Geochemical studies of hydrothermal fluids in the middle Okinawa Trough Back Arc Basin

中部沖縄トラフ背弧海盆海底熱水系の地球化学的研究

Jun-ichiro ISHIBASHI

Geochemical studies of hydrothermal fluids in the middle Okinawa Trough Back Arc Basin

by

Jun-ichiro ISHIBASHI

A dissertation submitted in partial fulfillment
of the requirements for the degree of Doctor of Science
in Chemistry in the graduate school of the University of Tokyo

Acknowledgments

I wish to express my sincere gratitude to Professor H. Sakai of Ocean Research Institute, University of Tokyo who inspired me throughout the course of this work, collaborated with me both on board and in the land laboratory, and carefully reviewed the manuscript. I am indebted to Professor H. Wakita of Laboratory for Earthquake Chemistry, University of Tokyo for continuous encouragement during my study, invaluable advice, and support for analyses of volatile components in his laboratory. I wish to express my grateful thanks to Drs. T. Tanaka, T. Naganuma, K. Mitsuzawa, T. Matsumoto and other members of Deep-Sea Research Group of JAMSTEC, Mr. Danno and members of the operation team of submersible "SHINKAI 2000", Captain Ochi and crew of tendership Natsushima, for their skillful cooperation through the hydrothermal fluid sampling programs in the dive missions. I wish to thank Drs. T. Gamo, F. Yanagisawa, E.-S., Kim, K. Shitashima, and M. Tsutsumi of Ocean Research Institute, for fruitful discussions, valuable suggestions, many helps in shipboard works and their providing me with data referred in this study. My thanks are extended to Dr. Y. Sano of Laboratory for Earthquake Chemistry, University of Tokyo for help in the helium isotopic measurements and QMS analyses, and to the members of the laboratory for their valuable comments and encouragement. I am grateful to Dr. Y. Nojiri of National Institute for Environmental Studies for his great support in the trace element analyses and valuable suggestions, Dr. H. Chiba of Okayama University for useful advice and discussion on the chemical species calculation.

I wish to thank Professor T. Oomori of the University of Ryukyus and members of the laboratory, for assistance on board work and in supplies of experimental equipment during the stay in the Okinawa Island.

Abstract

In order to reveal geochemical characteristics of hydrothermal systems in the middle Okinawa Trough Back Arc Basin, chemical compositions of hydrothermal fluids, both major and minor components including volatile components were studied.

Hydrothermal activities of high temperature fluid venting were located at two sites, the Jade site and Clam site, in the middle Okinawa Trough in 1988. They are the first observation of hydrothermal system within the continental margins.

During dive missions of Japanese submersible "SHINKAI 2000" in 1989, fluid samples were collected from both the Jade and the Clam sites, using samplers developed for this purpose. Measurement of pH and alkalinity of the fluids were conducted on board. Concentrations of Li, Na, K, NH_3, Mg, Ca, Sr, Ba, Mn, Fe, B, Al, SO_4, Cl and SiO_2 were analyzed. Contents of volatile composition such as CO_2, CH_4, He, H_2S and H_2 and isotopic composition of CO_2, CH_4, He and H_2S were also determined.

Major element composition of the Jade fluid is mostly comparable to the MOR fluids, except for K enrichment by about a factor of two in the former. Rough estimation of activities of major elements indicates that the Jade fluid is equilibrated with quartz, calcite and probably feldspars and their replaced minerals at about 300 C. This suggests that the Jade fluid composition is mainly controlled by these equilibrium systems during hydrothermal interaction. The high K content of the Jade fluid is attributed to high content of the rocks with which the

fluid reacted. A close comparison of the K content in the Jade fluid with those obtained by experimental seawater-volcanic rock interaction supports that the Jade fluid has experienced hydrothermal interaction with intermediate to acidic volcanic rocks.

High NH_3 content and minor element composition indicate that these components are incorporated into the Jade fluid during fluid-sediment interaction. Theoretical estimation of the in-situ pH during fluid-sediment interaction revealed that coupling of the high NH_3 content and fluid saturation with calcite controls pH and alkalinity of the fluid effectively.

The Clam fluid shows characteristic features indicating that it has experienced hydrothermal interaction at as low temperature as 100 C. Major element composition suggests that the Clam fluid is a mixture between high temperature fluid and entrained seawater. High alkalinity indicates oxidation of organic matter by sulfate reduction during fluid-sediment interaction. Chemical and isotopic compositions of sulfur species support that this reduction occurs at low temperature.

Significant enrichment in CO_2 and CH_4 is another specific character of the hydrothermal fluid in the middle Okinawa Trough. The CO_2 content of the Jade fluid is more than one order of magnitude higher than those of the MOR fluids. He isotopic composition of the Jade fluid suggests its magmatic origin. Carbon isotopic composition and high $CO_2/^3He$ ratio indicate that the dominant part of CO_2 in the Jade fluid was derived from magma origin of the Island Arc type. Contrary to this, CH_4 of the Jade

fluid is overwhelmed by thermogenic one, according to its isotopic composition.

The Clam fluid shows the lower $^3He/^4He$ ratios than the Jade fluid. This suggests a contribution of radiogenic He. The Clam fluid shows higher $CO_2/^3He$ ratio than the Jade fluid, which is attributed to fluid-sediment interaction. However, correlation between the ratios of $CO_2/^3He$ and $^3He/^4He$ is ambiguous. Isotopic composition of CH_4 in the Clam fluid is similar to that of the Jade fluid, supporting that CH_4 is derived from the fluid-sediment interaction at low temperature.

In summary, two prominent processes during hydrothermal interaction control fluid composition of both the Jade and Clam fluids. Interaction with acidic igneous rocks of the Island Arc type controls composition of major elements including CO_2 and H_2S. Interaction with sedimentary matter determines contents of minor elements including CH_4. The latter interaction is responsible for regulation of pH and alkalinity of the fluid. The Clam fluid has experienced low temperature hydrothermal interaction within the sedimentary layer, which causes distinctive features in its composition from the Jade fluid.

CONTENTS

List of figures

List of tables

Chapter 1.

Introduction
- Previous geochemical studies of hydrothermal system

1-1. Submarine hydrothermal system

Since high temperature fluid venting from the seafloor was discovered in 1977 at spreading axes of Galapagos Ridge and East Pacific Rise (Corliss et al., 1979; RISE Project Group, 1980), submarine hydrothermal system has been considered as one of the most interesting and important targets in oceanography. Numerous studies on this subject were conducted as a part of investigation of the mid-oceanic ridge (MOR) system. They have revealed that hydrothermal activity is an ubiquitous concomitant phenomenon to the ocean floor spreading activity. The MOR systems where well-developed fracture system concurs with shallow heat source magma, provide favorable environment to development of hydrothermal system.

Seawater, which penetrates into young oceanic crust through the fracture system, is heated up by the magma and ascends back to the seafloor due to its volume expansion. High temperature and high pressure condition promotes chemical reactions between seawater and crustal materials during hydrothermal circulation. Chemical composition of the fluid evolves from that of original seawater, while the crust suffers alteration. Furthermore, the fluid circulation causes transport of elements leached from the reactant materials to the seafloor surface. Venting of fluid induces mineral deposition on the seafloor due to drastic change in physical and chemical properties by mixing with ambient

seawater. Chemical processes within hydrothermal system play an important role in alteration of both fluid and the crust, in transfer of elements, and in mineral deposition.

1-2. Geochemical features of hydrothermal fluid

Table 1-1 compiles data of chemical composition of hydrothermal fluids obtained from the MOR systems. Their geochemical signatures compared with seawater are summarized as:

(1) depletion of Mg and SO_4: While both are major components of seawater, their contents are almost zero.

(2) strong acidity: pH of 3 - 4 is significantly lower than that of deep seawater of 7.8.

(3) enrichment in Ca and K: To compensate Mg depletion, Ca and K contents increase.

(4) enrichment in heavy metals: Contents of other trace cations are also enriched relative to seawater. Their enrichment factors are greater than 10^5, due to considerably low contents of metal elements in deep seawater.

(5) high SiO_2 content: SiO_2 content is close to or even higher than the saturation at temperature and pressure of interaction.

(6) reductive condition: A significant amount of sulfide ion exists.

(7) positive $\delta^{18}O$ value: Isotopic composition strongly indicates that the fluid is in oxygen isotopic equilibrium with silicates at high temperature.

(8) volatile component of magmatic origin: Isotopic composition of volatile components supports that they are derived from magmatic source.

As will be discussed in the following sections, these features are attributed to chemical reactions taking place between seawater and reactant rocks, at high temperature of 300-400°C and high pressure of 300-500 bars.

1-3. Controlling factors of major element composition

Mottl (1983a) summarized the following three principal mechanisms during hydrothermal interaction as factors which control chemical species in fluid. (1) fluid equilibria with minerals, (2) kinetic effects of leaching reaction, (3) elemental abundance in reactant matter and W/R ratio (mass abundance ratio of fluid over reactant rock). Among of them, he considered the fluid mineral equilibria determines eventually major element composition of hydrothermal fluid.

Mottl (1983b) considered that the reaction paths during hydrothermal circulation consists of two stages, earlier "fluid-dominated stage" and following "rock-dominated stage".

Prominent reactions in the earlier stage are formation of Mg-rich secondary minerals and anhydrite deposition (Seyfried and Bischoff 1981). Mg-silicate forms through reactions such as:

$$3Mg^{2+} + 4SiO_{2(aq)} + 4H_2O = \underset{\text{talc}}{Mg_3Si_4O_{10}(OH)_2} + 6H^+ \quad \text{--- (1-1)},$$

which removes Mg from and add H^+ into fluid. The latter attacks primary minerals and glass in the reactant rocks converting them to hydrated secondary phases, which cause mobilization of cations including heavy metals (Seyfried and Bischoff, 1981). SO_4 is also removed from seawater by precipitation of anhydrite as:

$$Ca^{2+} + SO_4^{2-} = \underset{\text{anhydrite}}{CaSO_4} \quad \text{--- (1-2)}$$

With Ca being leached from rocks, anhydrite precipitation continues until complete removal of SO_4 is attained. Formation of both Mg-silicate and anhydrite occurs at temperature above 150°C under adequate low W/R ratio (Seyfried and Mottl, 1982). Hydrothermal interaction in this stage is characterized by leaching of elements from primary minerals and glass. Fluid does not approach to saturation with minerals except for anhydrite and calcite due to fluid dominant condition. Fluid composition is controlled by kinetic effects of leaching reactions, elemental abundance in reactant rock and W/R ratio during interaction.

As leaching reaction progresses, fluid would become to be saturated with certain minerals. Elevated temperature to about 300°C and decreased W/R ratio accelerate saturation (Seyfried et al., 1988). In this stage, fluid composition is controlled by equilibria with mineral assemblages constituting altered phase. For example, a series of cation exchange reactions among feldspars controls contents of Na, Ca and pH (Berndt et al., 1989) as:

$$\underset{\text{anorthite}}{CaAl_2Si_2O_8} + 2Na^+ + 4SiO_2 = \underset{\text{albite}}{2NaAlSi_3O_8} + Ca^{2+} \quad \text{--- (1-3a)}$$

$$3\underset{\text{anorthite}}{CaAl_2Si_2O_8} + Ca^{2+} + 2H_2O = \underset{\text{clinozoisite}}{2Ca_2Al_3Si_3O_{12}(OH)} + 2H^+ \quad \text{--- (1-3b)}$$

$$2\underset{\text{anorthite}}{CaAl_2Si_2O_8} + 2SiO_2 + Na^+ + H_2O = \underset{\text{albite}}{NaAlSi_3O_8} + \underset{\text{clinozoisite}}{Ca_2Al_3Si_3O_{12}(OH)} + H^+ \quad \text{--- (1-3c)}$$

In summary, major element composition of fluid evolves as below. Mg and SO_4 are completely removed from fluid in the earlier stage. During this stage, Na, Ca, K and other cations are extracted from primary minerals and glass of reactant matter. Once fluid ensues to be saturated with secondary minerals, equilibria with them control composition of the fluid. Final major element composition is determined by the equilibria with assemblage of altered minerals.

Some calculative studies reinforced the model of fluid equilibria with minerals. Bowers et al.(1988) calculated chemical affinities of prominent precipitation reactions and indicated that ten venting fluids collected from the EPR (East Pacific Rise) were close to or at saturation with minerals which constitute greenschist facies. Bowers and Taylor (1985) and Bowers (1989) demonstrated that fluid evolution during whole reaction paths in hydrothermal interaction can be simulated by step-wise calculation.

1-4. Controlling factors of minor element composition

Since minor elements do not form independent altered minerals, ion exchange for major element is considered as a reaction which distributes them into mineral phases. Li and B are considered to be rarely involved into secondary minerals (Seyfried et al., 1984) and called as "soluble element". Content of such elements could quantitatively be estimated from W/R ratio and elemental abundance in reactant matter. Because these elements accumulate in fluid with increasing degree of leaching

from reactant rock and do not precipitate forming mineral phase, their contents would be useful to constrain alteration processes during hydrothermal interaction.

1-5. Volatile components of hydrothermal fluid

Volatile components of hydrothermal fluid are considered to be extracted from occluded gas in glassy materials of reactant rock.

The He isotopic composition of the EPR fluid is common to that in basaltic rock collected at the same site, supporting that the He in the fluid came from the basaltic rock (Lupton et al., 1980). Welhan and Craig (1983) demonstrated that both CO_2 and CH_4 in the EPR 21°N fluid are also derived by the same mechanism, based on their isotopic compositions and abundance ratios to ^3He coupled with data of basalt glass. Further study on volatile components of the EPR 13°N fluid (Merlivat et al., 1987) and of the Southern Juan de Fuca fluid (Evans et al., 1988) demonstrated that this model is also applicable to other MOR systems.

In the case of the MOR systems where no other significant source exists in the neighborhood, chemical and isotopic compositions of volatile components in hydrothermal fluid provide us with direct information of their magmatic sources.

1-6. Hydrothermal interaction in the sediment-hosted systems

Hydrothermal systems generally develop within sediment-free region where the oceanic crust has not aged since its generation. Contrary to such "sediment-starved hydrothermal system", some hydrothermal systems are recognized as developing in environment

where spreading center is covered with thick sedimentary layer. Such "sediment-hosted hydrothermal system" occurs in areas adjacent to continent which provides abundant sedimentary matter such as terrestrial detritus or clay minerals. The Guaymas Basin in the Gulf of California (Koski et al, 1985; Von Damm et al., 1985b) and the Escanaba Trough in the Gorda Ridge (Koski et al., 1988) have been well studied as examples of the sediment-hosted ridge system.

In the sediment-hosted hydrothermal system, fluid circulates within thick sedimentary layer as well as within the oceanic crust. Hydrothermal interaction between fluid and sedimentary matter controls fluid composition in different way from fluid-rock interaction.

Organic matter in sedimentary layer has high reactivity at high temperature condition. It decomposes to CO_2, CH_4, NH_3 and other lower organic compounds through thermal degradation and oxidation reactions. Involvement of these species into fluid significantly affects pH and alkalinity of the fluid. (Von Damm et al., 1985b). Volatile composition is also modified appreciably because sedimentary layer is usually a larger source of these species than magmatic source (Welhan and Lupton, 1987).

Furthermore, the shift of pH and alkalinity induce mineral deposition to alter metal element composition and may affect the fluid equilibria with minerals which in turn modify major element composition (Simoneit, 1985). Bowers et al.(1985) demonstrated that calculative simulation of interaction between EPR-type fluid and sedimentary matter can well predict chemical composition of

the Guaymas fluid, both increase in pH and signifant low metal elements contents. Apart from the organic matter decomposition, dissolution of inorganic minerals such as calcite and/or anhydrite would affect fluid composition.

Thornton and Seyfried (1987) conducted an experimental study on the fluid-sediment interaction at condition of 350°C, 500 bars. They discussed each reaction path mentioned above in detail, and expressed overall reactions which occur during the experiment as :

$$0.27(C_{106}H_{263}O_{110}N_{16}P) + 2.6Mg^{2+} + 3.4Na^{+} + 7.7SiO_2 + 2.6H_2O + 1.3KAlSi_3O_8 + 1.7CaSO_4 + 1.7FeO + 1.7CaAl_2Si_2O_8$$

$$= 0.85Mg_3Si_4O_{10}(OH)_2 + 0.42KAl_3Si_4O_{10}(OH)_2 + 3.4NaAlSi_3O_8 + 3.4CaCO_3 + 1.7FeS + 1.7CH_4 + 4.3NH_4^{+} + 0.27H_3PO_4 + 0.85K^{+} + 1.7H_2CO_3 + 10.7CH_3COOH + 3.4H^{+} \quad ---- \ (1\text{-}4)$$

1-7. Hydrothermal systems in the continental margins

Fig. 1-1 illustrates global distribution of the submarine hydrothermally active sites that have been identified up to date (1990). Because the MOR system has been investigated most energetically with great interest of tectonic study until quite recently, hydrothermal systems are discovered mainly there.

However, recent studies have expanded their exploration area and succeeded to discover hydrothermal activities in various tectonic settings. Loihi submarine volcano in hot spot region (Malahoff et al., 1982), spreading axis of the Mariana back arc basin (Craig et al., 1987) and spreading axis of the North Fiji Basin (Auzende et al., 1990) are such examples.

The Okinawa Trough is a back arc basin in a nascent stage, as will be discussed in Chapter 2. Although thick continental crust remains below the area, rifting-induced fracture systems and heat supplied by Island Arc type magmatic activity provide conditions favorable to hydrothermal circulation. Hydrothermal activities located in the middle Okinawa Trough are the first identification of hydrothermal system which develops within the continental margins.

The main purposes of this thesis are to study geochemical signature of the hydrothermal fluids of the middle Okinawa Trough back arc basin, both in elemental and volatile compositions, and to discuss reactions responsible for their unique composition. In Chapter 2, geological background of the hydrothermal system in the Okinawa Trough will be summarized. Analytical methods used in this study will be described in Chapter 3. Analytical results on major and trace elements will be discussed in Chapter 4. Chapter 5 will be devoted to volatile components. The concluding remarks based on the discussion in Chapter 4 and 5 will be given in Chapter 6.

Table 1-1 Compilation of elemental fluid composistion of hydrothermal fluids obtained form the MOR systems

component		EPR 21N	EPR 13N	EPR 11N	SJFR	MAR	GSC	Seawater
pH(25°C)		3.3-3.8	3.92	3.1-3.7	3.2	3.7-3.9		7.8
Li	μM	891-1322	688	484-884	1110-1810	510	689-1142	26
Na	mM	432-510	560	290-577	700-800	846		463
K	mM	23.2-25.8	29.6	18.7-32.9	37.3-51.6	23.7	18.7-18.8	9.8
Rb	μM	27-33	14.1	15-25	28-37	10.7	13.4-21.2	1.3
NH_4	mM	<0.01						<0.01
Be	nM	10-37			95-150	38.3	11-37	0.0
Mg	mM	0	0	0	0	0	0	52.7
Ca	mM	11.7-20.8	55	10.6-35.2	77.3-96.4	9.9-10.5	24.6-40.2	10.2
Sr	μM	65-97	175	38-135	230-312	51	87	87
Ba	μM	<15					17.2-42.6	0.14
Mn	μM	700-1000	800-120	742-925	2610-4480	492	360-1140	<0.001
Fe	μM	750-2420	1050-1850	1640-6470	1030-1870	1830-2180		<0.001
B	μM	500-550				518-530		416
Al	μM	4.0-5.2		12.9-13.6	1.9	5.2		20
SO_4	mM	0.0-0.6	0	0	-1.7--0.5			27.9
Cl	mM	489-579	740	338-686	896-1090	559		541
AT	meq	-0.50--0.19		-0.28--1.02	0	-0.24--0.06	0	2.3
SiO_2	mM	15.6-19.5	22	14.3-20.6	22.7-23.3	18.3	21.9	0.16

all unit are in per kg

EPR 21°N: 21°N East Pacific Rise (Von Damm et al. 1985a)
EPR 13°N: 13°N East Pacific Rise (Michard et al., 1984)
EPR 11°N: 11°N East Pacific Rise (Bowers et al., 1988)
SJFR : Southern Juan de Fuca Ridge (Von Damm et al., 1987)
MAR : Mid Atlantic Ridge at Kane (Campbell et al., 1988)
GSC : Galapagos Spreading Center (Edmond et al., 1979)

B concentrations are from (Spivack and Edmond, 1987)

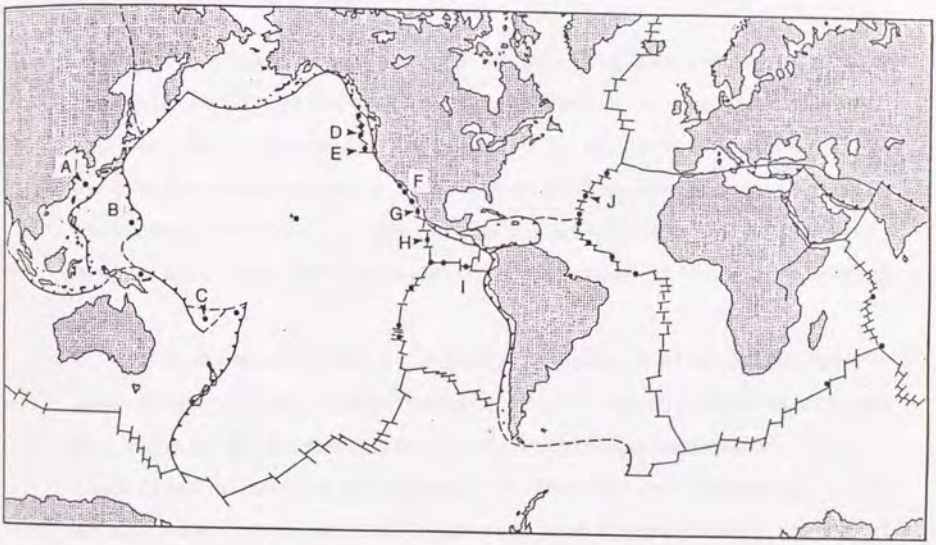

Fig. 1-1 Global distribution of major identified submarine hydrothermal systems (modified after Rona 1988)

A: Middle Okinawa Trough; B: Mariana Trough
C: North Fiji Basin; D: Juan de Fuca Ridge
E: Gorda Ridge; F: Guaymas Basin;
G: East Pacific Rise 21°N; H: EPR 13°N
I: Galapagos Spreading Center; J: Mid-Atlantic ridge

Chapter 2.

Geological background of hydrothermal systems in the middle Okinawa Trough

2-1. The Okinawa Trough

The Okinawa Trough is a NE-SW trending depression of 1200 km long and about 100 km wide, located between the Ryukyu Islands and East Sea (fig. 2-1). This trough is divided into three parts by its depth and location, the northern Okinawa Trough of depth shallower than 1000 m, the middle Okinawa Trough of 1000 m to 2000 m depth and the southern Okinawa Trough of 2000 m to 2300 m depth.

The Okinawa Trough is a back arc basin behind the Ryukyu trench-arc system. Along the axis of the trough, several grabens are aligned en echelon (fig. 2-2). Previous studies for geological structure and history of the Okinawa Trough (e.g. Lee et al., 1980; Kimura, 1985; Letouzey and Kimura, 1985; Sibuet et al., 1987), attribute them as formed with extensional tectonic situation. While some studies (Kimura, 1985; Sibuet et al., 1987) proposed the Southern Okinawa Trough is in the beginning stage of seafloor spreading, others (e.g. Oshima et al., 1988) argued against this. Recent studies (e.g. Japanese DELP 1988 Group, in preparation) demonstrated some lines of evidence favorable for the latter hypothesis. They agreed that the present extensional stage of the Okinawa Trough remains in a rifting stage prior to a spreading stage, which is characterized by development of normal faulting and crustal extension in brittle continental crust.

2-2. Previous studies on the middle Okinawa Trough

At the axial part of the middle Okinawa Trough, Kimura et al.(1986) found several distinct grabens which are surrounded by normal faults and which contain elongated parallel ridges and scattered small knolls. Among them, the Iheya Graben (shown by an arrow mark in fig. 2-2) where this structure appears most clearly, has been chosen for a detail investigation area.

Fig. 2-3 is a precise seabeam map of this area. The prominent ridge (named as Iheya Ridge) located at the axis of the Iheya graben consists of basalt and basaltic andesite (Kimura et al., 1986; Naka et al., 1989; Ishizuka et al., 1990). On the other hand, abundant occurrence of acidic rocks of dacite and rhyolite and extensive distribution of "woody pumice" were observed at small knolls (named as Iheya Knolls) in the eastern area of the Iheya Ridge (Uyeda et al., 1985; Momma et al., 1989). Honma et al.(1987) revealed common signature of the calc-alkaline rocks of the island arc type in both type rocks based on their chemical and isotopic compositions. This bi-modal volcanism may be taken to indicate extensional activity in the Iheya Graben (Kimura et al., 1986).

At any sites in the middle Okinawa Trough, oceanic back arc basalt has not appeared. Seismic refraction study (Nagumo et al., 1986) indicated a 5 km thick layer which is attributed to granitic continental crust and the lack of the oceanic crust. Parallel lineation of magnetic anomalies on the seafloor has not been recognized (Kitahara et al., 1986).

The basaltic rock at the Iheya Ridge shows K-Ar ages of 0.22

- 0.42 Ma, indicating very recent volcanic activity (Kimura et al., 1986). Microseismic study (Ouchi et al, 1989) demonstrated ceaseless occurrence of numerous small earthquakes further support for the presently active state of the middle Okinawa Trough. Yamano et al. (1986a; 1986b; 1989) reported extremely high and localized heat flow anomalies, and attributed them to be caused by an intrusive body younger than 3×10^5 year and shallower than 3.5 km.

In summary, the geological and geophysical lines of evidence attribute the tectonic setting of the Iheya Graben to be in an initial stage of rifting within continental crust and in a most active part of the middle Okinawa Trough.

2-3. Sedimentary environments around the middle Okinawa Trough

The Okinawa Trough is also characterized as extensive sedimentation. As easily speculated from its location, enormous amount of terrestrial matter is supplied from the Asia continent and the East Sea continental shelf. High sediment accumulation would cause burial of unoxidized organic matter, and would induce good condition for its rapid diagenesis. In the case that a heat source exists under sedimentary layer, it would enhance this reaction.

2-4. Hydrothermal activities in the middle Okinawa Trough

One low temperature activity (Hibiscus site) and two high temperature sites (Jade site and Clam site) have been found in the Iheya Graben up to date (1990). They are the first observations of hydrothermal circulation within the continental

crust margin. Fig. 2-4 illustrates localities of these hydrothermal activities.

In July 1986, direct evidence of hydrothermal activity was witnessed during the dive mission of Japanese submersible SHINKAI 2000 (Kimura et al., 1988). Small mounds composed of hydrothermal precipitation of Fe-smectite and Fe-oxyhydroxide (Masuda et al., 1987), and shimmering fluid of 2-3°C higher temperature than ambient seawater were observed. This site (named as "Hibiscus site") was located at the Natsushima 84-1 Knoll (27 34.4 N, 127 08.6 E, fig. 2-3:A) which consists of acidic rocks and faces the south side of a small basin where high heat anomalies had been recorded (Yamano et al., 1986a).

Preliminary results of chemical composition of the Hibiscus fluid (Gamo et al., 1987b) demonstrated low pH, high methane content and high $^{3}He/^{4}He$ value. However, these anomalies were not so significant, which suggest a low temperature hydrothermal activity of the Hibiscus site, together with evidence from hydrothermal precipitation.

In 1986, R/V Hakuho Maru of the Ocean Research Institute, University of Tokyo, occupied this area to make further survey on hydrothermal activity. During this cruise, hydrothermal plume was detected in the water column around the Hibiscus site, by measuring CH_4 content and He isotope anomalies (Ishibashi et al., 1986). The results were very promising, indicating the presence of hydrothermal vents, probably much more active than the Hibiscus site.

Following this, two high temperature hydrothermal fields

were discovered in this area in 1988. In the following sections, geological settings of these sites are summarized briefly.

2-5. Geological settings of the Jade site at the Izena Cauldron

The high temperature hydrothermal activity accompanying extensive sulfide mineralization was located at the Izena Cauldron (27°16′N, 127°05′E, fig.2-3:B) (Halbach et al., 1989). This site was discovered during the cruise of German research vessel "Sonne" in June of 1988, and named as "Jade site".

The Izena Cauldron is a rectangular (6 km x 3 km) depression located at about 30 km southeast apart from the Iheya Ridge. Several observation conducted by the submersible "SHINKAI 2000" reported occurrence of rhyolite (Tanaka et al., 1990), dacite (Nakamura et al., 1989), woody pumice and tuff breccia with consolidated sediment (Kato et al, 1989) at the outer wall of the Izena Cauldron.

Hydrothermal field lies within a NNE-trending 1000 x 200 m elongated belt zone along the north-eastern wall of the Cauldron at depth of 1450-1300 m (see fig. 2-4). Dive missions of the SHINKAI 2000 in 1988 and 89 (Nakamura et al., 1989; Aoki and Nakamura, 1989) and survey cruises of DK89-1-OKN (Momma et al, 1989) and GH89-3 investigated regional distribution of the activities in the Jade site.

Fig. 2-5 summarizes these results in a map (Tanaka et al., 1990). At the center part, the "Black smoker" chimney vigorously emits fluid of 320°C upwards to height of 15 m with fine suspension. Several hydrothermal mounds of angular sulfides blocks were distributed. Around the Black smoker, several groups

of chimneys were located which discharge clear fluid of 220°C or lower temperature. Collected ore samples show occurrence of sphalerite, tetrahedrite, galena, chalcopyrite, pyrite, barite and anhydrite. From their mineral composition, they are considered to be a modern analogue of the Kuroko-type mineralization in the Northeast Honshu, Japan (Halbach et al., 1989; Urabe, 1989; Nakamura et al., 1990).

On the outskirt part, native sulfur layers and white pockmark zones consisting of altered minerals and precipitates were observed (Tanaka et al., 1990; Nakamura et al., 1990). In two of the white pockmarks, venting of "liquid CO_2 bubble" was witnessed (Sakai et al., 1990b).

2-6. Geological settings of the Clam site at the Iheya Depression

Another active high temperature hydrothermal field was located at a northern foot of the Iheya Ridge (27°33′N, 126°58′E, fig. 2-3:C). A deep-tow TV camera system of research vessel KAIYO caught biological community and temperature anomaly in June 1988 (Momma et al., 1989). This site was named as "Clam site" according to intensive biological activity which forms clusters of giant clams, tube worms and shrimps.

TV camera observation by KAIYO and Sonne, and dive missions of the SHINKAI 2000 in 1988, 1989 and 1990 have been carried out at this site. The hydrothermal activity is confined within a narrow area of a radius of less than 1 km (see fig. 2-6) on a flat gentle slope of 1400 m depth of the Iheya depression. Although the Iheya Ridge is considered to be the center of the

present activity in the Iheya Graben, other intense activities have not been discovered at any area around it.

The most remarkable geological feature in the Clam site is carbonate crust which covers the seafloor. Some of them are piled up to form a small mound and some of them are collapsed along a fissure. Collected samples of the crust were identified as silica-mangno-calcite and Mn-rich dolomite (Tanaka et al., 1989). Ore deposits of sulfide minerals have never been observed in the Clam site.

Hydrothermal fluid ventings concentrate within a narrow zone adjacent to a small hill (fig. 2-6). Clear fluid emerges out through fractures and cracks of the carbonate crusts, in places. Some of them form altered material or deposit on the seafloor, although large construction was never observed. Temperature of fluids was more than 100°C, but the highest measured temperature was limited to 210°C.

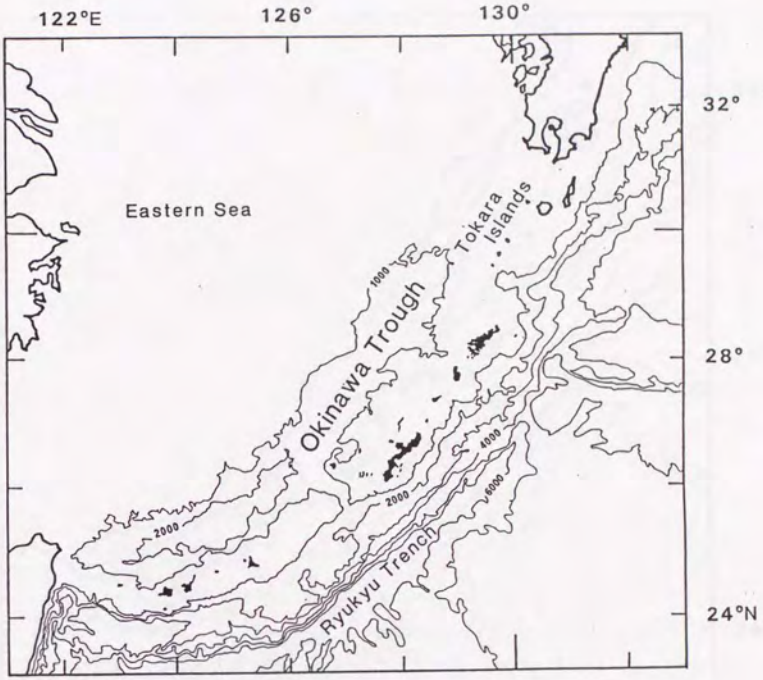

Fig. 2-1 A topographic map of the Okinawa Trough.

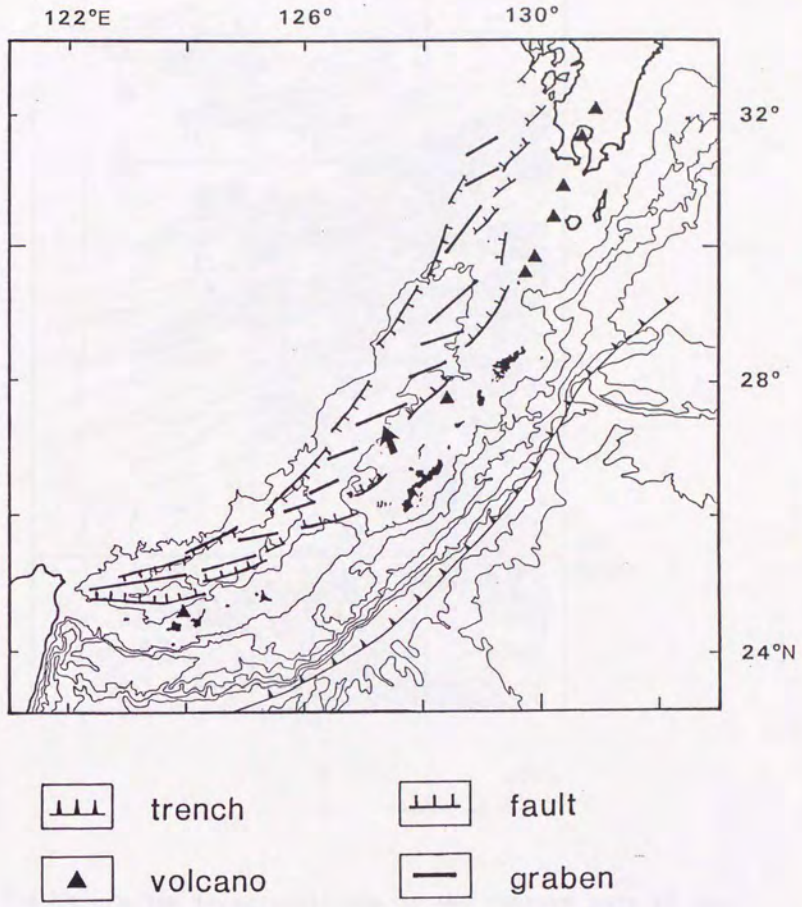

Fig. 2-2 An outline map of tectonic structure in the Okinawa Trough. An arrow mark indicates the Iheya Graben. (modified from Kimura, 1988)

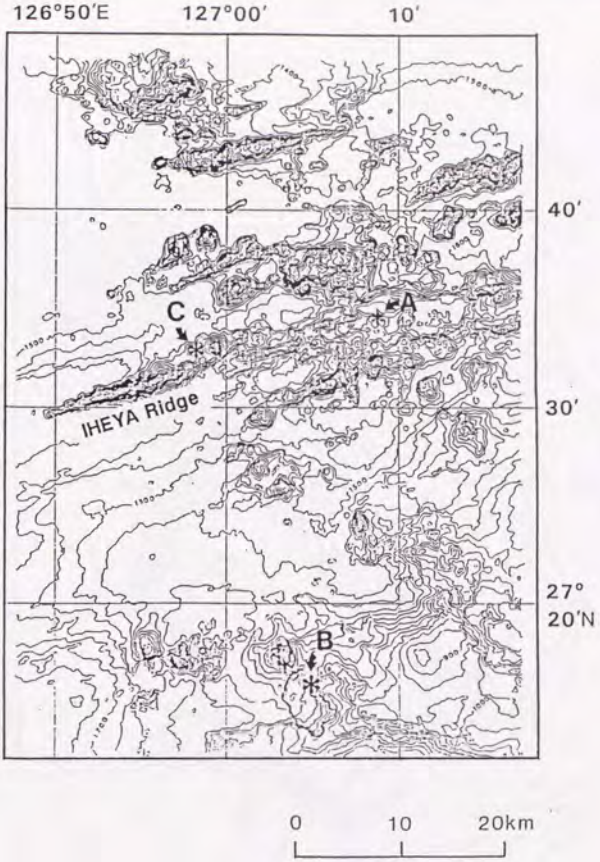

Fig. 2-3 A precise topographic map of the western part of the Iheya Graben. Every contours are in 100m.
(The original seabeam map was made by the Hydrographic Department, Martime Safety Agency of Japan; Katsura et al., 1986).

Asterisks mark indicate localities of the hydrothermal sites.
A: Hibiscus site on the Natsushima 84-1 Knoll
B: Jade site at the Izena Cauldron
C: Clam site at the Iheya Depression

Fig. 2-4 A map showing topography of the Izena Cauldron. Shaded area indicates the Jade site.

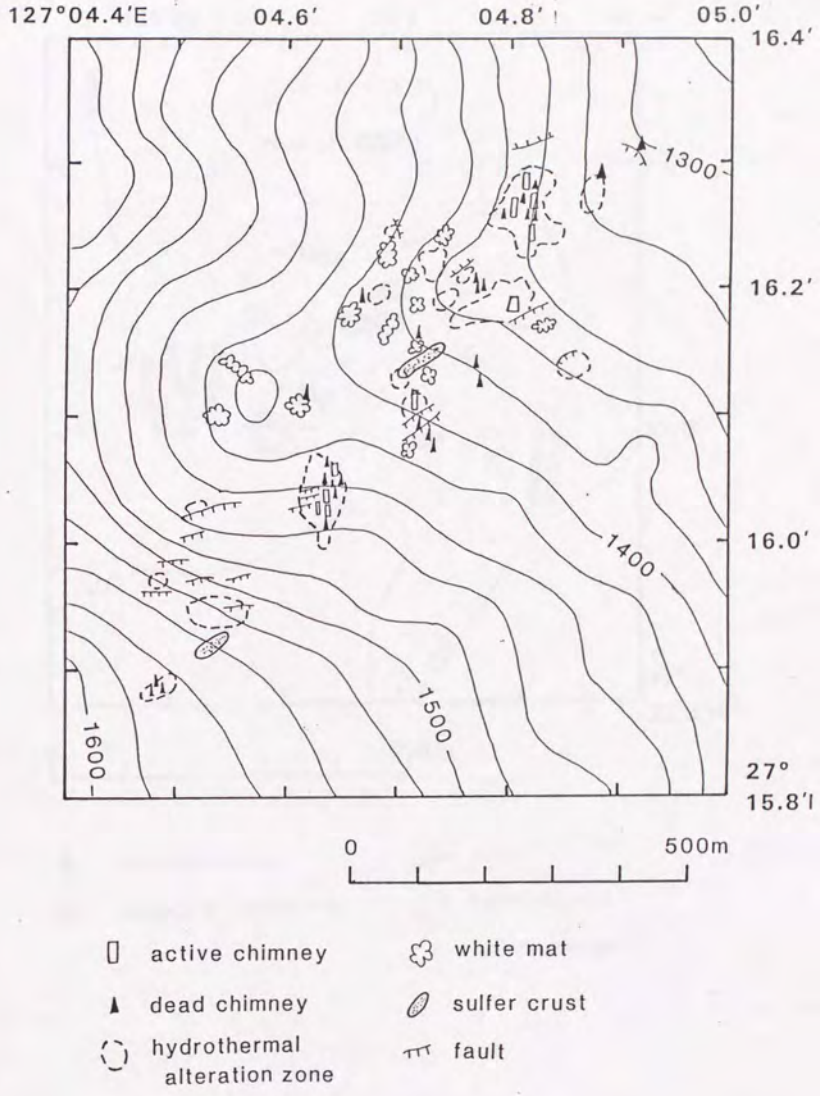

Fig. 2-5 A map showing distribution of hydrothermal activities in the Jade hydrothermal site. (modified from Tanaka et al.,1990)

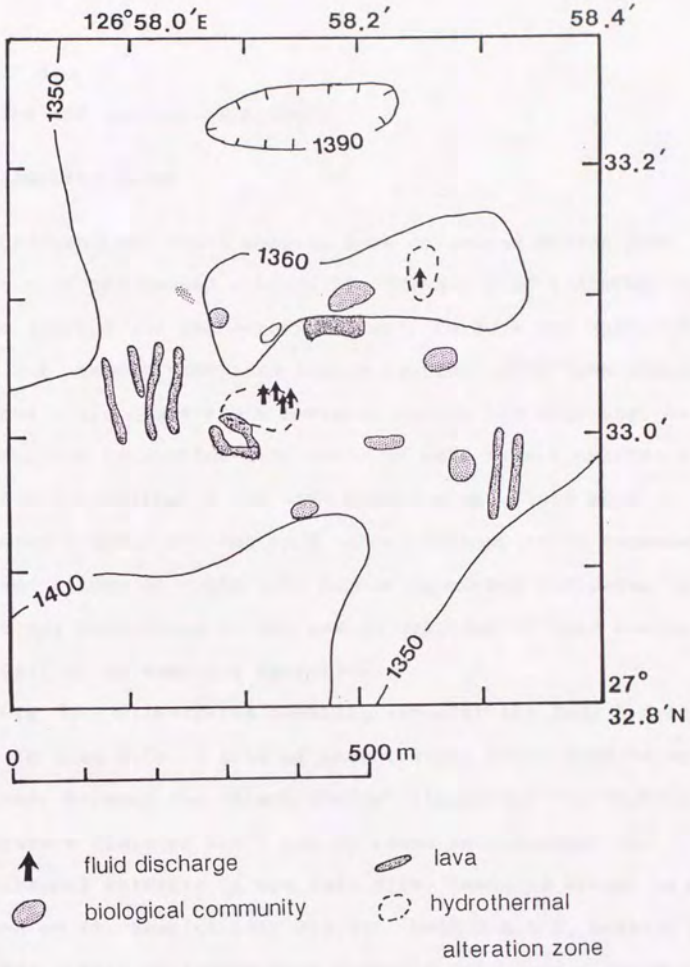

Fig. 2-6 A map showing distribution of hydrothermal activities in the Clam hydrothermal site.
(modified from Tanaka et al., 1989)

Chapter 3.

Sampling and analytical methods

3-1. Sampling sites

Hydrothermal fluid samples were collected during dive missions of the manned submersible SHINKAI 2000 (JAMSTEC; Japan Marine Science and Technology Center), in June and July, 1989. In table 3-1, sample names are listed together with each sampling site and fluid temperature measured during the sampling. As will be described in section 3-2, three or more sample cylinders were used for a sampling of the same hydrothermal fluid when a revolving sampler was employed. A set of samples is expressed in the same column in table 3-1. A Missing number indicates that no sample was introduced in the sample cylinder of that number due to a failure of sampling operation.

Fig. 3-1 illustrates sampling sites in the Jade hydrothermal site. In this site, 7 sets of hydrothermal fluid samples were obtained. Because the "Black Smoker" discharges the highest temperature fluid of 320°C and it seems to represent the hydrothermal activity in the Jade site, sampling target was focused on it. Samples D413-RV1,2,3, D413-RV4,5,6, D414-AL and D414-RV2,3 were collected from chimneys which are a few meters to the west of the "Black Smoker". The fluid discharging from these chimneys were clear and of about 150°C temperature. D422-RV2,3 and D423-RV2,3 were obtained from the top of the "Black Smoker" chimney, directly. D423-RV4,5,6 were taken at another venting site, where small chimneys emit clear fluid. This sampling site was about 200 m apart from the "Black Smoker". During the

sampling D415-M and D424-M, it was tried to collect "liquid CO_2 bubble" as described in section 5-3-7, and only the latter sampling was successful.

At the Clam site, 5 sets of samples were collected at three vents in a small region of the same hydrothermal alteration zone. D416-AL, RV1,2 were collected at a fissure where clear fluid of 220°C emerged. About a month after this sampling, two dives, D426 and D427 revisited the same site and collected the samples from the same vent as D416 or at least a vent very close to the former. Samples D416-RV4,5,6 were collected at other vents about 30 m apart from the fissure (fig. 3-2). D416-M and D427-M2, M3 were bottom seawater samples collected apart from these vents but within the hydrothermal active region.

3-2. Sampling equipments

Specific sampling equipments were developed for this dive study in the Ocean Research Institute (ORI) (Sakai et al., 1990c). Three types of water samplers were employed. The details of the first device is described in the following paragraphs. The second is a titanium sampler which is employed by American submersible "Alvin" (Von Damm et al., 1985a). The third is a cylinder sampler made of acrylic resin, used for collecting low temperature sample. Its one end has a cap which is open before sampling and can be triggered to be shut off with rubber band at seafloor.

Fig. 3-3 shows an outline of the revolving valve sampler. It consists of a sucking gear pump, 6 titanium cylinders, a

revolving switch valve, Teflon tubing, and a titanium inlet tube. Each cylinder has an O-ring sealed piston. As the gear pump pumps out distilled water which had occupied an upper room of the cylinder, the piston moves upwards introducing sample waters into a lower room. A check valve between the sample cylinder and the Teflon tubing prevents backward flow of the sample water after completion of the pumping. With rotation of the revolving switch valve, the next cylinder becomes to be ready for sampling.

The gear pump and the revolving switch valve can be controlled from a submersible cabin. While the inlet tube is set up as close to a vent as possible, the sampler is operated for collecting hydrothermal fluid. At the same time of the sampling, fluid temperature is monitored using a Platinum- thermometer attached to the top of the inlet tube. It takes about 15 minutes to fill up one sample room of 780 ml capacity.

The drawback of the revolving sampler is that the water which occupied inlet and Teflon tubes in prior to sampling (see fig. 3-3) was inevitably introduced into the sampling cylinder and contaminated the hydrothermal fluid. In order to obtain the fluid sample free from such contamination, two or more successive sampling of the same hydrothermal fluid was necessary. While the sample in the first cylinder was diluted by distilled water or the former sample, nearly pure fluid sample should be obtained in the last cylinder of a series of the successive sampling.

The revolving sampler is of advantage to collect volatile-rich fluid sample. Gas evolution from hydrothermal fluid trapped in the sample cylinder often causes significant pressure increase on the return to sea surface to induce leakage of volatile

components from the sample. The revolving sampler assures an extra space for gas evolution, by adjusting the piston to pause at a half-way of its full drive. Thus, the movement of the piston compensates for the pressure increase during the recovery of the sampler. Sample leakage due to gas evolution was considered to be sufficiently prevented.

3-3. Sample transfer procedure

After the recovery of the submersible "SHINKAI2000", both aqueous and evolved gas phases of a fluid sample were transferred from the sample cylinder, at on board laboratory in the tendership Natsushima.

Fig. 3-4 is a schematic diagram showing the on board transfer and storage procedures of the gaseous sample. At the first step, the evolved gas in an over-pressurized cylinder was taken out using a plastic syringe and its volume was measured under atmospheric pressure. It was, then, transferred to a storage bottle after procedures described in the next paragraph. After inner pressure became balanced to atmospheric, the gaseous portion remained in the sampler was pushed out by moving the piston and treated in the same way.

After the volume measurement, the sample was shaken with 1N $Zn(CH_3COO)_2$ solution to collect H_2S as ZnS. It was then introduced into saturated $Ba(OH)_2$ solution to precipitate $BaCO_3$. Residual gas (R-gas) was transferred into another plastic syringe for volume measurement. At the last step, the R-gas was transferred to a leaded glass bottle evacuated beforehand.

When all the gaseous portion was taken out, position of the piston was recorded to know sample volume of the aqueous portion (sample volume of the gaseous portion was measured during its transfer). The aqueous sample was aliquoted to each sampling bottle and stored after chemical treatment as follows.

1. 5 ml were drawn into a N_2 purged polystyrene bottle and capped (with no head space) for pH measurement.

2. 30 ml were drawn into a N_2 purged polystyrene bottle and capped (with no head space) for alkalinity titration.

3. 30 ml were drawn into a 60 cm long copper tubing and sealed at both ends with steal clumps for He analysis.

4. 30 ml were drawn into a N_2 purged glass vial and capped with septum (with no head space) after poisoned by $HgCl_2$ for dissolved CO_2 analysis. A duplicate was prepared for CH_4 and other volatile components analyses.

5. 30 ml were drawn into a N_2 purged polystyrene bottle and $Zn(CH_3COO)_2$ was added to precipitate ZnS for H_2S analysis.

6. 30 ml were drawn into a polystyrene bottle for nutrient analysis. 2 ml of this sample were diluted immediately with by ten times with distilled water. Both samples were stored in a refrigerator until analyses.

7. 60 - 100 ml were drawn into a polystyrene bottle for major elements. This was filtered with 0.4 μm nucleopore filter and then divided into two portions. The one was acidified with HCl or HNO_3 for cation analyses, and the other was stored without any treatment for anion analyses.

8. The remainder of the sample was then drawn into the teflon bottle and acidified with distilled HNO_3 for analyses of

heavy metal elements.

3-4. Analytical methods of elemental components

Analytical methods of major and minor elemental components are summarized in table 3-2 with their analytical precision. Most of them follow conventional methods employed for hydrothermal fluid or seawater analyses (e.g. von Damm et al., 1985a).

Measurement of pH and titration for alkalinity were done as soon as possible after the sample split. Colorimetric analyses of SiO_2 and NH_4 were conducted within 24 hours after recovery of the sample. Other analyses were conducted in the land based laboratory in the ORI and in the National Institute for Environmental Studies (NIES). Anions were analyzed by Dr. E.-S. Kim of ORI. Contents of Na are calculated from charge balance, because of poor precision of spectrophotometric analysis.

3-5. Analytical methods of volatile components

The hydrothermal fluid samples were often recovered in two separated phases, gaseous and aqueous phases, although they must be in a single liquid phase on the seafloor condition. Since volatile components distributed in both phases, their composition in the original fluid was estimated as below. Composition in gaseous and aqueous phases were determined by analyses of respective sample. Based on the sample volume of both gaseous and aqueous phases which were measured during the sample transfer, the total amount of each volatile component in the whole obtained sample was calculated. Composition in an original fluid was

determined on the assumption that both the evolved gaseous portion and the aqueous portion of the obtained sample were neither lost nor added during the sample recovery and that they were in a single aqueous phase on the sampling condition.

CO_2 content in the gaseous portion was determined by volumetry during the sample transfer procedure, measuring volume change before and after the alkali dissolution.

Composition of the R-gas sample was determined by a Quadrupole mass spectrometer (QMS) analysis conducted in the Laboratory for Earthquake Chemistry, University of Tokyo (LEC). Contents of CH_4, N_2, O_2, Ar, and CO_2 were measured comparing with analyses of synthesized standard gases. In the case that content of CO_2 in the R-gas sample was not negligible, the result of volumetry was corrected with it. Some total gas samples without alkali dissolution were also analyzed with QMS system and their results of CO_2 content were checked with volumetric results.

Gas chromatographic technique was employed for the analysis of H_2 content in several samples. These samples were also gas chromatically analysed for CH_4 and N_2 to check the QMS results. analysis. The gas chrmatographic analyses were conducted by Dr. F. Yanagisawa of ORI. In these cross checks, analytical results show agreement with each other.

The CO_2 and CH_4 in the aqueous phases were analyzed on the samples stored in glass vials. The CO_2 (by Dr. T.Gamo) and CH_4 analysis were conducted in ORI, using the gas chromatographic technique after purge of dissolved gas from the aqueous samples (Gamo and Horibe, 1980; Gamo et al., 1987a).

The He isotopic ratios of the R-gas samples were measured in LEC using a high resolution mass spectrometer, after purification of samples after Sano and Wakita (1988). The carbon isotopic ratios of CO_2 in the gaseous phases were measured in ORI, after releasing CO_2 from the $BaCO_3$ precipitates. The CO_2 in the aqueous phases were separated during the quantitative analysis with GC, and its isotopic composition was also measured in ORI by Dr. T. Gamo. The carbon isotopic ratios of CH_4 were measured on the CO_2 samples produced by combustion of the R-gases with CuO furnace at 800°C, by Mr. M. Tsutsumi of ORI. The H_2S was convereted to $BaSO_4$ for the gravimetric measurement of the concentrations as well as for the isotopic ratio measurements by Dr. E.-S. Kim of ORI.

Table 3-1. List of hydrothermal fluid samples

dive	sample name	site	temp.(°C)	Note
D413	RV1,2,3	Jade	<220	
	RV4,5,6	Jade	<220	
D414	AL	Jade	30-150	
	RV2,3	Jade	30-150	
D415	M	Jade		Bottom seawater[3]
D416	AL	Clam	90-100	
	RV1,2	Clam	90-100	
	RV4,5,6	Clam	90-100	
	M	Clam		Bottom seawater
D422	RV2,3	Jade	320±10	Only gas phase[4]
D423	RV2,3	Jade	320±10	
	RV4,5	Jade	30-150	
D424	RV4	Jade		Extracted gas from sediment[5]
	M	Jade		Liquid CO_2 bubble[6]
D426	RV3,5,6	Clam	90	
D427	RV1,3,5,6	Clam	90-100	
	M1	Clam		Bottom seawater above the vent
	M2	Clam		Bottom seawater
	M3	Clam		Bottom seawater

1) Samples listed in the same column were obtained in the same series of sampling procedure (see text)

2) Prefix of sample names indicates the equipment used for sampling as
   RV: Revolving valve sampler
   AL: Alvin type sampler
   M: Acrylic corer sampler

3) Bottom seawater including little amount of liquid CO_2 bubble

4) Aqueous phase were lost during sampling recovery due to pressure increase of gaseous phase.

5) Spontaneously extracted gas accumulated in the sample room, which probably originated from sediment in the inlet tube.

6) Evolved gas from liquid CO_2 bubble and hydrate

Table 3-2. Analytical methods of elemental components

element	method	precision
pH	electrode	3%
Li	ICP emission spectrophotometry	3%
Na	calculation from charge balance	5%
K	atomic absorption spectrophotometry	3%
NH_4	colorimetry (nitroprusside method)	10%
Mg	atomic absorption spectrophotometry	3%
Ca	atomic absorption spectrophotometry	3%
Sr	ICP emission spectrophotometry	3%
Ba	ICP emission spectrophotometry	3%
Mn	atomic absorption spectrophotometry	3%
Fe	ICP emission spectrophotometry	5%
B	ICP emission spectrophotometry	5%
Al	ICP emission spectrophotometry	5%
SO_4	ion chromatography	5%
Cl	ion chromatography	5%
Alk.	titration	5%
SiO_2	colorimetry (molybdate blue method)	10%

Table 3-3. Analytical methods for volatile components

component	phase	method
CO_2	gas	volumetry during the alkali dissolution
		QMS
	liquid	Gas chromatography after Gamo et al.(1980) [1]
CH_4	gas	QMS
	liquid	Gas chromatography after Gamo et al.(1987a)
H_2	gas	Gas chromatography [2]
He	gas	QMS
H_2S	gas	gravimetry [3]
	liquid	gravimetry [3]
$^3He/^4He$	gas	Mass spectrometry after Sano and Wakita (1988)
$\delta^{13}C(CO_2)$	gas	Mass spectrometry
	liquid	Mass spectrometry [1]
$\delta^{13}C(CH_4)$	gas	Mass spectrometry [4]

1) analyzed by Dr. T.Gamo
2) analyzed by Dr. F.Yanagisawa
3) analyzed by Dr. E.S. Kim
4) analyzed by Mr. M.Tsutsumi

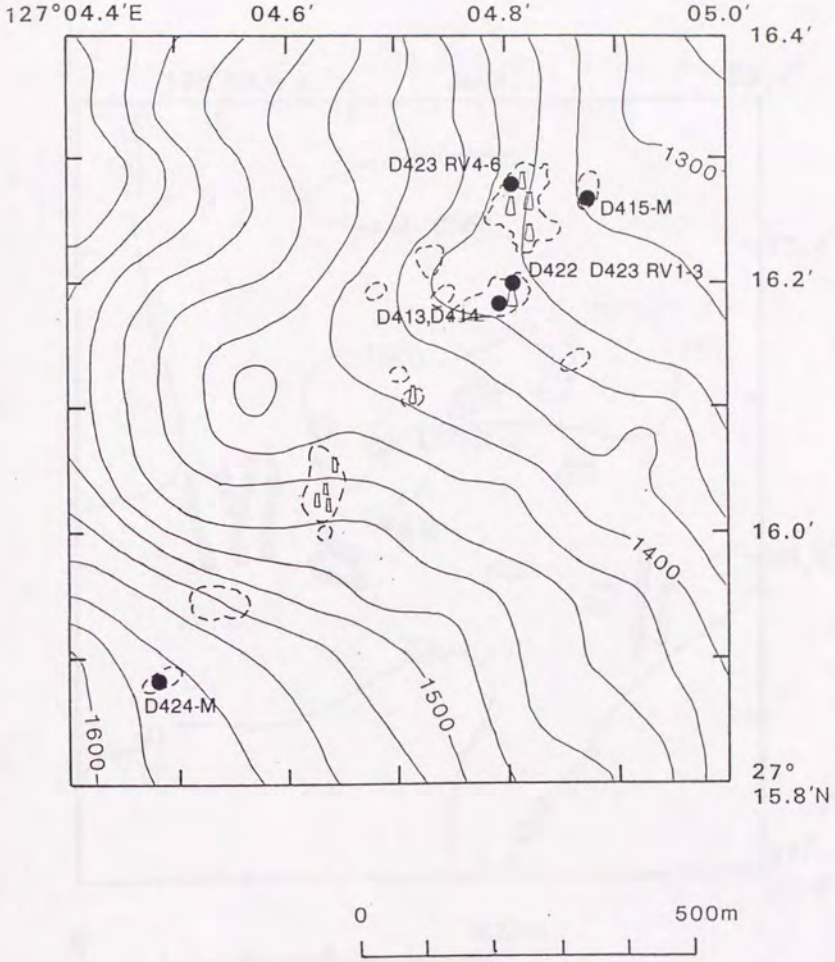

Fig. 3-1 Map showing sampling locations in the Jade site

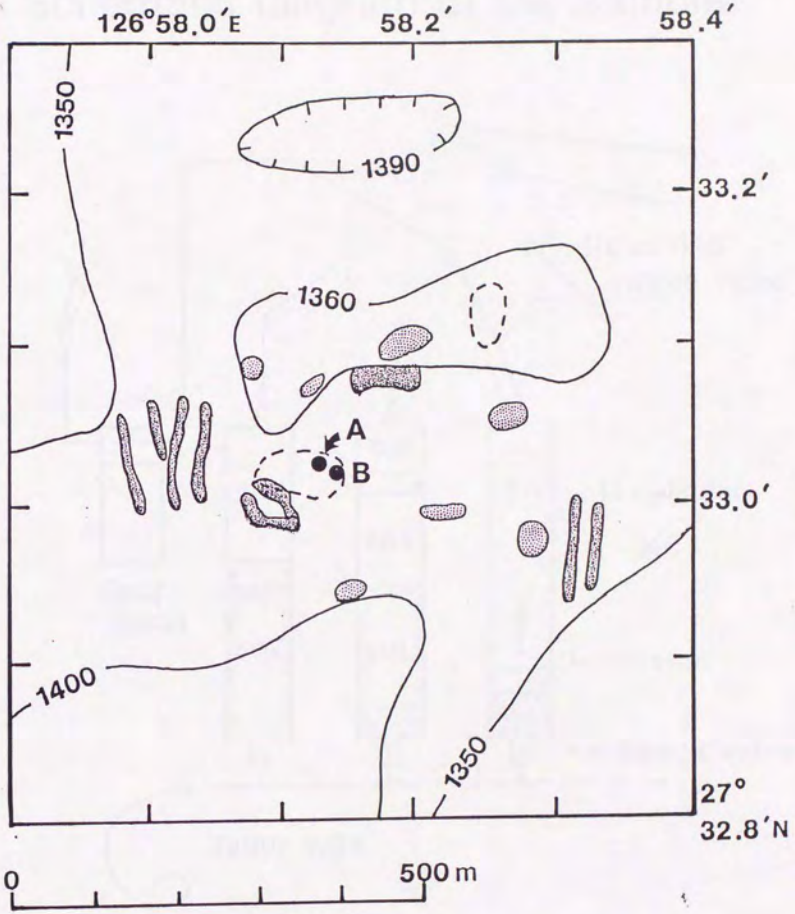

Site A: D416-AL,RV1,2 D426 D427

Site B: D416-RV4,5,6

Fig. 3-2 Map showing sampling locations in the Clam site

Schematic diagram of the sampler

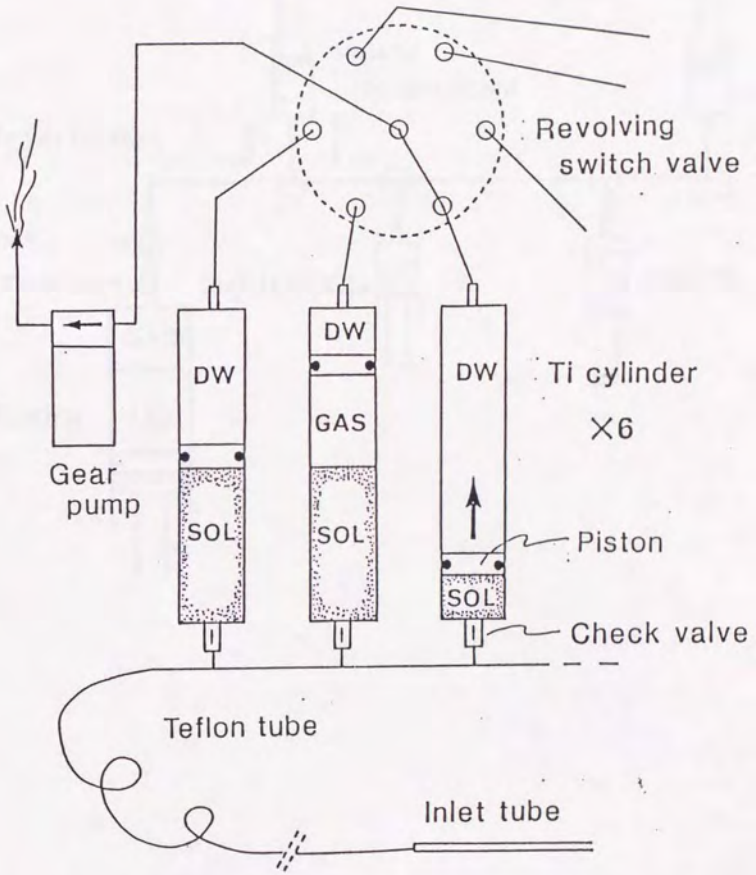

Fig. 3-3 Schematic diagram of the revolving valve sampler (Sakai et al., 1990c)

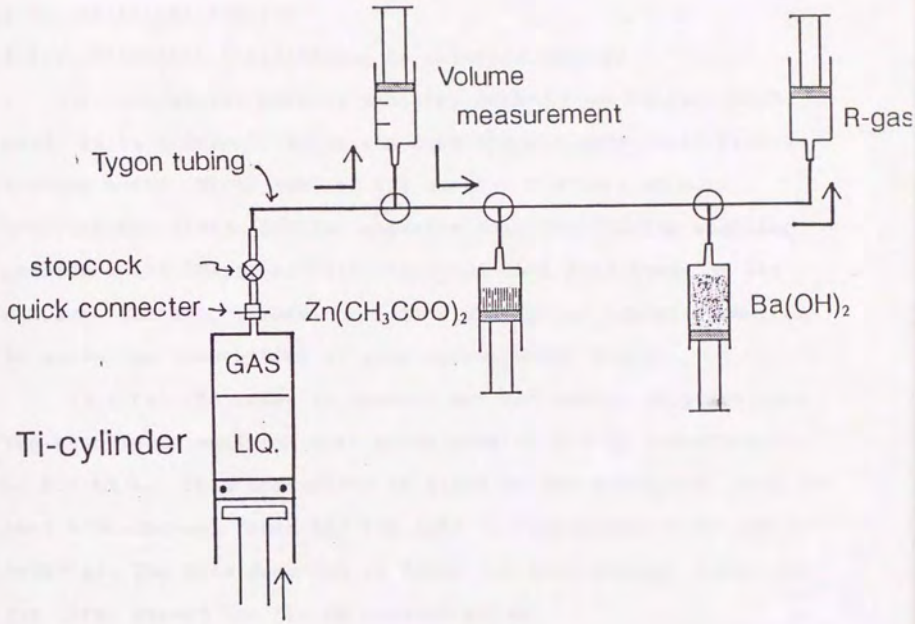

Fig. 3-4 Schematic diagram of transfer procedure of the evolved gas sample

Chapter 4.

Major and minor element compositions of the Jade and Clam site hydrothermal fluid

4-1. Analytical results

4-1-1. Elemental compositions in obtained samples

As long as the present sampling method (see Chapter 3) is used, it is difficult to obtain pure hydrothermal fluid from a venting point. Water samples are usually mixtures of pure hydrothermal fluid, ambient seawater entrained during sampling procedure and distilled water remained in a dead space of the sampler. Therefore, some correction and estimation are required to asses the composition of pure hydrothermal fluid.

At first, in order to correct for the sample dilution, all the results of analyses were normalized to the Cl concentration of 550 mM/kg. This correction is based on the assumption that the pure hydrothermal fluid has the same Cl concentration as ambient seawater. The data reported in table 4-1 were already corrected for this, except for the Cl concentration.

4-1-2. Estimation of the Jade fluid endmember

It is well established that the composition of an endmember hydrothermal fluid is estimated by extrapolation of Mg content to zero (Von Damm et al., 1985a). This conventional estimation is based on the presumption that the endmember hydrothermal fluid is Mg-free (see section 1-3) and that each component of the fluid is considered to be conservative in the mixing with ambient seawater during sampling.

In fig. 4-1, content of each component is plotted against Mg

content. All the components in the Jade fluid samples show good linear relationships, except for Ba. D423-RV3 was a sample obtained from the high temperature fluid of 320°C, which emanated from the "Black smoker". This sample contained Mg only of 1.1 mM/kg, supporting the presumption for the conventional endmember estimation. With respect to Ba, it is not conservative in the mixing of the fluid and seawater, probably due to precipitation of barite.

The least square fitting (LSQ) was employed for extrapolation to Mg = 0 as usual. At the first column in table 4-2, the estimated composition of the Jade endmember fluid is presented. At the second column, analytical result of D423-RV3 is listed for comparison. With respect to pH and Ba, the values in the second column were taken as values of the endmember.

4-1-3. Estimation of the Clam fluid endmember

Contrary to the Jade fluid, all of the Clam fluid samples show as low temperature as 100°C and as high Mg content as about 35 mM/kg. Moreover, the highest observed temperature was 220°C. It is not justifiable to adopt the conventional estimation method to the Clam fluid without discussion.

Fig. 4-2 illustrates the relationship between SO_4 content and $\delta^{34}S(SO_4)$ value of the Jade and Clam fluid samples. All the Jade fluid samples have constant $\delta^{34}S$ value identical to ambient seawater, supporting simple mixing between SO_4-free hydrothermal endmember and ambient seawater. However, the Clam fluid samples show remarkable enrichment in ^{34}S and negative correlation between $\delta^{34}S(SO_4)$ value and SO_4 contents. As mentioned above, the

conventional estimation method requires Mg and SO_4 free endmember. However, such endmember obviously could not constitute the SO_4 relationship observed in the Clam fluid samples. The Clam fluid endmember, if it exists, should contain a significant amount of ^{34}S-enriched SO_4.

Therefore, hydrothermal endmember should be decided on another basis. Sakai et al.(1990a) proposed a possible endmember according to the observed fluid temperature. On the assumption that the temperature of 220°C represents the minimum endmember temperature, its composition was estimated as Mg = 22±3 mM/kg and SO_4 = 10.0±0.3 mM/kg, respectively, according to extrapolation of relationship between observed temperature and Mg content.

However, this estimation seems to conflict with anhydrite solubility of fluid as illustrated in fig. 4-3. A dashed line indicates solubility product of anhydrite at each temperature estimated for hypothetical mixture between the Jade endmember fluid and ambient seawater. Due to the abundant SO_4 content in seawater and low anhydrite solubility at higher temperature, hydrothermal fluid becomes to be oversaturated with anhydrite practically in all the range of mixing. The endmember of 220°C, if exist, must show depletion in Ca and SO_4. However, this consideration does not agree with composition of the observed Clam fluid samples.

Therefore, the obtained samples which show temperature around 100°C are assumed to have experienced the last stage of hydrothermal interaction at such low temperature, and has not suffered mixing with ambient seawater during sampling procedure. As Gamo et al.(1991) has already noted, the Clam fluid samples do

not show so good lineation in Mg diagrams as the Jade fluid samples. Especially, components affected by fluid-sediment interaction such as pH, alkalinity and NH_3, show different relationships at each venting. This variable relationship would assure that low temperature interaction is characteristic to the Clam fluids.

Based on the above discussion, the endmember composition of the Clam fluid was not estimated here. D427-RV3 is taken as a representative of the Clam fluid based on its good condition during sampling and the lowest Mg content. Its chemical composition is listed at the forth column in table 4-2.

4-2. Elemental components in the Jade fluid

4-2-1. Comparison with the Mid Oceanic Ridge hydrothermal fluid

Table 4-3 compiled the chemical compositions of submarine hydrothermal fluids so far studied, including the Jade fluid. Fig. 4-4 illustrates comparison of cation composition between the Jade fluid and the EPR fluid (EPR21°N, OBS vent) as a representative of the MOR type fluids.

As discussed in Chapter 1, the chemical composition of submarine hydrothermal fluids is distinguished from that of seawater in (1) depletion of Mg, SO_4, (2) low pH, (3) enrichment in Ca, K and other cations, (4) significant enrichment in heavy metals, (5) high SiO_2 content, (6) existence of H_2S. The Jade fluid also shows all of these features.

It is also notable that, in some components, the Jade fluid shows enrichment or depletion beyond a range of variation so far observed in the MOR type fluids. High pH and alkalinity compared

to the EPR hydrothermal fluids are most characteristic and are similar to the fluid in the sediment-hosted Guaymas Basin. The Jade fluid is characterized also by higher contents of K, Li and Ba, and lower contents of trace metals such as Fe and Mn than the MOR fluids.

4-2-2. Physical properties

At the Jade site, the maximum observed temperature was 320°C. This value is comparable to those observed at other submarine hydrothermal systems (see table 4-3). As mentioned in Campbell et al.(1988b), 350°C seems to be the upper limit of exit temperatures of the submarine hydrothermal fluids, although it is not well confirmed what causes this restriction. The Jade fluid temperature is close to this limit, suggesting that it emanates immediately after hydrothermal interaction.

Fig. 4-5 illustrates a phase diagram of seawater (Bischoff and Rosenberg, 1985). As will be discussed in Chapter 5, the Jade fluid is significantly enriched in CO_2. Dissolved CO_2 would increase total vapor pressure and they would lower the boiling point of the Jade fluid. The partial pressure of CO_2 is calculated according to the CO_2 mole fraction in the Jade fluid and Henry's law coefficients (estimated from Ellis and Golding, 1963), and a boiling curve of the Jade fluid is estimated as a dashed line drawn in fig. 4-5.

The observed temperature of the Jade fluid on the seafloor is plotted as a cross mark. As is seen, it is located close to the boiling curve. Thus, it is not surprising if the Jade fluid would have experienced two phase separation during its ascent.

Such an example of boiling was reported at the Axial Seamount in the Juan de Fuca Ridge (Massoth et al., 1989; Butterfield et al., 1990). Chemical composition of boiling fluid is characterized by lower contents of Na and Cl than those of seawater. However, with respect to the Jade fluid, none of the major elements showed notable depletion (table 4-1), assuring that the Jade fluid has not experienced the boiling procedure, at least, at present.

4-2-3. Major element composition

a) Quartz solubility

Chemical equilibrium between co-existed fluid and minerals is considered as a principal mechanism which controls chemical composition of hydrothermal fluid (see section 1-3). The most simple example is an equilibrium between dissolved SiO_2 and quartz (Fournier et al., 1983) expressed as:

$$SiO_{2(quartz)} = SiO_{2(aq)} \quad \text{--- (4-1)}$$

Fig. 4-6, illustrates isopleths of quartz solubility in seawater. The SiO_2 content of the Jade fluid is close to saturation concentration of quartz at temperature of 305 - 315°C and at pressure higher than 150 bars. This result indicates that hydrothermal interaction occurred at such temperature and that the SiO_2 content is controlled by the quartz equilibrium at this temperature range. However, it is difficult to know information about depth of a reaction zone, because the SiO_2 solubility is not sensitive for pressure at this range of temperature.

b) Estimation of in-situ pH

In order to know with what minerals the fluid is equilibrated, in-situ pH and activities of major cations and

anions must be estimated. Although some computation programs have been developed (Reed, 1982; Arnorsson et al., 1982; Bowers et al., 1988), a simple, semi-quantitative procedure was adopted in this study. Details of whole procedure and the thermodynamic constants used are described in chapters 6 and 7 of Henley et al.(1984). Its outline is summarized below.

The first step is the estimation of in-situ pH at high temperature condition where hydrothermal interaction occurs. Using data of dissolution constants of aqueous weak acids and bases (Arnorsson et al., 1982) and activity coefficients of dissolved species (determined by Debye-Huckel algorithms), distribution of all species is determined at the temperature where pH was measured. And a charge balance is determined taking account of the measured pH value. Then, all species were redistributed at the high temperature condition. Thus, an in-situ pH value is determined uniquely. In the case where phase separation occurred prior to the pH measurement, degassed components must be taken into account in the redistribution procedure.

In this study, some steps are omitted to simplify the computation. The ionic strength of the fluid is fixed as 0.55 at 25°C and 0.45 at 300-350°C and an iteration of feedback steps is omitted. Uncharged species, hydroxide complexes, organic ligands, and organic acids are disregarded. And through the whole procedure, a correction for pressure effect is not considered.

The estimated pH of the Jade fluid at 300°C was 4.83. The temperature of estimation was set at 300°C to use thermodynamic

data without extrapolation. Distribution of principal weak acid-base species at this temperature is illustrated in fig. 4-7(a). This figure expresses that the Jade fluid has intense buffer capacity by NH_3-NH_4^+ dissociation. Although total CO_2 amount is larger than total NH_3 amount, dissociated species of bicarbonate and carbonate ion are less than an ammounium ion in the pH range of the Jade fluid.

In order to confirm the validity of the estimation procedure, in-situ pH values of some other hydrothermal fluids were calculated and comparison with reffered values are listed in table 4-4. The species distribution diagram for the EPR fluid is shown in fig. 4-7(b). Deviation between the estimated value by this study and the referred value was as high as 1.2 unit in pH. However, this is not desperate situation. Bowers et al.(1988) inferred that the estimated in-situ pH of the EPR fluid shifts from 3.5 to 4.5 by using modified thermodynamic data base. Even in the case of using a well-developed computation program, it is generally difficult to determine an absolute value of in-situ pH, due to large errors derived from chemical analyses (especially pH measurement at room temperature) and thermodynamic data set.

However, in the case of the Jade fluid, a unique principal dissociation equilibrium of NH_3-NH_4^+ represents buffer capacity of the fluid. This is likely to assure that the approximate procedure is enough applicable for the estimation of in-situ pH of the Jade fluid. In such condition, dissociations of other ion complexes have only fairly negligible effects, at least, in consideration for a relative shift of pH.

Consideration of calcite dissolution equilibrium would

provide another support for the estimated value of in-situ pH. Because of the abundant CO_2, the Jade fluid is expected to be equilibrated with calcite. Using the estimated in-situ pH and dissociation constants of carbonates, the solubility product of calcite in the Jade fluid is calculated to be logQ = -14.02. This is very close to the solubility of calcite of logK = -13.93 at 300°C, as shown in fig. 4-8. This result indicates agreement between two independently estimated pH values: one is based on the charge balance of fluid with dissociation constants of weak acid-base (especially NH_3 in this case) and another is on the contents of Ca and total CO_2 with an equilibrium constant of calcite dissolution.

c) Equilibrium between fluid and almino-silicates

Alteration reactions of feldspars to form clays are considered to be one of the principal fluid interactions involving primary almino-silicate minerals. For example, the equilibrium of the reaction:

$$3KAlSi_3O_8 + 2H^+ = KAl_3Si_3O_{10}(OH)_2 + 6SiO_2 + 2K^+ \quad \text{--- (4-2)}$$

K-feldspar K-mica quartz

which involves dissolved K^+ and H^+, would control the relationship between activities of these cations.

Fig. 4-9 illustrates activity diagrams in the system Na_2O-K_2O-Al_2O_3-H_2O. A plot of fluid composition on this diagram provides enough information on whether the fluid is equilibrated with each alteration reaction. Using the estimated value of in-situ pH and activity coefficients, activity ratios of $a(K^+)/a(H^+)$ and $a(Na^+)/a(H^+)$ of the Jade fluid are plotted in

Fig. 4-9. For comparison, data of some hydrothermal fluids listed in table 4-4 (using pH value on each reference) are also plotted.

All the fluids except for the Guaymas fluid, gather around the joint between K-feldspar, muscovite, albite and paragonite, although a large uncertainty in the calculation causes their scattering. This suggests that the equilibria of reactions between feldspars and the secondary minerals control contents of Na and K in the Jade fluid. Nakamura et al.(1990) described that secondary micas or mica/montmorillonite mixed layer minerals occurred at the center of the Jade hydrothermal field. This observation may provide further support for the estimation based on fluid composition.

Bowers et al.(1988) investigated several fluid interactions with minerals constituting the greenschist facies assemblage, and concluded that the EPR fluid compositions are controlled by the overall mineral equilibria among such assemblages. The above result for the Jade fluid agrees with a part of this conclusion.

d) factors regulating major cation composition

Enrichment in K content is one of the characteristics of the Jade fluid. Control of major element composition by fluid equilibria with minerals implies that calculative approach could reveal which mineral assemblages are responsible for the K enrichment of the Jade fluid. However, there would be little chance to obtain such conclusion by calculative approach due to incompletion and/or large uncertainty of thermodynamic data at present.

Difference in major fluid composition between the Jade and the MOR fluid may be attributed to difference in secondary

mineral assemblage with which fluid is equilibrated. Because formation of altered minerals is principally governed by precipitation from the fluid which has leached element from primary minerals and glass, it would be controlled by elemental abundance in the reactant rock. Enrichment in K of the Jade fluid may reflect a high K content in the reactant rock.

Table 4-5 compiles data of major cation compositions of natural hydrothermal systems and experimental seawater-rock interaction systems. Fushime (located in the Kyushu Island) is taken as a representative of a geothermal system within andesitic rocks (Yoshimura et al., 1985). As an indicator of cation composition, Sakai et al.(1990a) proposed "K-index" as K/(K+2Ca). In order to check its possible improper change due to calcite precipitation, Na/(Na+K) ratio is also listed in the same table.

These two factors in the fluids obtained by experimental fluid-rock interaction support the contention that the factor increases with increasing acidity of the rocks interacted. Based on this, it is possible to distinguish hydrothermal fluids interacted with acidic rocks from those interacted with basaltic rocks; The Jade fluid obviously belongs to the former group.

Sakai et al.(1990a) concluded that the reactant rock of the Jade fluid would be andesite based on their composition similar to the Fushime fluid. However, as shown in table 4-5, fluid-sediment interaction shows tendency of higher K-index, although its effect is not clear only from this data. Furthermore, not andesite, but rhyolitic and dacitic rocks were observed so far in the Izena Cauldron (Tanaka et al, 1990; Kato et al., 1989).

Further studies on fluid interaction with acidic rocks would be necessary to provide constraint on the reactant matter of the Jade hydrothermal site.

4-2-4. Control of pH and alkalinity

As was described in section 2-3, the Okinawa Trough hydrothermal system is located on seafloor favorable for the development of the sediment-hosted hydrothermal system. The Jade fluid shows characteristic signature, especially in pH and alkalinity, of hydrothermal interaction within sedimentary layer.

Thermal degradation of organic matter is one of such fluid-sediment hydrothermal interactions. It would be expressed in a simple scheme as:

$$(CH_2O)_{106}(NH_3)_{16}(H_3PO_4) = 53CH_3COOH + 16NH_3 + H_3PO_4 \text{ --- (4-3)}$$

where CH_3COOH is used to represent a complex assemblage of short chain hydrocarbons. Under an adequate condition, it tends to proceed to decarboxylation as:

$$CH_3COOH = CH_4 + CO_2 \text{ --- (4-4)}$$

As a result of total degradation, NH_3, CO_2 and CH_4 and other organic species were produced and they would be added into hydrothermal fluid. The thermal degradation is often accompanied with oxidation of organic matter, which can be expressed as:

$$CH_3COOH + 2O_2 = 2CO_2 + 2H_2O \text{ --- (4-5)}$$

As an oxidant, Fe^{3+} in rock and SO_4^{2-} in seawater would be available.

Another important reaction is dissolution or precipitation of calcite. Dissolution of calcite is expressed as:

$$CaCO_3 + 2H^+ = Ca^{2+} + H_2CO_3 \text{ --- (4-6)}$$

This dissolution equilibrium depends on pH of fluid. Increase in pH induces precipitation of calcite as shown in (4-6).

A shift of pH and alkalinity of fluid caused by fluid-sediment interaction is estimated using the pH estimation procedure described in the previous section. Values of pH and alkalinity of the fluids were calculated for given changes in CO_2 or NH_3. Results are illustrated in fig. 4-10.

Change of CO_2 content induces very little effect to both pH and alkalinity of the fluid (fig. 4-10(a)), because the fluid originally contains abundant CO_2 as H_2CO_3 of which dissociation is suppressed by NH_3-NH_4^+ buffer (see also fig. 4-7(a)). Change of NH_3 affects pH and alkalinity of the fluid (fig. 4-10(b)). A pH shift of 0.3 - 0.7 unit occurs for 1 mM change of NH_3 in 1 kg fluid. The shift in alkalinity is proportional to that of NH_3. Change of HCO_3^- ion induces shift in both pH and alkalinity; the effect is almost equivalent to that of NH_3 (fig. 4-10(c)). Dissolution of calcite is a model case for HCO_3^- addition into the fluid, while its precipitation represents HCO_3^- deduction. These reactions would be expressed as:

$$CaCO_3 = Ca^{2+} + CO_3^{2-} \quad \text{--- (4-7a)}$$

$$CO_3^{2-} + H_2CO_3 = 2HCO_3^- \quad \text{--- (4-7b)}$$

$$2NH_4^+ + 2HCO_3^- = 2NH_3 + 2H_2CO_3 \quad \text{--- (4-7c)}$$

In the Jade fluid, NH_3-NH_4^+ buffer quantitatively substitutes addition and deduction of HCO_3^- as expressed in (4-7c). Change of NH_4^+ is also estimated (fig. 4-10(d)), although no proper model reactions occur in hydrothermal fluid.

Based on the above estimation, thermal degradation of organic matter obviously is responsible for an increase of pH and

alkalinity of fluid mainly due to addition of NH_3. Total effect of the fluid-sediment interaction on the Jade fluid may be evaluated as below. At first, oxidation of organic matter accompanied by thermal degradation is unlikely, because it would induce a significant increase in fluid alkalinity which is not the case with the Jade fluid. Secondly, the most part of CO_2 was considered to be derived from magmatic source, as will be discussed in Chapter 5. And CO_2 change within a mM/kg range from fluid-sediment interaction does not affect fluid signature, as fig. 4-10(a) indicates. Therefore, the effect of organic degradation could be represented by that caused by addition of NH_3 into fluid. Fig. 4-11 indicates the result of pH and alkalinity shifts of the fluid caused by change in NH_3 content from 0 to 5.05 mM/kg.

Two possible models are selected for the simulation of fluid-sediment interaction. In the first case, the fluid is assumed to have been undersaturated with calcite through fluid-sediment interaction. In this model, NH_3 addition is only the changes to be considered. As shown in fig. 4-11(a), pH and alkalinity increased by NH_3 addition. Hypothetical Jade fluid which was free from fluid-sediment interaction has an alkalinity of -3.0 meq/kg and a pH of around 2.7. These values are significantly lower than those of the MOR fluids, suggesting the hypothetical fluid of this model is unlikely to exist.

The second simulation is based on the assumption of fluid saturation with calcite through fluid-sediment interaction. In this model, calcite deposition concurs with NH_3 addition. Results

are shown in fig. 4-11(b). Calcite precipitation of 2 mM/kg and alkalinity increase of 1 meq/kg occur with the addition of the addition of 5 mM/kg NH_3. And shift of pH is limited to less than 0.2 unit in this case. The hypothetical NH_3-free fluid show the pH and alkalinity comparable to the MOR fluids, with reasonable changes in Ca and CO_2.

Coupling of the NH_3 addition and calcite precipitation keeps the pH and alkalinity of fluid in a steady state, after once NH_3 addition led the pH into this range. Unless dissolved Ca is exhausted, NH_3 addition caused by thermal degradation of organic matter results in calcite precipitation only, without affecting the pH and fluid composition.

4-2-5. Minor element composition

Contents of "soluble element" such as Li and B in the fluid depend on the elemental abundance in the reactant rock and the W/R ratio of the interaction (see section of 1-4). The Jade fluid shows Li and B contents twice and ten times that of the EPR fluids, respectively. Due to lack of data about reactant rocks in the Jade hydrothermal system, no quantitative estimation can be made at present. The characteristically high B content might suggest an involvement of sedimentary matter.

Contents of heavy metals such as Fe and Mn in fluid would be significantly affected by factors such as pH, redox condition and fluid temperature. The Jade fluid shows Fe and Mn contents lower than the EPR fluids but comparable to the Guaymas fluids. This feature may be attributed to the high pH of the fluid which lowered solubility of these elements. However, it is notable that

the Jade fluid has ability to form sulfide mineral deposition on the seafloor in spite of this pH condition.

4-3. Elemental components in the Clam fluid

4-3-1. Comparison with the Jade fluid

The Mg diagrams (fig. 4-1) provide general signatures of the Clam fluid. In table 4-2, chemical composition of the Clam fluid is listed in comparison with hypothetical mixture between the Jade endmember and the ambient seawater at the same Mg content.

Major element composition of the Clam fluid seems to show good agreement with the hypothetical mixture. Components affected by fluid-sediment interaction show great difference from the hypothetical mixture.

4-3-2. Major element composition

Two reaction models are considered to explain major element composition of the Clam fluid. The first model is to assume that low temperature hydrothermal interaction at 100 - 200°C controls the Clam fluid composition. The second model presumes that the Clam fluid is a mixture between the high temperature hydrothermal fluid and entrained seawater and that it has been modified by fluid-sediment interaction at low temperature.

Major element composition favors the latter model. Simple mixing easily explains the Mg versus major elements linearity (fig. 4-1). This supports the model that the primary high temperature Clam fluid has almost the same major element composition as the Jade fluid and implies that the reactant rocks of the Clam site are acidic rocks similar to those at the Jade

site.

On the contrary, it is difficult to consider that only low temperature hydrothermal interactions between seawater and rocks are responsible for the fluid of such chemical composition. The formation of Mg-silicates accompanied with the cation exchange and anhydrite precipitation are the main reactions that take place at low temperature (see section 1-3). These reactions indeed proceed at as low temperature as 150°C (Seyfried and Bischoff, 1979) and only they control fluid composition until Mg and SO_4 is completely removed from fluid. Major element composition expected from cation exchanges seems to be different from the Clam fluid, supporting the mixing model.

4-3-3. Control of pH and alkalinity

Significantly high alkalinity in the Clam fluid, together with its enrichment in NH_3 and CH_4 and high pH, strongly suggest that fluid-sediment interaction is important in the interpretation of the Clam fluid composition.

In-situ pH of the Clam fluid (D427-RV3) at 100°C is calculated to be 5.10 (table 4-4), using the same procedures as described before. The shift of pH and alkalinity was also estimated for the Clam fluid and are illustrated in fig. 4-12. Effects caused by NH_3 and HCO_3^- with pH shift are less than those in the Jade fluid. As illustrated in fig. 4-7(c), the carbonate dissociation system provides a dominant buffer capacity of the Clam fluid over the NH_3-NH_4^+ system that has a smaller dissociation constant at low temperature than at high temperature of the Jade fluid. The Clam fluid seems to have strong buffer

capacity against the addition of species supplied by thermal degradation of organic matter due to the abundant H_2CO_3 in the fluid.

A mixing of the high temperature Jade type fluid and ambient seawater could not explain high alkalinity of the Clam fluid, because both endmembers have 0 - 2.5 meq/kg alkalinity. High alkalinity of the present Clam fluid should be induced by fluid-sediment interaction.

As shown in fig. 4-12, the alkalinity shift of the Clam fluid is proportional to addition of NH_3 or HCO_3^-. The NH_3 content of the Clam fluid is 3.93 mM/kg, which is not enough to explain high alkalinity (= 9.54 meq/kg) of the Clam fluid. Dissolution of 4-5 mM calcite per 1 kg fluid may also induce a necessary alkalinity increase. However, such an increase was not noticed in the Clam fluid. Therefore, thermal degradation and calcite dissolution are difficult to explain the high alkalinity of the Clam fluid.

4-3-4. Sulfate reduction during fluid interaction

Oxidation of organic matter during fluid-sediment interaction would induce fluid of high alkalinity. In the Clam fluid, SO_4 derived from seawater is available as an oxidant. The reaction can be expressed as:

$$(CH_2O)_{106}(NH_3)_{16}(H_3PO_4) + 53SO_4^{2-} + 106H^+ =$$
$$106CO_2 + 16NH_3 + 53H_2S + 106H_2O + H_3PO_4 \text{ --- (4-8)}$$

Chemical and isotopic compositions of sulfur species of the obtained samples are summarized in table 4-6. The stoichiometry of (4-8) indicates that 1 mM/kg reduction of SO_4 produces

2 meq/kg of alkalinity. The Clam fluid shows 6.2 mM/kg higher H_2S content and 1.0 mM/kg lower SO_4 content than the hypothetical mixture of the Jade type high temperature fluid and entrained seawater. The SO_4 reduced to form the excess H_2S of the fluid is enough to create the alkalinity of 9.54 meq/kg in the Clam fluid. Unbalance between the increase of H_2S and the decrease of SO_4 may be attributed to dissolution of anhydrite, which may also explain the slightly higher Ca content in the Clam fluid than the hypothetical fluid.

The sulfate reduction also raises pH of the fluid, but this effect would be compensated by the carbonate buffer system. Saturation of the Clam fluid with calcite at 100°C (see fig. 4-8) suggests that calcite precipitation also may have controlled the pH through the fluid-sediment interaction. It is difficult to simulate the total effect of fluid-sediment interaction as well as in the case of the Jade fluid, due to the large variation range of composition.

The isotopic compositions of sulfur species (table 4-6) would provide a strong support for the oxidation of organic matter coupled with sulfate reduction. The isotopic exchange equilibrium between SO_4 and H_2S in solution is expressed (Ohmoto and Lasaga, 1982) as:

$$1000*\ln\alpha(SO_4\text{-}H_2S) = 6.463*10^6/T + 0.56 \quad (T \text{ in K})$$

The fractionation at 100°C is calculated to be +47.0 per mill. The deviation of $\delta^{34}S(SO_4\text{-}H_2S)$ of the observed Clam fluid is +25.6 per mill, which means that isotopic equilibrium is not attained.

Therefore, kinetic isotope effect during reduction is considered to control the isotopic compositions of the fluid. Experimental study of SO_4 reduction at 100°C (Grineko et al., 1969) reported that $^{32}SO_4$ reacts faster than $^{34}SO_4$ with a factor of 1.019. Based on this result, $\delta^{34}S(SO_4)$ value at time t is estimated as (Ohmoto and Rye, 1979):

$$\delta^{34}S(SO_4)_{(t)} = \delta^{34}S(SO_4)_{(0)} + 1000 * (F^{(1-k)} - 1)$$

where F is the fraction of SO_4 remaining at time t, and k is kinetic effect. Assuming that k = 1.020, F = 0.835 and $\delta^{34}S(SO_4)_{(0)}$ = +20.7 per mill, $\delta^{34}S(SO_4)_{(t)}$ is calculated to be +24.3 per mill. This value agrees with the observed isotope ratio of +25.6 per mill of the Clam fluid.

On the same assumption, the $\delta^{34}S(H_2S)$ of produced H_2S is estimated as:

$$\delta^{34}S(H_2S)_{(t)} = \delta^{34}S(H_2S)_{(0)} + \{\delta^{34}S(SO_4)_{(0)} - \delta^{34}S(SO_4)_{(t)} * F\}/(1-F),$$

in the case of reduction in a closed system. Calculated $\delta^{34}S(H_2S)$ is +2.5 per mill. This value is in fair accord with the observed value of +1.4 per mill.

Both chemical and isotopic compositions of sulfur species of the Clam fluid are attributed to oxidation of organic matter by sulfate reduction during fluid-sediment interaction at low temperature.

4-3-5. Minor element composition

Both Li and B in the Clam fluid show higher contents than those in the Jade fluid at the same Mg content. An enrichment factor of each specie is estimated from table 4-2 as the ratio of

its content in the Clam fluid to that in the Jade fluid at Mg = 35.0 mM/kg. The enrichment factors for Li and B are very close to each other (Li=2.00, B=1.95).

Since these elements behave as "soluble elements", their higher contents in the Clam fluid than the Jade fluid suggests that W/R ratios in the Clam system is smaller than the Jade fluid. Common enrichment factors of about 2.0 in Li and B imply that the W/R ratio of the Clam fluid is about half that of the Jade fluid. This explanation is accordance with the difference in the geological settings of two sites. While the Jade site is located on the slope of the cauldron wall, the Clam site is at the bottom of the depression. This implies thicker sedimentary layer at the Clam site induces fluid interaction with sediment at lower W/R ratio.

The Clam fluid shows substantially a lower Fe content than the Jade fluid. Other sulfide-forming metal elements in the Clam fluid show similar depletion (Shitashima, K. unpublished data). These may be attributed to the lower solubility of these elements at lower temperature and/or at higher pH of the Clam fluid. Only Mn in the Clam fluid shows the higher content than in the Jade fluid, which may be attributed to reductive condition of the Clam fluid as will be discussed in Chapter 5.

4-4. Summary

The Jade hydrothermal fluid shows a high vent temperature of 320°C and the major element composition similar to the MOR hydrothermal fluids. The Jade fluid is in equilibrium with quartz

and calcite, and probably with feldspars and their altered minerals at high temperature condition. This suggests that these overall fluid equilibria with minerals control the major element composition. The K content in the Jade fluid is nearly twice that in the MOR fluid. This high K content in the Jade fluid is explained as being due to interaction between seawater and acid volcanic rocks, rather than interaction between seawater and basaltic rocks. High contents of Li and B in the Jade fluids is also attributed to similar fluid-rock interaction as the major element composition.

Other components of the Jade fluid are affected obviously by fluid-sediment interaction. Thermal degradation of organic matter contributes NH_3 to fluid, which coupled with calcite saturation, controls pH and alkalinity of the Jade fluid within a narrow range in spite of high NH_3 content.

The Clam fluid does not show high temperature as the Jade fluid. The Mg and SO_4 contents and sulfur isotopic composition of SO_4 suggests that the Clam fluid is formed by mixing between high temperature hydrothermal fluid and entrained seawater and that the mixed fluid has experienced fluid-sediment interaction at low temperature.

Major element composition of the Clam fluid supports this mixing model. It implies that the primary high temperature fluid had similar composition to the Jade fluid. It is also notable that its major element composition is not significantly modified after mixing.

Significantly high alkalinity of 9.54 meq/kg of the Clam fluid indicates oxidation of organic matter during fluid-sediment

interaction. Chemical and isotopic compositions of sulfur species of the Clam fluid support that SO_4 in entrained seawater acts as an oxidant of organic matter. Buffering capacity by dissolved carbonate species and dissolution-precipitation equilibrium of calcite would control pH of the Clam fluid. Depletion of metal elements in the Clam fluid compared to the Jade fluid may be attributed to lower temperature and/or higher pH.

Table 4-1 Analytical results of elemental composition of the obtained samples

DIVE	Sample	Cl (mM)	Mg (mM)	Li (uM)	Na (mM)	K (mM)	NH4 (mM)	Ca (mM)	Sr (μM)	Ba (μM)
Jade site										
D413	RV1	293	58.5	65	----	14.2	----	12.8	103.4	2.66
	RV2	507	50.5	130	----	14.5	0.31	11.5	93.0	4.64
	RV3	523	50.8	100	462.8	13.4	0.24	11.4	89.4	3.47
	RV4	518	43.7	345	----	22.2	0.92	13.1	92.4	3.05
	RV6	515	43.1	398	458.1	24.0	1.04	13.5	98.0	3.87
D414	RV2	476	53.1	166	457.8	17.1	0.43	12.9	98.2	3.94
D423	RV2	484	21.5	1029	450.5	46.0	3.48	18.5	97.4	4.39
	RV3	528	1.1	1869	428.5	73.6	5.07	22.9	115.3	60.64
	RV4	358	38.1	----	----	16.0	0.46	11.0	----	----
	RV5	500	46.4	281	464.9	19.6	0.61	13.0	91.6	2.61
D424	RV2	103	44.0	----	477.6	10.8	----	10.3	----	2.24
Clam site										
D416	AL	516	48.7	443	463.6	18.5	1.60	13.0	87.6	2.59
	RV1	285	40.9	793	----	26.9	----	14.7	89.4	4.29
	RV2	474	41.3	984	453.9	28.8	3.10	15.8	87.5	4.08
	RV4	521	39.6	513	----	18.0	1.77	12.0	76.2	2.81
	RV5	514	46.1	531	459.9	20.0	1.85	13.3	86.0	4.40
	RV6	513	50.3	184	468.3	12.8	0.62	11.2	86.9	1.91
	M	551	53.0	20	476.7	9.9	0.01	10.6	86.1	0.10
D426	RV5	364	----	----	----	7.5	----	5.4	----	----
	RV6	373	40.3	936	457.0	27.6	3.73	15.4	84.9	6.32
D427	RV1	514	35.5	1296	459.9	32.0	4.56	16.0	83.3	4.42
	RV2	266	36.8	1139	----	33.1	----	13.7	87.9	8.97
	RV3	510	35.0	1300	458.2	31.9	3.92	16.1	82.7	3.76
	RV6	524	33.8	1288	450.3	31.8	4.01	15.6	79.8	3.91
	M-1	665	38.9	385	----	14.6	1.53	10.4	69.4	2.09
	M-2	551	53.2	18	473.5	10.2	0.00	10.4	85.3	0.13
	M-3	554	53.4	18	473.3	10.0	0.00	10.5	85.1	0.14

Table 4-1 Analytical results of elemental composition of the obtained samples (continued)

DIVE	Sample	Cl (mM)	Mg (mM)	Mn (μM)	Fe (μM)	B (mM)	Al (μM)	SO4 (mM)	AT (meq)	SiO2 (mM)	pH
Jade site											
D413	RV1	293	58.5	----	----	----	----	28.3	----	----	5.44
	RV2	507	50.5	26.8	1.77	0.635	0.72	25.2	1.96	1.5	5.01
	RV3	523	50.8	20.8	1.42	0.590	0.05	24.3	2.36	1.1	5.09
	RV4	518	43.7	70.5	----	----	----	22.0	2.40	3.5	4.89
	RV6	515	43.1	81.8	2.28	1.110	0.94	21.8	2.35	3.4	4.87
D414	RV2	476	53.1	35.2	1.87	0.742	0.35	27.3	2.51	2.1	5.47
D423	RV2	484	21.5	213.7	11.58	2.040	2.94	12.8	1.93	6.5	4.77
	RV3	528	1.1	374.3	21.65	3.444	4.83	0.0	1.92	12.9	4.72
	RV4	358	38.1	----	----	----	----	26.4	----	1.5	5.08
	RV5	500	46.4	55.0	2.27	0.836	1.79	25.6	2.37	1.8	4.90
D424	RV2	103	44.0	----	----	----	----	23.5	----	----	5.21
Clam site											
D416	AL	516	48.7	166.8	2.48	1.302	1.45	25.4	5.33	4.3	5.60
	RV1	285	40.9	----	----	----	----	20.6	----	----	5.49
	RV2	474	41.3	371.9	11.64	2.406	30.41	18.8	10.30	6.3	5.63
	RV4	521	39.6	195.8	0.00	----	----	19.6	6.04	4.6	5.50
	RV5	514	46.1	313.2	9.09	1.285	13.88	22.7	3.94	3.2	5.30
	RV6	513	50.3	108.5	3.48	0.726	1.72	25.8	2.51	1.4	5.39
	M	551	53.0	1.0	2.31	0.408	2.40	30.7	2.28	0.5	7.31
D426	RV5	364	----	----	----	----	----	----	----	----	5.27
	RV6	373	40.3	380.1	2.97	2.200	1.61	19.6	7.64	4.0	5.33
D427	RV1	514	35.5	506.7	2.38	2.734	1.25	18.4	9.41	5.2	5.42
	RV2	266	36.8	532.1	----	----	----	19.4	----	----	5.23
	RV3	510	35.0	508.7	2.48	2.770	0.86	17.0	9.52	5.6	5.42
	RV6	524	33.8	----	2.51	2.976	0.85	16.2	----	5.3	----
	M-1	665	38.9	131.3	9.64	1.000	0.28	20.2	4.43	1.6	5.31
	M-2	551	53.2	0.3	0.91	0.420	0.30	29.3	2.32	0.1	6.42
	M-3	554	53.4	0.2	1.13	0.427	0.61	29.5	2.31	0.1	7.07

Table 4-2 Estimated composition of the Jade and Clam fluid

component	unit[1]	method	Jade LSQ[2]	Jade D423-RV3	Jade mix [3]	Clam D427-RV3	Seawater[4]
T	°C		320	320	120	100	3.8
pH / 25°C			(4.7)	4.72	---	5.42	7.31
Li	uM	ICP	1858	1869	653	1300	33.2
Na [5]	mM	calc.	430	428	454	458	467
K	mM	AA	73.7	73.6	32.5	31.9	11.4
NH_4	mM	color.	5.32	5.06	1.84	3.93	0.04
Mg	mM	AA	0.0	0.0	35.0	35.0	53.0
Ca	mM	AA	23.2	22.9	15.2	16.1	11.1
Sr	uM	ICP	112	115	97.5	82.7	89.7
Ba	uM	ICP	(60)	60	-----	3.8	0.1
Mn	uM	AA	375	374	132	508	7.6
Fe	uM	ICP	21.3	21.6	7.06	2.48	0.0
B	mM	ICP	3.41	3.44	1.47	2.77	0.48
Al	uM	ICP	4.88	4.83	1.93	0.86	0
SO_4	mM	IC	0.5	0.0	18.0	17.0	26.9
Cl [6]	mM	IC	550	550	550	550	550
AT [7]	meq	titr.	1.88	1.92	2.20	9.54	2.32
CO_2	mM	[8]	207.3	208.9	73.4	88.7	2.4
H_2S	mM	[8]	13.1	13.6	4.15	9.44	0
SiO_2	mM	color.	12.5	12.9	4.8	5.6	0.8

1) all units are in per kg
2) values in parenthies are analytical results of D423-RV3 sample
3) hypothetical fluid mixture of the Jade endmember and seawater
4) values estimated by the LSQ calculation (assumed as Mg= 53.0 mM/kg)
5) Na content is calculated from charge balance
6) Cl content is assumed as constant in all samples
7) titration alkalinity
8) from chapter 5

Table 4-3 Compilation of endmember fluid composistion of submarine hydrothermal systems (extracted from Von Damm, 1990)

component		Okinawa Jade	EPR21°N OBS(1)	EPR21°N OBS(2)	EPR13°N No.2	EPR11°N No.4	SJFR plume	MAR MARK-1	Guaymas Vent 4	Mt. Axial VM	Seawater
T	(℃)	350	350	350	354	347	224	350	315	299	
pH(25°C)		4.7	3.4	3.4	3.1	3.1	3.2	3.9	5.9	3.4	7.8
Li	μM	1858	926	926	592	884	1720	843	873	204	26
Na	mM	430	432	439	551	472	796	510	485	159	464
K	mM	73.7	23.5	23.2	27.5	32	51.6	23.6	40.1	7.6	9.8
Rb	μM		28		19	24	37	10.5	66.0		1.3
NH_4	mM	5.32	<0.01						12.9		<0.01
Be	nM		15				95	38.5	29		0.0
Mg	mM	0	0	0	0	0	0	0	0	0	52.7
Ca	mM	23.2	15.6	15.6	53.7	22.5	96.3	9.9	34.0	10.2	10.2
Sr	μM	112	81	76	182	80	312	50	226		87
Ba	μM	60	8						54		0.14
Mn	mM	0.37	0.96	1.02	2.39	0.76	3.59	0.49	0.139	0.162	<0.001
Fe	mM	0.021	1.66	1.53	10.3	6.47	18.7	2.18	0.077	0.007	<0.001
Zn	μM		106		5	105	900	50	19	2.3	0.01
Pb	nM		308		27	50			230	101	0.01
B	mM	3.41	0.50				0.49	0.51	1.57	0.50	0.416
Al	μM	4.88	5.2		19.8	12.9	1.9	5.3	3.7		0.020
SO_4	mM	0	0.5	0	0	0	-0.5	0	0.06	0	27.9
Cl	mM	550	489	500	712	563	1090	559	599	188	541
Br	mM			0.80	1.15	0.94	1.83	0.84	1.06	0.24	0.840
alk.	meq	+1.88	-0.4	-0.54	-0.73	-1.02		-0.064	+8.10	+0.58	+2.3
SiO_2	mM	12.5	17.6	17.6	19.4	18.8	23.3	18.2	13.8	13.5	0.16
H_2S	mM		7.30	7.6	8.2	8.0	3.5	5.9	4.8	19.5	0
CO_2	mM		(5.72)						(21)	160	2.3

all unit are in per kg

Data References

EPR21°N (1): East Pacific Rise 21°N, OBS vent (Von Damm et al. 1985a)
EPR21°N (2): Resampling of OBS fluid 4 years after (1) (Campbell et al., 1988a)
EPR13°N : East Pacific Rise 13°N, vent No.2 (Bowers et al., 1988)
EPR11°N : East Pacific Rise 11°N, vent No.4 (Bowers et al., 1988)
SJFR : Southern Juan de Fuca Ridge, plume vent (Von Damm et al., 1987)
MAR : Kane fracture at the Mid Atlantic Ridge (Campbell et al., 1988)
Guaymas : Guaymas Basin, vent 4 (Von Damm et al., 1985b)
Mt. Axial : Axial seamount at the Juan de Fuca Ridge, VM (Massoth et al., 1989)

B data are from Spivack and Edmond (1987)
Br data are from Campbell and Edmond (1989)
References of CO_2 data are noted in table 5-4

Table 4-4 Results of in-situ pH estimation

Site	fluid	measured pH	in-situ pH	temp.* (°C)	reference
Okinawa	Jade	4.73	4.83	300	
	Clam	5.42	5.10	100	
EPR21°N	OBS	3.4	3.65	350	
			3.54		1)
			4.47		2)
Guaymas	vent 4	5.9	5.23	300	
			6.47		1)
Experimental fluid		6.19	4.9	300	
			5.1		3)

* temperature at which pH is estimated

1) Bowers et al.(1985)
2) Bowers et al.(1988)
3) Thornton and Seyfried (1987)

Table 4-5 Cation compositions of various hydrothermal fluids

		Rock type	Na (mM/kg)	K (mM/kg)	Ca (mM/kg)	K/(K+Na)	K/(K+2Ca)
Jade			430	73.7	23.2	0.146	0.614
Clam			442	47.9	19.9	0.098	0.546
Fushime	1)	andesite	408	65.0	22.3	0.137	0.593
Experiment	2)	andesite	469	48.0	13.8	0.093	0.635
	3)	andesite	468	28.6	36.5	0.058	0.281
	4)	rhyolite	525	60.1	6.7	0.103	0.818
	5)	rhyolite	562	55.0	6.9	0.089	0.799
Guaymas Basin	6)	sediment	485	43.1	34.0	0.082	0.388
Experiment	7)	sediment	405	31.7	23.7	0.073	0.401
EPR 21°N	8)	basalt	432	23.2	15.6	0.051	0.426
EPR 13°N	9)	basalt	551	27.5	53.7	0.048	0.204
EPR 11°N	10)	basalt	472	32.0	22.5	0.063	0.416
Juan de Fuca	11)	basalt	661	37.3	84.7	0.053	0.180
Experiment	12)	basalt	477	12.5	20.4	0.026	0.235
	13)	diabase	455	11.7	28.2	0.025	0.172

1) borehole fluid sample from the geothermal well named C in the table 1 of Akaku et al.(1988)
2) T=300 °C, P=1000 bars, W/R=2.3 (Shiraki et al., 1987)
3) average of 3 runs; T=300 °C, P=1000 bars, W/R=5 (Hajash and Chandler, 1985)
4) T=300 °C, P=1000 bars, W/R=5.1 (Shiraki et al., 1987)
5) average of 4 runs; T=300 °C, P=1000 bars, W/R=5 (Hajash and Chandler, 1985)
6) fluid from the vent No.4 (Von Damm et al., 1985b)
7) T=350 °C, P=500 bars, W/R=3 (Thornton and Seyfried, 1987)
8) fluid from the OBS vent (Von Damm et al., 1985a)
9) fluid from the vent No.2 (Bowers et al, 1988)
10) fluid from the vent No.4 (Bowers et al., 1988)
11) fluid from the vent No.1 (Von Damm et al., 1987)
12) T=300 °C, P= 500 bars, W/R=10 (Seyfried and Bischoff, 1981)
13) T=300 °C, P= 500 bars, W/R=10 (Seyfried and Bischoff, 1981)

Table 4-6 Chemical and isotopic composition of sulfur species of the Jade and Clam samples (modified from Gamo et al.1991)

Sample	SO_4 (mM/kg)	$\delta^{34}S(SO_4)$ (per mill CDT)	H_2S (mM/kg)	$\delta^{34}S(H_2S)$ (per mill CDT)	alkalinity (meq/kg)
Jade site					
D413 RV6	21.8	20.6	4.10	7.7	2.35
D423 RV2	12.8	20.7	7.96	7.6	1.93
D423 RV3	0.0		13.66	7.4	1.92
Clam site					
D416 RV2	18.8	25.7	7.10	-0.2	10.30
D416 RV5	22.7	21.4	3.73	3.0	3.94
D426 RV6	19.6	24.0	7.54	0.9	7.64
D427 RV3	17.0	25.6	9.44	1.4	9.52
hypothetical fluid					
mixture	18.0	20.7	4.16	7.6	2.20

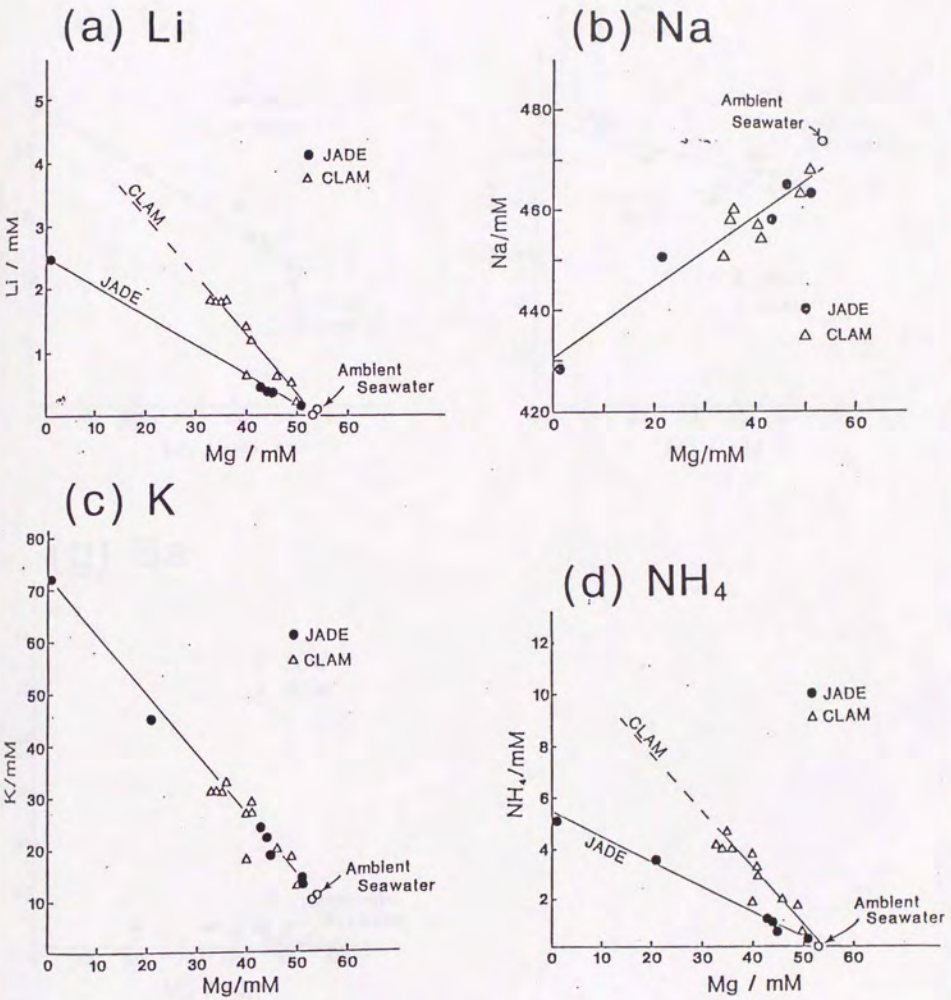

Fig. 4-1 Relationship between concentration of each component and Mg for the obtained samples

(a) Li vs Mg, (b) Na vs Mg, (c) K vs Mg, (d) NH4 vs Mg

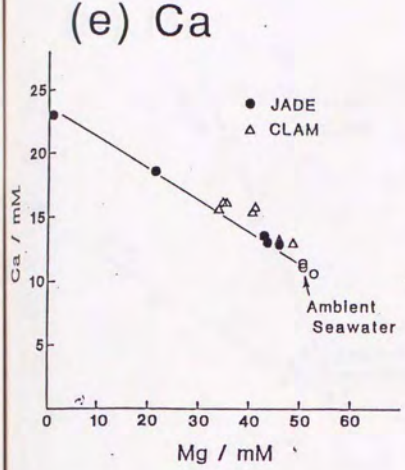

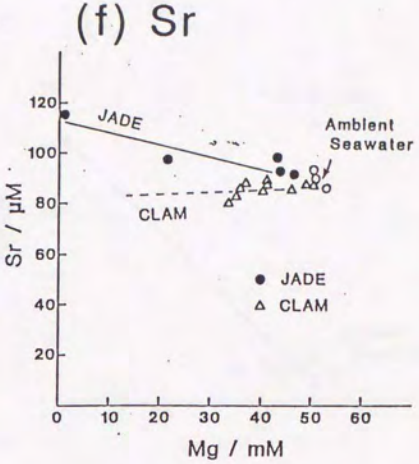

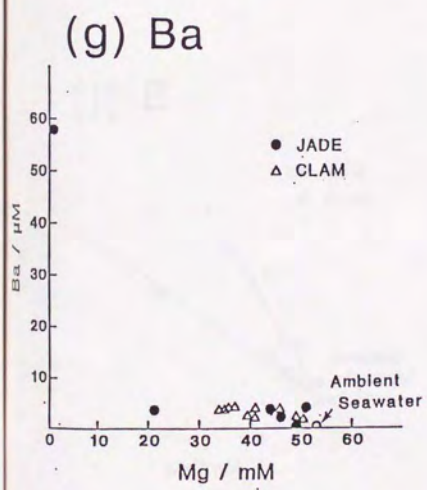

Fig. 4-1 Relationship between concentration of each component and Mg for the obtained samples (continued)

(e) Ca vs Mg, (f) Sr vs Mg, (g) Ba vs Mg

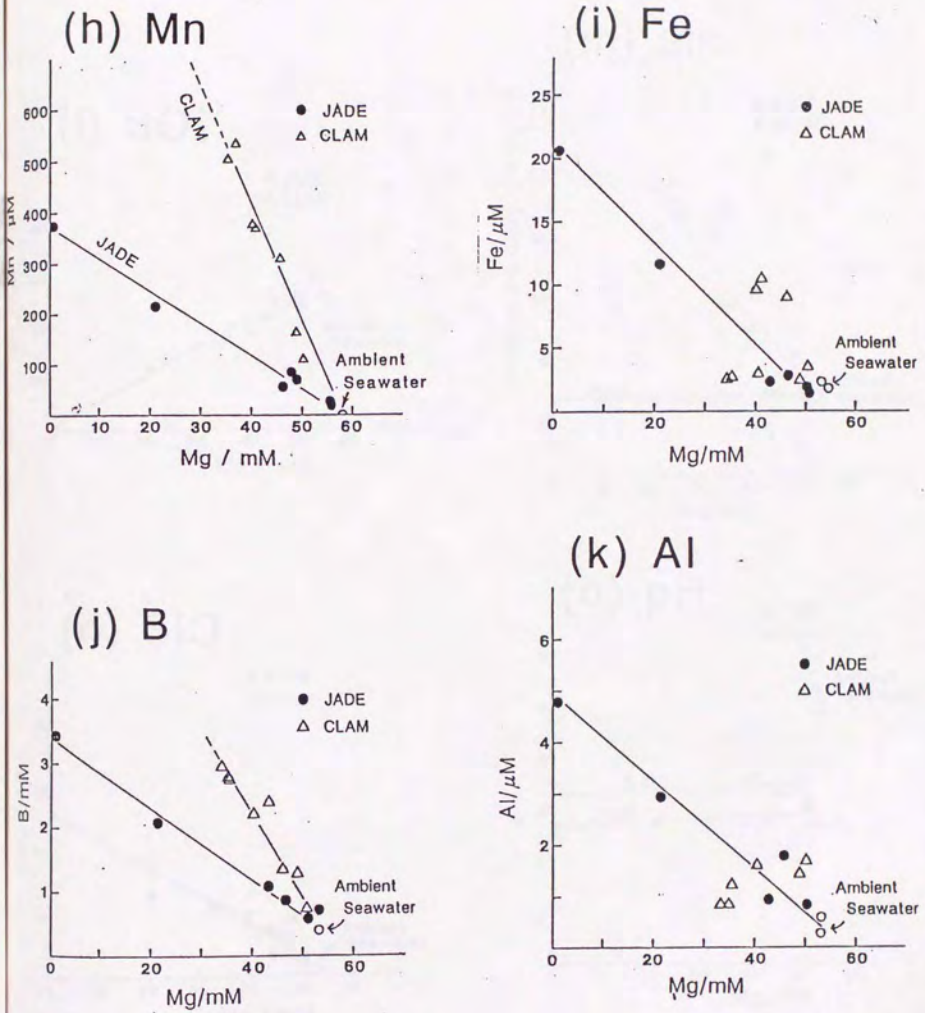

Fig. 4-1 Relationship between concentration of each component and Mg for the obtained samples (continued)

(h) Mn vs Mg, (i) Fe vs Mg, (j) B vs Mg, (k) Al vs Mg

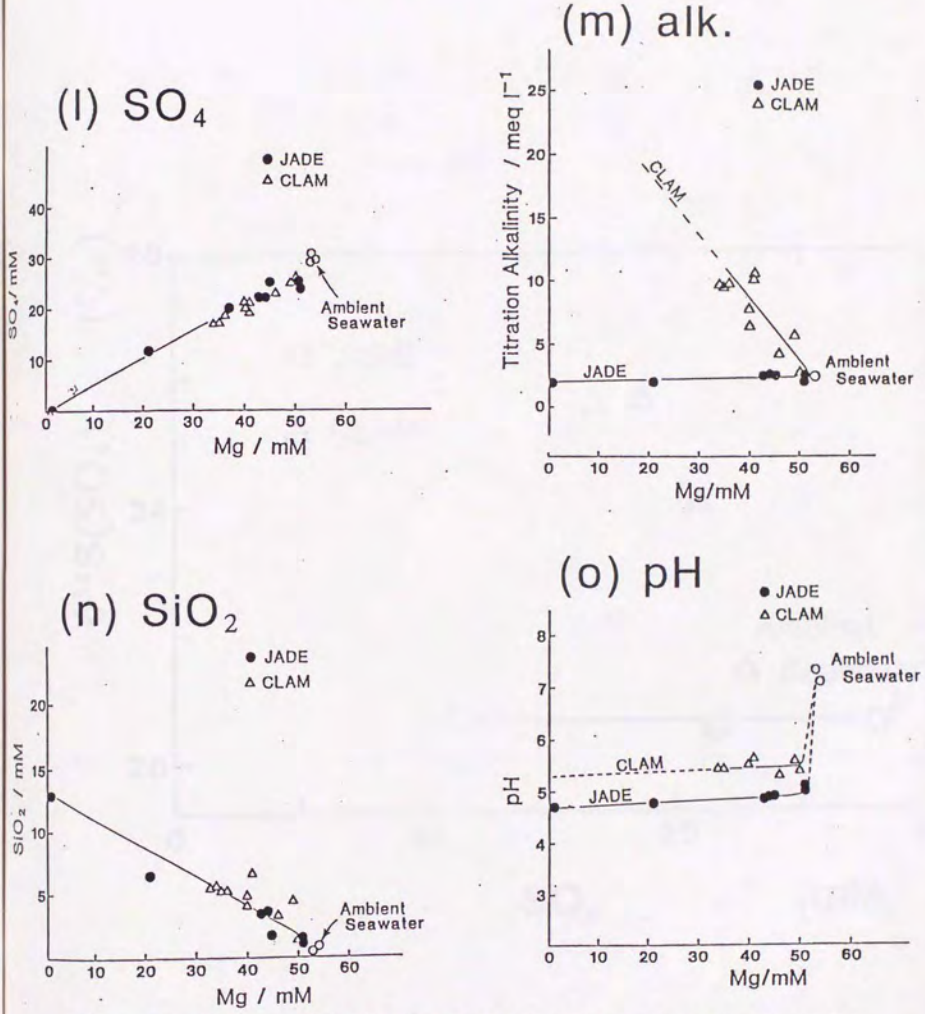

Fig. 4-1 Relationship between concentration of each component and Mg for the obtained samples (continued)

(l) SO_4 vs Mg, (m) alkalinity vs Mg, (n) SiO_2 vs Mg, (o) pH vs Mg

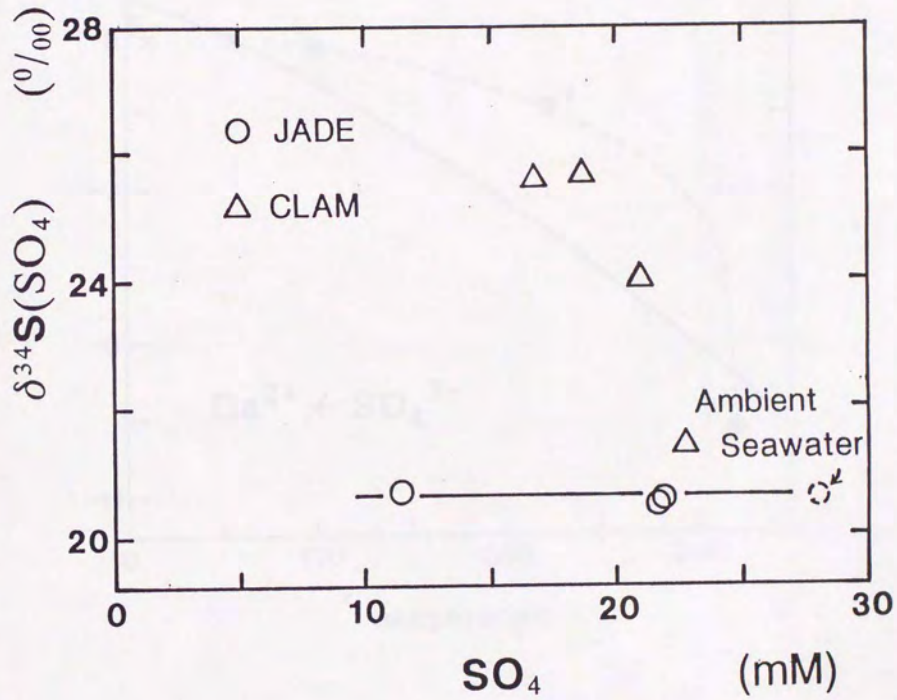

Fig. 4-2 Relationship between SO_4 concentration and its isotopic composition (modified from Gamo et al., 1991)

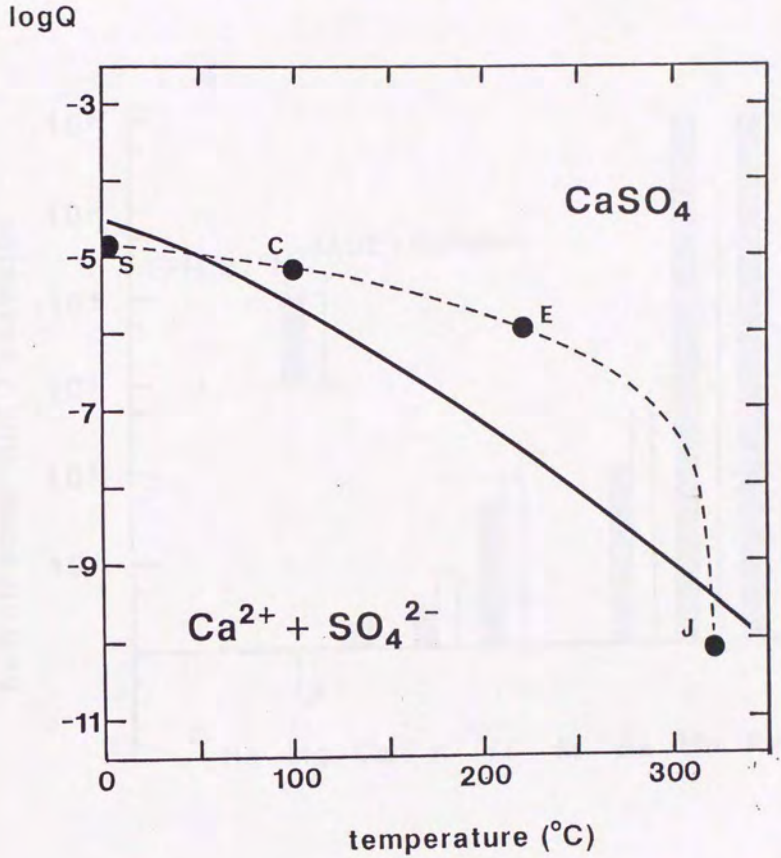

Fig. 4-3 Solubility curve of anhydrite

A dashed line indicates anhydrite solubility products of hypothetical mixture at its temperature

A Circle plots solubility product of each fluid as
S: Seawater, C: D427-RV3, J: D423-RV3,
E: The estimated endmember by Sakai et al.(1990a)

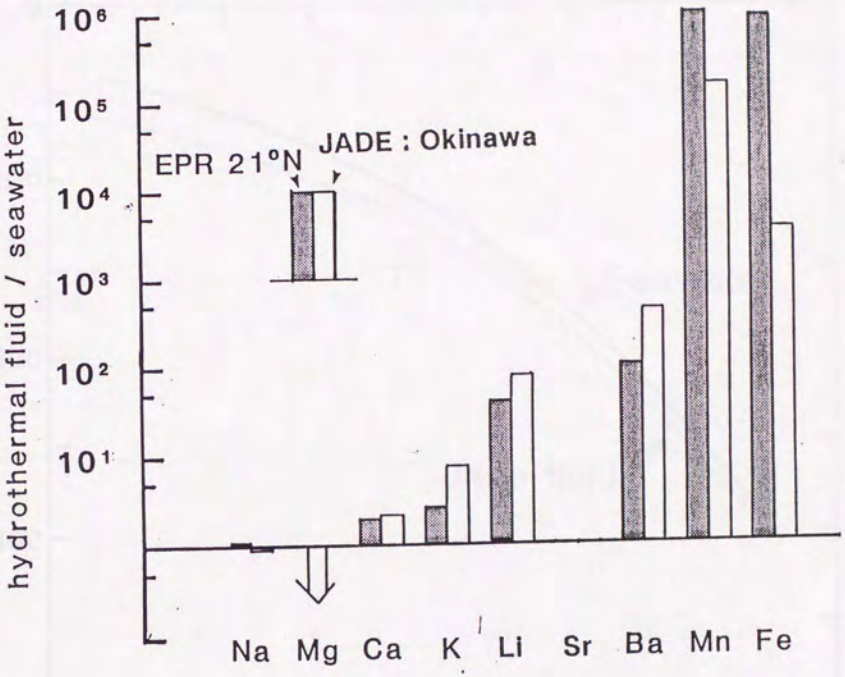

Fig. 4-4 Comparison of hydrothermal fluid composition between the Jade fluid and the EPR 21°N fluid.

Ratios of each content to that of seawater are expressed in logarithm scale.

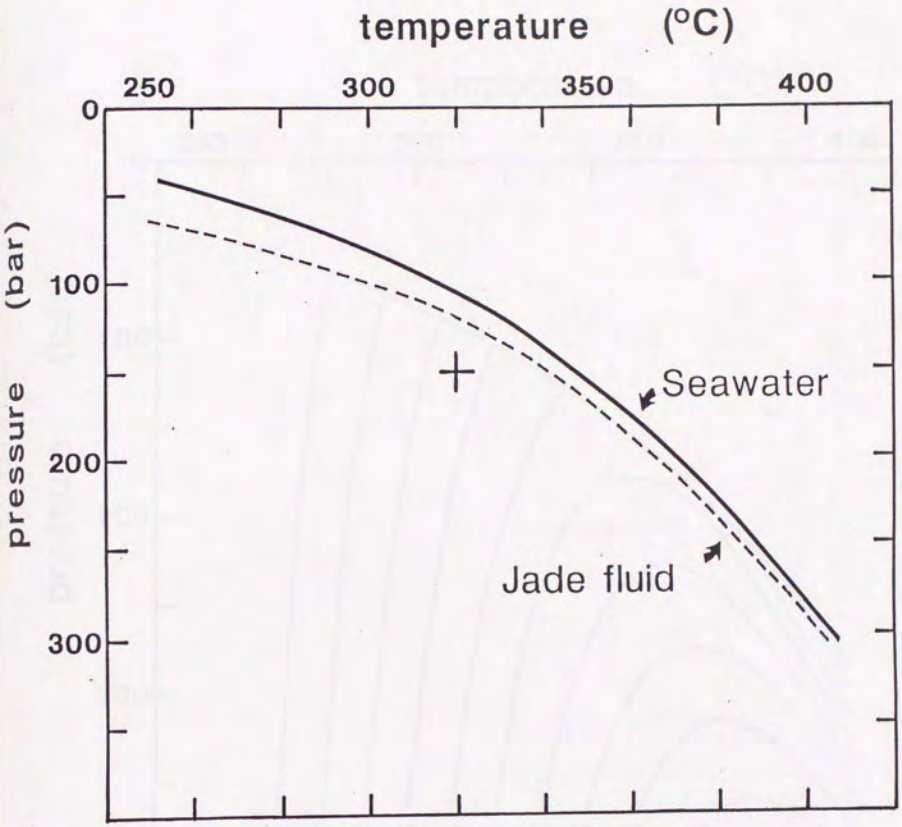

Fig. 4-5 A boiling curve of seawater and the Jade fluid (calculated from Bischoff and Rosenbauer, 1985)

A dashed line indicates a boiling curve of the Jade fluid considering CO_2 content

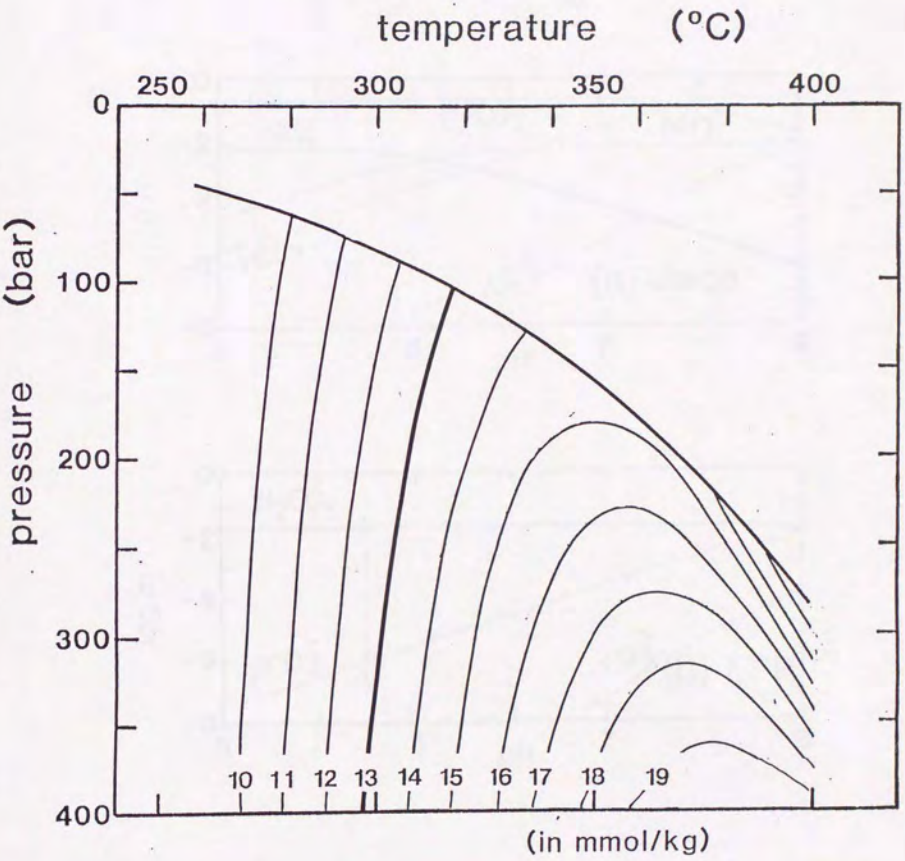

Fig. 4-6 Isopleths of quartz solubility in seawater (calculated from Bischoff and Rosenberg, 1985)

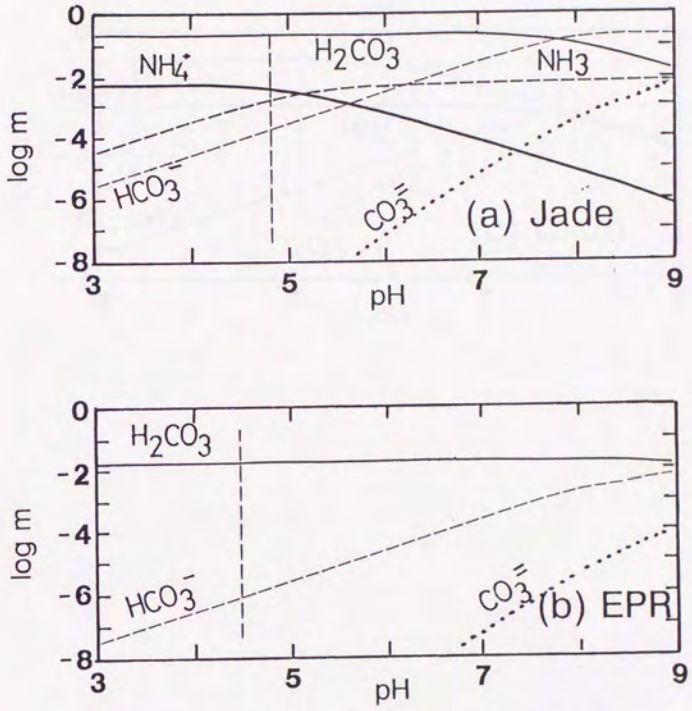

Fig. 4-7 Morality vs pH diagrams for the principal weak acid-base species in hydrothermal fluids
(a) Jade fluid at 300°C (b) EPR-OBS fluid at 300°C

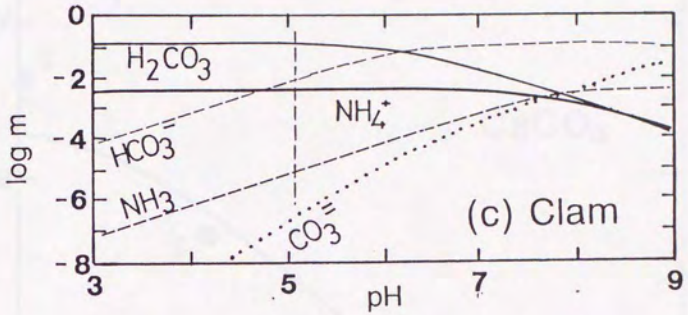

Fig. 4-7 Morality vs pH diagrams for the principal weak acid-base species in hydrothermal fluids (continued)
(c) Clam fluid at 100°C

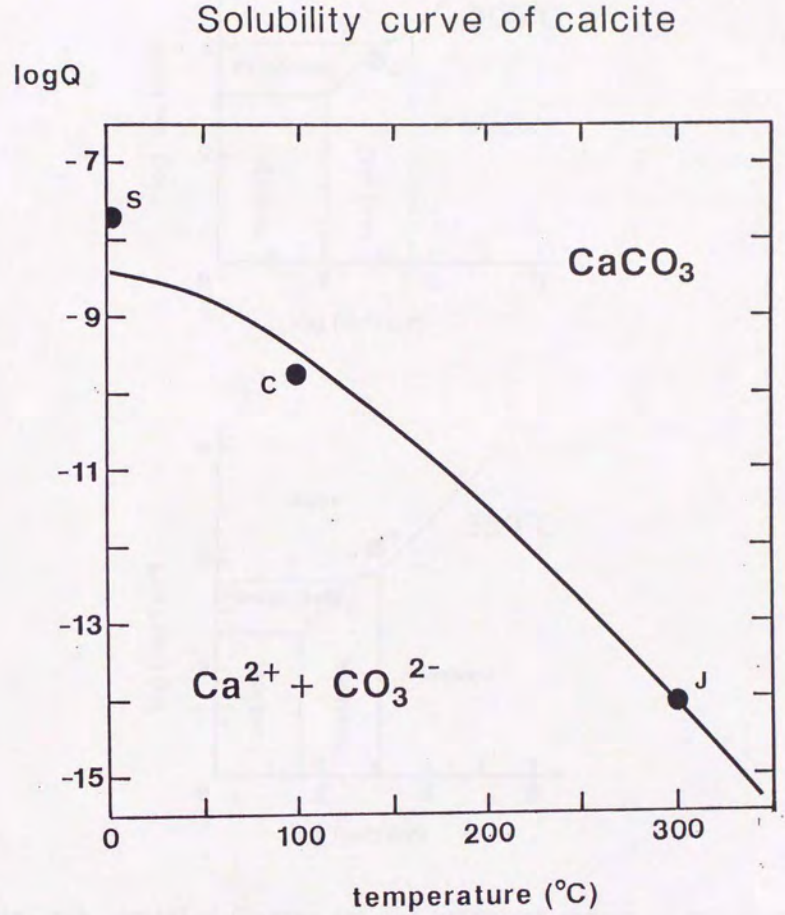

Fig. 4-8 Solubility curve of calcite

A circle plots solubility product of each fluid using value of its estimated pH as
S: Seawater, C: D427-RV3, J: D423-RV3

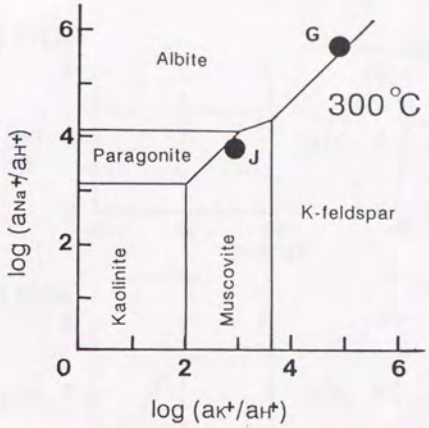

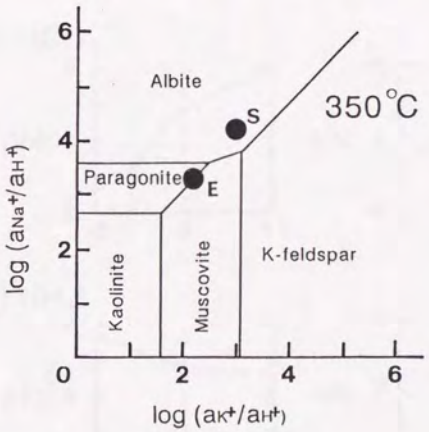

Fig. 4-9 Activity diagram for the principal phases in the system Na_2O-K_2O-Al_2O_3-H_2O at 300°C and at 350°C and 1kb with quartz saturation (from Bowers et al.,1984)

A circle plots activity ratios of each hydrothermal fluid according to the calculation in this study
J: D423-RV3, G: Guaymas Basin, E: EPR-OBS
S: Experimental study of fluid-sediment interaction (Thornton and Seyfried, 1987)

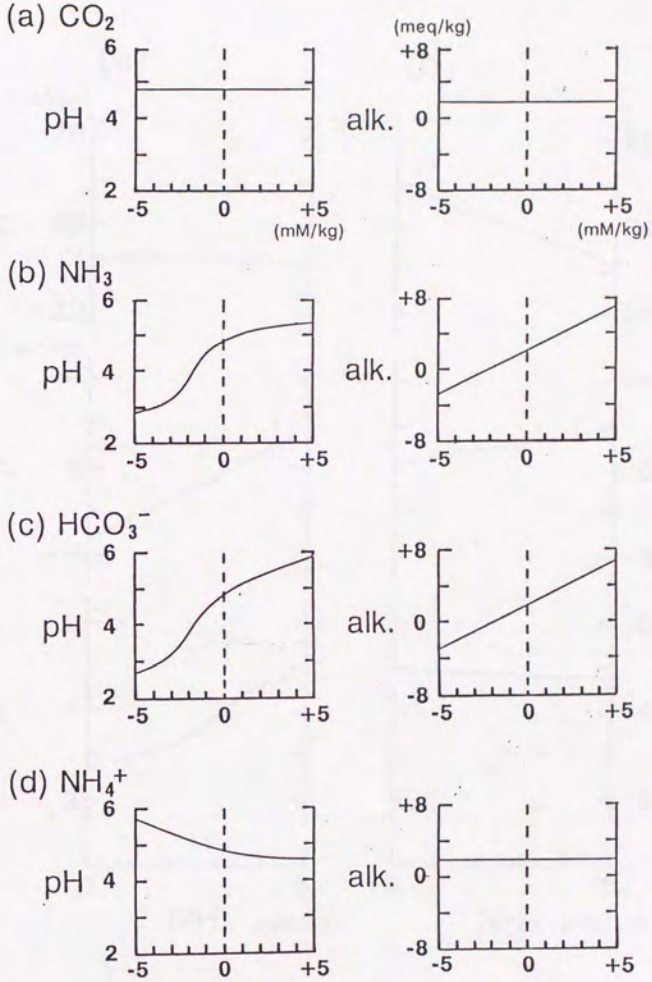

Fig. 4-10 Effect estimation caused by addition or deduction of acid-base species to the Jade fluid at 300°C.
(a) CO_2 (b) NH_3 (c) HCO_3^- (d) NH_4^+

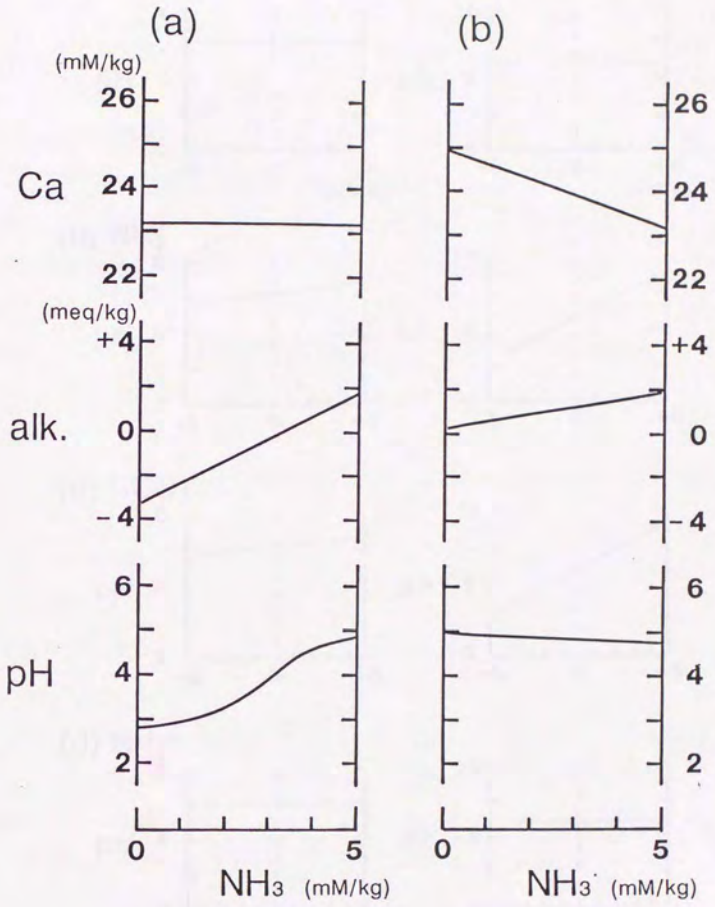

Fig. 4-11 Simulation of shift of pH, alkalinity and Ca content of the Jade fluid induced by NH_3 addition
(a) without calcite deposition model
(b) with calcite deposition model

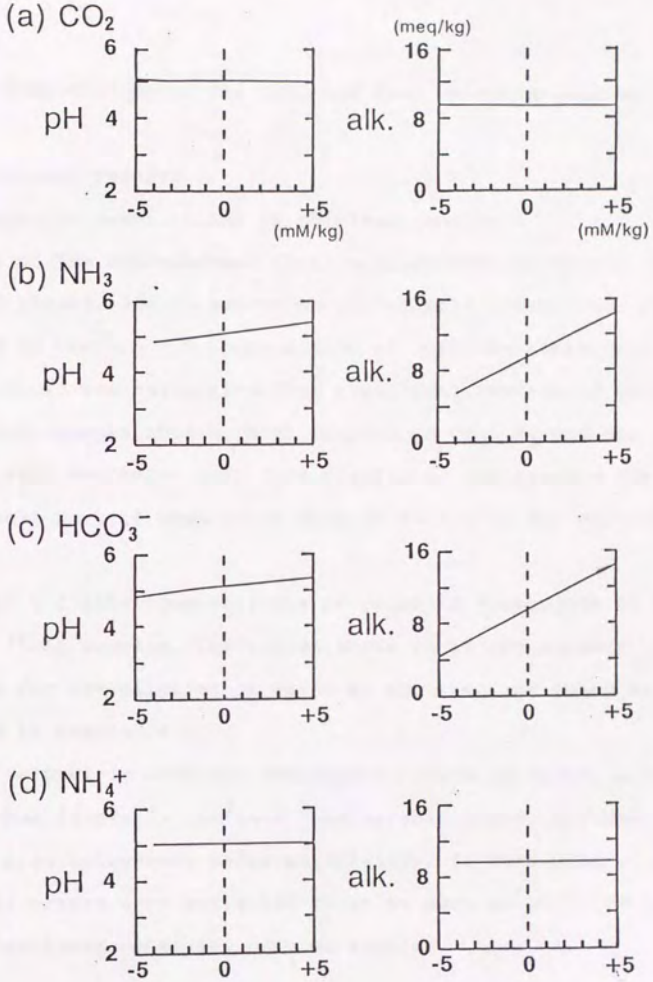

Fig. 4-12 Effect estimation caused by addition or deduction of acid-base species to the Clam fluid at 100°C.
(a) CO_2 (b) NH_3 (c) HCO_3^- (d) NH_4^+

Chapter 5.

Volatile compositions of the Jade and Clam site hydrothermal fluid

5-1. Analytical results

5-1-1. Volatile compositions in obtained samples

Most of the hydrothermal fluid samples were recovered in two separated phases, due to evolution of volatile components. As mentioned in section 3-5, composition of volatile components in original fluid was calculated from analytical results of both gaseous and aqueous phases. With respect to CH_4, H_2 and He, contents were estimated only from results of the gaseous portion, because most part of them (more than 99 %) are in the gaseous phase.

Table 5-1 lists compositions of volatile components in the analyzed fluid samples. The values shown in it are already corrected for the dilution by water at the sampling tubes as mentioned in Chapter 4.

The volumetric analysis employed on board is rather a crude method, thus it likely includes considerable error. The QMS analysis also introduces large uncertainty. In this study, analytical errors were estimated to be as much as 10 to 20 % based on duplicate analyses of some samples.

5-1-2. Isotopic compositions

Table 5-2 presents analytical results of $^3He/^4He$ ratio and $^4He/^{20}Ne$ ratio with a corrected $^3He/^4He$ ratio ($(^3He/^4He)_c$). The $(^3He/^4He)_c$ value was adjusted for an air-derived He by assuming that all the Ne in the sample was derived from atmosphere.

Correction formula are cited below table 5-2. In this study, the atmosphere-derived component is assumed to be the air-saturated seawater (ASSW) in which the $^4He/^{20}Ne$ ratio is 0.445 (Weiss 1971). $^3He/^4He$ ratios are expressed relative to the atmospheric $^3He/^4He$ ratio (its absolute ratio is 1.4×10^{-6}) as "R_{atm}". Errors on the $^3He/^4He$ ratios are one standard deviation of each measurement run, and those on the $^4He/^{20}Ne$ were estimated as about 10%, according to the previous consideration (Sano and Wakita, 1988).

All the Jade fluids show the uniform isotopic ratios of 6.2-6.8 R_{atm} after air-correction, except for D424-RV4 which is not fluid sample but evolved gas from sediment clogged the sampler tube (see footnote of table 3-1). Three samples from the Clam site also show rather uniform isotopic ratios of 3.9-4.1 R_{atm}.

Analytical results of carbon isotopic ratios are listed in table 5-3. Both carbon isotopic ratios of CO_2 and CH_4 are expressed in per mill deviation from the PDB standard as $\delta^{13}C$. Each $\delta^{13}C(CO_2)$ value of fluid was calculated from analytical results in the gaseous and the aqueous phases, in similar way to CO_2 content.

Because deep seawater originally contains considerable amounts of CO_2 as bicarbonate ions, its effect should be corrected. Assuming that CO_2 in each sample is a mixture of hydrothermally-derived and ambient seawater-derived components, the corrected $\delta^{13}C$ values for hydrothermal CO_2 were calculated. The analytical results of D416-M was taken as representative of chemical and isotopic compositions of ambient seawater. Corrected

values are listed in the third column of table 5-3. Because the hydrothermally derived CO_2 accounts for more than 90% of CO_2 in all the samples, correction is not so significant. Anyway, $\delta^{13}C(CO_2)$ values are uniform in each site, around -5.2 per mill at the Jade fluid and around -4.0 per mill at the Clam fluid.

5-2. Volatile compositions of the endmember fluids.

In fig. 5-1, relationships between each volatile component and Mg in the obtained samples are plotted. While the CO_2-Mg and H_2S-Mg diagrams show good linear relationships, CH_4-Mg and He-Mg diagrams defines only poor one. Because of their complexity, the volatile compositions of D423-RV3 and D427-RV3 are taken as the endmember compositions of the Jade and Clam fluid, respectively.

Both the Jade and Clam fluids of the middle Okinawa Trough hydrothermal systems are significantly enriched in volatile components compared to the MOR hydrothermal fluids. Table 5-4 summarizes volatile compositions of hydrothermal fluids so far studied. While the four MOR fluids show a similar composition, the Jade fluid shows more than one order of magnitude higher contents of CO_2 and CH_4 than them but is comparable with them in terms of H_2S and He. Although the Clam fluid composition can not be compared directly with other fluids, its tendency of enrichment in CO_2 and CH_4 is obvious. The enrichment of these volatile components in the Jade and Clam fluids is one of the most important geochemical features of the middle Okinawa Trough hydrothermal system.

5-3. Volatile components in the Jade fluid

5-3-1. Helium

Although He is a minor component of hydrothermal fluid, it has been proven to be the most sensitive tracer for magmatic processes (e.g. Lupton, 1983). Its isotopic ratio displays a wide variation between the mantle component enriched in primitive ^3He, and the crustal component enriched in radiogenic ^4He.

The Jade fluid samples show He isotopic ratios of 6.2 - 6.8 R_{atm} (table 5-2), which are lower than but close to those of the MOR fluids (= 7.5-10.0 R_{atm}). The coincidence of the isotopic composition between He in hydrothermal fluid and in basalt glass at the MOR suggests that the He in fluid is derived by leaching of basalt glass during hydrothermal interaction (see section 1-6). As shown in fig. 5-2, the Jade fluid shows the He isotopic ratio that is typical of volcanic discharges in the Island Arc. The elevated isotopic ratio would indicate that He in the Jade fluid is of mantle origin and that it was derived from magmatic source without significant contamination by crustal component.

The heat/^3He ratio of the Jade fluid is calculated as below. Content of ^3He is a product of the ^4He concentration (0.82×10^{-6} mol/kg) and the absolute $^3He/^4He$ ratio (8.61×10^{-6}), leading to a value of 7.1×10^{-12} mol/kg. Enthalpy of the Jade fluid is 1380 kJ/kg according to the thermodynamic property table (Bischoff and Rosenbauer, 1985). Then, heat/^3He ratio of the Jade fluid is 0.19×10^{18} J/mol(^3He).

Lupton et al.(1989) demonstrated that the heat/^3He ratios of the MOR fluids are in a narrow range (table 5-5). They considered that the heat/^3He ratio are converged as growth of mineral

precipitation through the fluid conduit in these matured system. They also suggest that the heat/^{3}He ratio in hydrothermal fluid would show different values in the case that He is supplied not by extraction from basalt, but by other procedure such as extensive degassing of volatile component from magmatic source. The heat/^{3}He ratio of the Jade fluid is in the similar range to those of the MOR fluids. This may suggest that the fluid circulation in the Jade system is in a steady condition as in the MOR systems and that the He in the Jade fluid has been extracted from volcanic rocks by seawater interaction.

5-3-2. Carbon dioxide

CO_2 is the most dominant volatile component of the hydrothermal fluids in the middle Okinawa Trough. Possible sources of CO_2 are: (1) magmatic origin (2) carbonate minerals, (3) organic origin (decarboxylation and thermocatalytic oxidation of organic matter).

Fig. 5-3 summarizes the isotopic composition of CO_2 of hydrothermal fluids and other magmatic gas discharges together with range of possible sources. $\delta^{13}C(CO_2)$ values of the Jade fluid are of -5.4 to -5.1 per mill PDB (table 5-3), which are in accordance with the MOR fluids and geothermal gases. These isotopic composition of CO_2 is attributed to magmatic origin (Truesdell and Hulston, 1980).

However, appropriate mixing of organic and carbonate carbon could produce such range of carbon isotopic composition (Allard 1983). Isotopic composition of marine carbonate has $\delta 13C(CO_2)$ near ±0 per mill, while that of organic carbon from sedimentary

matter is lower than -20 per mill (Hoefs, 1987). It is difficult to conclude its origin only from its isotopic evidence.

The content ratio of CO_2 to ^3He would be useful as another clue to the origin of CO_2, since ^3He is well confirmed as a mantle component. In this study, only two samples from the Jade site and one from the Clam site provide available data sets for this ratio, though they have large uncertainty and adequate only to rough discussion. Fig. 5-4 is a diagram showing the $CO_2/^3He$ versus $^4He/^3He$ relationship of these fluids.

In fig. 5-4, data of other magmatic gas discharges are plotted together. They may be classified into two groups. Data of the MOR fluids (from table 5-4) and geothermal gases in the Iceland (Sano et al., 1985a) gathered around the estimated MORB value (2×10^9) by Marty et al.(1987). Contrary to them, data of volcanic gases in Japanese Island Arc (Marty et al., 1989) have the higher $CO_2/^3He$ ($4.5\text{-}29 \times 10^9$) and slightly higher $^4He/^3He$ ratio than the first group. This high $CO_2/^3He$ ratio was considered as characteristic to the Island arc type magma based on the model that subducted materials are incorporated into magma generation underneath the Island Arc (Marty et al., 1987).

Values of the Jade fluids are plotted within the latter region. The $CO_2/^3He$ ratio of the Jade fluid supports that the major part of CO_2 originates from magma of the Island Arc type.

5-3-3. Methane

CH_4 is usually minor volatile species in hydrothermal fluid. As shown in table 5-4, CH_4 content in hydrothermal fluids vary widely over several orders of magnitude. The Jade fluid shows

significant enrichment in CH_4. The variety of CH_4 contents implies that CH_4 originates from several different sources. Four principal sources are generally considered (Welhan, 1988) as: (1) bacterial production (CO_2 reduction and CH_4 fermentation), (2) thermal breakdown of complex hydrocarbons, (3) outgassing of juvenile carbon as CH_4 from the mantle, (4) inorganic synthesis in reactions involving CO_2 and H_2.

Fig. 5-5 illustrates the distribution of $\delta^{13}C(CH_4)$ of hydrothermal fluids and geothermal fluids together with ranges for CH_4 of various origins. As Shoell (1988) reviewed, the isotopic composition of CH_4 is useful to identify its source. Biogenetic CH_4 is characterized by $\delta^{13}C(CH_4)$ lower than -60 per mill. Decomposition of organic matter at higher temperature would form thermogenic CH_4 within a range of -60 per mill to -20 per mill. More ^{13}C-enriched CH_4 ($\delta^{13}C$ = -20 to -7 per mill) is produced by inorganic process free from biogenetic sources.

The MOR fluids show a common isotopic composition of $\delta^{13}C(CH_4)$ value of -20 to -15 per mill, which is attributed as abiogenic CH_4 leached from occluded gas in basalt glass (Welhan and Craig, 1983). Similarity in $CH_4/^3He$ ratios between hydrothermal fluid and basaltic glass and lack of other possible sources in sediment-starved environment support this identification. Further evidence is the relationship between isotopic compositions of CH_4 and CO_2 (fig.5-6), which implies that both components have co-existed and attained isotopic equilibrium at around 600 - 700°C during basalt extrusion (Welhan, 1988).

The isotopic composition of CH_4 in the Jade fluid is -41 - -36 per mill (table 5-3). These values are quite different from those of the MOR fluids, but similar to those of the Guaymas Basin fluids and to several subaerial geothermal systems. The Jade fluid shows $CH_4/^3He$ ratio of 1.0×10^9 which is more than two orders of magnitude higher than the MOR fluids, implying CH_4 contribution from other sources than magmatic. Both results suggest that CH_4 of the Jade fluid is overwhelmingly of thermogenic origin.

Relationship between $\delta^{13}C(CO_2)$ and $\delta^{13}C(CH_4)$ would also support this model. Carbon isotopic fractionation between CO_2 and CH_4 in the Jade fluid is 33.2 per mill (fig. 5-6), which corresponds to the isotope exchange equilibrium at 200°C (Bottinga, 1969). This value is lower than the observed fluid temperature, indicating that two species are not in isotopic equilibrium.

5-3-4. Other volatile components

It has been proposed that H_2S of the MOR fluids originates from mixing of two sources; one leached from basalt and the other from reduction of seawater sulfate (e.g. Shanks et al., 1981). This model is based on the isotopic composition of H_2S of +1.3 - +5.5 per mill in the MOR fluids (Kerridge et al., 1983; Woodruff and Shanks, 1988).

The Jade fluid show $\delta^{34}S(H_2S)$ value of +7.4 - +7.7 per mill (table 4-6), which is higher than those of the EPR fluids. A similar mixing model could be applied to the Jade fluid with magmatic sulfur of higher $\delta^{34}S$ in the Island Arc than the MORB

(Ueda and Sakai, 1984; Allard, 1983). Alternatively, entrainment of seawater-derived sulfur reduced in the near-surface environment could produce ^{34}S-enriched H_2S (Woodruff and Shanks, 1988). It is difficult to judge which model is likely, at present.

Contents of H_2S and H_2 may be controlled by its redox state. Oxygen fugacity of the Jade fluid is calculated as below. Relationship between H_2 content and oxygen fugacity is controlled by redox equilibrium :

$$H_2O = H_2 + 1/2O_2 \quad \text{--- (5-1)}$$

A value of $\log f(O_2)$ in the Jade fluid at 300 C is calculated by using H_2 content, the Henry's law coefficient of H_2, and the equilibrium constant of (5-1), which leads to $\log f(O_2) = -31.0$. Relationship between H_2S content and oxygen fugacity is estimated by redox equilibrium :

$$SO_4^{2-} + 2H^+ = H_2S + 2O_2 \quad \text{--- (5-2)}$$

From pH value and activities of H_2S and SO_4 estimated in section 4-2-3, $\log f(O_2)$ is estimated. Activity of SO_4 is determined as $10^{-6.05}$ according to the anhydrite deposition equilibrium. Value of $\log f(O_2)$ in the Jade fluid at 300°C is -30.6. This accordance of estimated $\log f(O_2)$ values between H_2-H_2O couple and H_2S-SO_4 couple supports that the contents of these species are indeed controlled by redox state of the fluid, although it could not be confirmed what reactions control this redox state.

If CH_4 and CO_2 occur in the Jade fluid are in chemical equilibrium (5-3) the $\log f(O_2)$ value estimated from CH_4-CO_2 couple would also be consistent with the values calculated above.

$CH_4 + 2O_2 = CO_2 + 2H_2O$ --- (5-3)

The result of calculation is $\log f(O_2) = -36.2$, which suggests little possibility that the CH_4 in the Jade fluid is supplied by reduction of CO_2. Slow reaction rate of (5-3) at the temperature range of the Jade fluid suggests that such reduction does not occur in the Jade fluid.

5-3-5. Venting of liquid CO_2

Venting of liquid CO_2 observed in the Jade site (Sakai et al., 1990b) is a good demonstration of the significant enrichment in CO_2 of the Jade hydrothermal system. This interesting phenomenon was witnessed at two sites which are 300 - 500 m apart from the center of activity in the hydrothermal field (localities are shown in fig. 3-1: D415-M and D424-M). Fig. 5-7 is a phase diagram for the system of CO_2 and H_2O. The P-T condition of the discharge sites (depth 1550m; pressure 150 bars; temperature 3.8°C) is plotted in the region where both liquid CO_2 and CO_2-hydrate stably exists.

The liquid CO_2 bubbles were sampled successfully at the site of D424-M and analyzed by the same methods as volatile components in the fluid samples. Chemical composition was obtained to be CO_2: 86.2%, H_2S: 2.3%, CH_4: 11.2%, corrected with amount of N_2 and O_2 which are attributed as contaminant from air during handling of the sample. This composition is in good agreement with the compositions of volatile component in the hydrothermal fluids at the Jade site. He isotopic composition also shows this similarity (table 5-2).

These data strongly suggest that the liquid CO_2 has the same

magmatic origin as the volatile components dissolved in the hydrothermal fluids. Because the CO_2 content in the Jade fluid is far less than the saturation level at any possible P-T condition, the mechanism of generation of the phase-separated CO_2 fluid is likely to be rather complex.

5-4. Volatile components in the Clam fluid

5-4-1. Helium and carbon dioxide

The Clam fluid shows the distinct $^3He/^4He$ ratios from the Jade fluid. They are 3.9 - 4.1 R_{atm} (table 5-2), which are higher than atmospheric value but evidently lower than those of the magmatic source in the Island Arc. The isotopic composition in this range is frequently observed in various gas discharges, such as hot spring gases in the Island Arc area.

The lower isotopic composition indicates that He in the Clam fluid is a mixture with radiogenic He. Mixing between the high temperature fluid and the entrained seawater can not explain the lower He isotopic composition of the Clam fluid, because He in bottom seawater has isotopic composition nearly equivalents to atmospheric component, which is excluded in the correction calculation (see section 5-1-2). The mixing ratio between magmatic and radiogenic He can be calculated on the assumption that the former has the same isotope ratio as the Jade fluid (= 6.6 R_{atm}) and that the latter is 0.011 R_{atm} based on the radiogenic production rate of he in the continental crust (Gerling et al., 1971). The radiogenic component comprises about 38 % of the total He in the Clam fluid.

Two mechanisms of involvement of radiogenic He in the Clam

fluid may be possible. First, assimilation of lower crustal materials during magma genesis would produce low $^3He/^4He$ in the source magma. The assimilation model is proposed by Ishizuka et al.(1990) to explain the genesis of andesite magma at the Iheya Graben. The He in the Clam fluid possibly originated from such magma source.

Second, even the source magma has the same $^3He/^4He$ ratio as the Island Arc type magma, dilution by radiogenic He leached from crustal matter during hydrothermal circulation in sedimentary layer would result in the low $^3He/^4He$ ratios in the Clam fluid. Sedimentary piles of continental source, which cover the area around the Clam site are possible sources of radiogenic He.

The Clam fluid shows the higher $CO_2/^3He$ ratio than the Jade fluid (fig. 5-4). Although He depletion shown in Mg diagram (fig. 5-1 (d)) is doubtful due to large analytical error, CO_2 is more enriched in the Clam fluid than the Jade fluid at the same Mg content (fig. 5-1 (a)).

Some hot spring gases in Japan (Urabe, 1985) show $CO_2/^3He$ ratios in the similar range to the Clam fluid, as plotted in fig. 5-4. In these gases, higher $CO_2/^3He$ ratio may be correlated with lower $^3He/^4He$ ratio. Poreda et al.(1988) attributed the high $CO_2/^3He$ and low $^3He/^4He$ values of hot spring gases in the Island Arc to the mixing of two endmembers, low-$^3He/^4He$ (=0.01 R_{atm}), high-$CO_2/^3He$ gases($>10^{11}$) derived from decarbonation reaction in the crustal region and the high-$^3He/^4He$, the low-$CO_2/^3He$ gases from the mantle. The lower W/R ratio in the Clam fluid supported by its minor element composition (see section 4-3-5), implies

that the Clam fluid extracted both radiogenic He and crustal carbon during the fluid-sediment interaction more efficiently than the Jade fluid.

Alternatively the $^3He/^4He$ and $CO_2/^3He$ ratios of the Clam fluid are affected by independent factors. The oxidation of organic matter in the fluid-sediment interaction of the Clam fluid (see section 4-3-4) may be responsible for the higher CO_2 content in the Clam fluid than in the Jade fluid, whereas mechanisms such as assimilation of crustal material in magma generation may be possible fro the low $^3He/^4He$ ratio. Accumulation of more precise data of fluids is necessary for further discussion of these two possibilities.

5-4-2. Other volatile components

The isotopic composition of CH_4 in the Clam fluid suggests thermogenic origin as in the Jade fluid. Higher CH_4 contents may be attributed to more effective fluid-sediment interaction in the Clam site than the Jade site.

While the H_2S content in the Clam fluid is increased by the sulfate reduction coupled with organic matter oxidation (see section 4-3-4), H_2 content may be controlled by redox state. More reductive environment in the Clam fluid may be responsible for the higher H_2 content than the Jade site. Accumulation of precise concentration of H_2 in hydrothermal fluid is needed content data would be useful to discuss redox state, however, only few samples were available to analysis at present.

5-5. Summary

The hydrothermal fluids of the middle Okinawa Trough show

significant enrichment in CO_2 and CH_4 and have comparable contents of He and H_2S compared to the MOR fluids.

The Jade fluid shows the $^3He/^4He$ ratio of 6.2-6.8 R_{atm}, which suggests magmatic He. The $CO_2/^3He$ ratio of 15-30 x 10^9 and $\delta^{13}C(CO_2)$ around -5 per mill suggest that the most part of CO_2 originates from magmatic source as well as He. Both $^3He/^4He$ ratio and $CO_2/^3He$ ratio of the Jade fluid are good accordance with the values of the Island Arc type magma estimated from those of volcanic gases in the Island Arc area.

Contrary to this, CH_4 in the Jade fluid is thermogenic in origin derived from fluid-sediment interaction, based on its $\delta^{13}C(CH_4)$ values of -36 to -40 per mill. The contents of H_2S and H_2 in the Jade fluid seems to be controlled by the redox condition of the fluid possibly governed by fluid-sediment interaction.

The Clam fluid shows $^3He/^4He$ ratio of 3.9-4.1 R_{atm} due to mixing with crustal He. The Clam fluid also shows higher $CO_2/^3He$ ratio than the Jade fluid, which may be ascribed to incorporation of excess CO_2 into fluid during fluid-sediment interaction. However, its correlation with the low $^3He/^4He$ is ambiguous at present.

Oxidation of organic matter coupled with sulfate reduction is responsible for the higher H_2S contents and the lower $\delta^{34}S(H_2S)$ values in the Clam fluid than the Jade fluid. The content of CH_4 and H_2 may also be controlled by the fluid-sediment hydrothermal interaction.

Table 5-1 Analytical results of gas composition of the obtained samples

Sample		CO_2 (mM/kg)	CH_4 (mM/kg)	H_2 (mM/kg)	He (uM/kg)	H_2S[1] (mM/kg)
Jade Site						
D413	RV6	55.4	2.40		0.46	
D423	RV2	112.6	3.25	0.01	0.23	7.96
	RV3	208.9	7.66	0.02	0.82	13.66
	RV5	25.6				1.66
Clam Site						
D416	RV2	86.3	3.08		0.12	
	M	2.4				
D426	RV6	77.9	5.15	0.13		7.54
D427	RV1	85.2		0.19		
	RV3	95.6	5.41		0.14	9.44

1) from Gamo et al.(1991)

Table 5-2 Analytical results of He isotopic composition

Sample		$^3He/^4He$ (R_{atm})	$^4He/^{20}Ne$	$(^3He/^4He)c$ (R_{atm})
Jade Site				
D413	RV5	6.407 ± 0.024	4.35	6.84
	RV6	4.794 ± 0.033	1.14	6.27
D422	RV3	6.506 ± 0.039	57.70	6.54
D423	RV3	6.177 ± 0.031	19.24	6.26
	RV5	5.890 ± 0.130	4.90	6.23
D424	RV4	2.597 ± 0.032	0.48	5.79
	M	6.452 ± 0.036	15.61	6.57
Clam Site				
D416	RV2	3.750 ± 0.027	7.85	3.87
D426	RV6	3.388 ± 0.030	1.55	4.01
D427	RV3	3.868 ± 0.041	4.38	4.09

$$(^3He/^4He)c = \frac{[\ (^3He/^4He)sample - r\ ]}{(\ 1 - r\ )}$$

$$r = \frac{(^4He/^{20}Ne)air}{(^4He/^{20}Ne)sample}$$

Table 5-3 Analytical results of carbon isotopic composition

Sample		CO_2 (mM/kg)	$\delta^{13}C(CO_2)$ (per mil)	$\delta^{13}C(CO_2)$ [1] (per mil)	CH_4 (mM/kg)	$\delta^{13}C(CH_4)$ (per mil)
Jade Site						
D413	RV6	55.4	(-4.0)		2.40	-36.1
D416	M	2.4	-0.9			
D422	RV3					-40.7
D423	RV2	112.6	-5.0	-5.1		
	RV3	208.9	-5.3	-5.3		
	RV5	25.6	-4.7	-5.4		
D424	M					-36.4
Clam Site						
D426	RV6	77.9	-3.6	-3.7	5.15	-41.2
D427	RV1	85.2	-3.9	-4.0		
	RV3	95.6	-4.1	-4.2		

1) Corrected for deep seawater carbonate

$$\delta^{13}C(‰) = \left[\frac{(^{13}C/^{12}C)\text{sample}}{(^{13}C/^{12}C)\text{standard}} - 1\right] \times 1000$$

Table 5-4 Chemical and isotopic composition of volatile components in hydrothermal fluids

component	Jade	Clam	EPR 21°N	EPR 13°N	SJFR	Endeavour	Guaymas	Seawater
CO_2 (mM)	209	95.6	8.0	10.8-16.7	3.9-4.4	5-11	16-24	2.3
H_2S (mM)	13.7	9.44	6.6-8.4	2.9-12.2	3.0-4.4	---	3.8-6.0	0
CH_4 (μM)	7600	5400	45-65	27-55	82-118	500-1400	12000-16500	0.01
H_2 (μM)	20	190	227-1275	---	196-527	25-75	(600-850)*	---
He (μM)	0.82	0.14	0.9-2.2	1.4-2.6	---	-----	---	0.0018
$CO_2/^3He$ ($x10^9$)	18-30	131-142	0.8	0.3-0.7			(4.5)*	
$CH_4/^3He$ ($x10^6$)	810-1100	5100-7400	3.5-6.5	1.4-2.1			3200	
$H_2/^3He$ ($x10^6$)	2.8	26	22-124	---			(1660)*	
$\delta^{13}C(CO_2)$! (‰PDB)	-5.2	-4.0	-7.0	(-5.5--4.1)!	-9.7--6.8		-10.5--3.4	
$\delta^{13}C(CH_4)$ (‰PDB)	-40.7--36.1	-41.2	-17.6--15.0	-19.5--16.6	-20.8--17.8		-50.8--43.2	
$\delta^{34}S(H_2S)$ (‰CDT)	7.4-7.6	-0.3-3.0	1.3-5.5	2.3-5.2	4.0-7.4		---	
$^3He/^4He$ (Ratm)	6.1-6.9	3.9-4.1	7.8	7.4-7.6	---		7.0	

Units are in per kg
Carbon isotopic ratios are expressed in per mill deviation from PDB standard
Sulfur isotopic ratios are expressed in per mill deviation from CDT standard
Helium isotopic ratios are expressed in ratio to atmospheric He

! Isotopic composition of CO_2 in hydrothermal fluid is estimated considering correction for deep seawater bicarbonate. (data of EPR 13°N is not uncorrected)

Data sources

EPR 21°N : East Pacific Rise 21°N (Craig et al., 1980; Welhan and Craig, 1983; Lilley et al., 1983; Woodruff and Shanks, 1988)
EPR 13°N : East Pacific Rise 13°N (Merlivat et al., 1987; Bluth and Ohmoto, 1988)
SJFR : Southern Juan de Fuca Ridge (Evans et al., 1988; Shanks and Seyfried, 1987)
Guaymas : Guaymas Basin (Welhan, 1988; Welhan and Lupton 1987; Lupton, 1983)
* calculated from data cited in (Welhan et al., 1988)
Endeavour: Endeavour ridge (Lilley et al., 1989; Kadko et al., 1990)

Table 5-5 Compilation of heat/^{3}He ratios in hydrothermal fluids (Lupton et al., 1989; Baker and Lupton, 1990)

site	fluid temp. (°C)	heat/^{3}He (10^{18}J/mol)	^{3}He/^{4}He (R_{atm})
Venting fluid			
Jade site	320	0.19	6.4
EPR 21°N	350	0.23	7.8
EPR 13°N	300	0.10	7.5
Galapagos Rift	20	0.19	7.8
Juan de Fuca	400	0.10	7.9
Guaymas Basin	315	1.5	7.0
Hydrothermal plume			
Cleft segment at Juan de Fuca			
megaplume-1986		0.66	7.9
steady state plume-1986		0.044	7.9
-1987		0.039	7.9
-1988		0.072	7.9

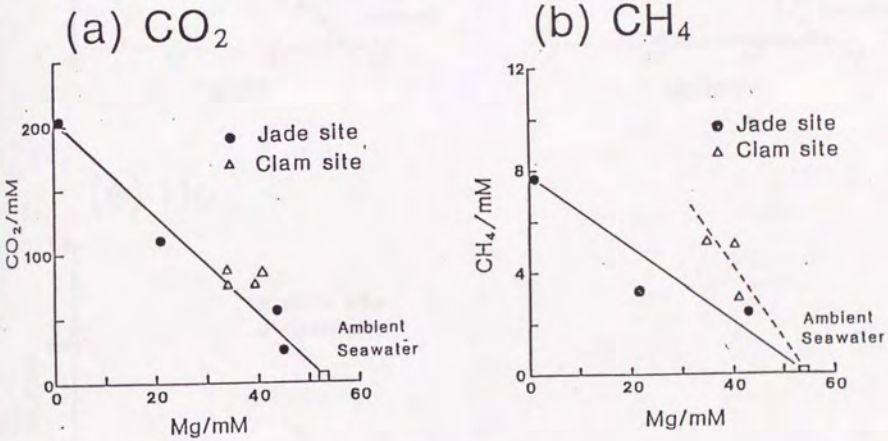

Fig. 5-1 Relationship between concentration of each volatile component and magnesium
(a) CO_2 vs. Mg (b) CH_4 vs. Mg

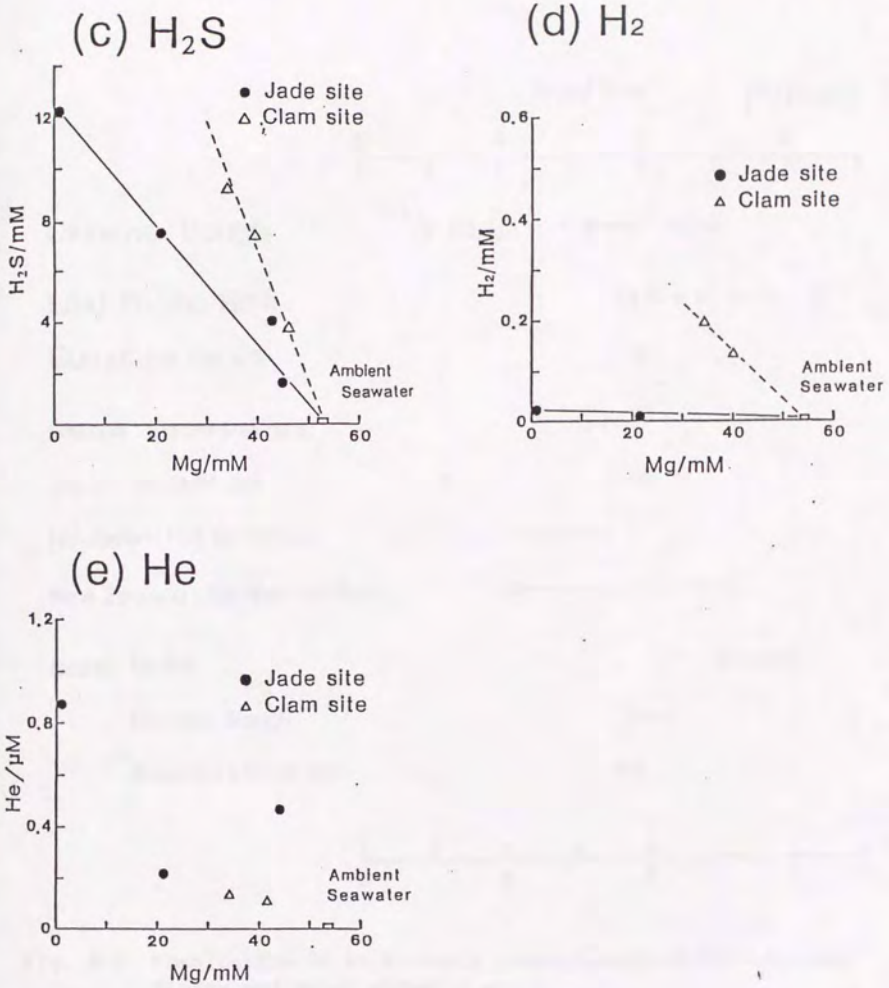

Fig. 5-1 Relationship between concentration of each volatile component and magnesium (continued)
(c) H_2S vs. Mg (d) He vs. Mg (e) H_2 vs. Mg

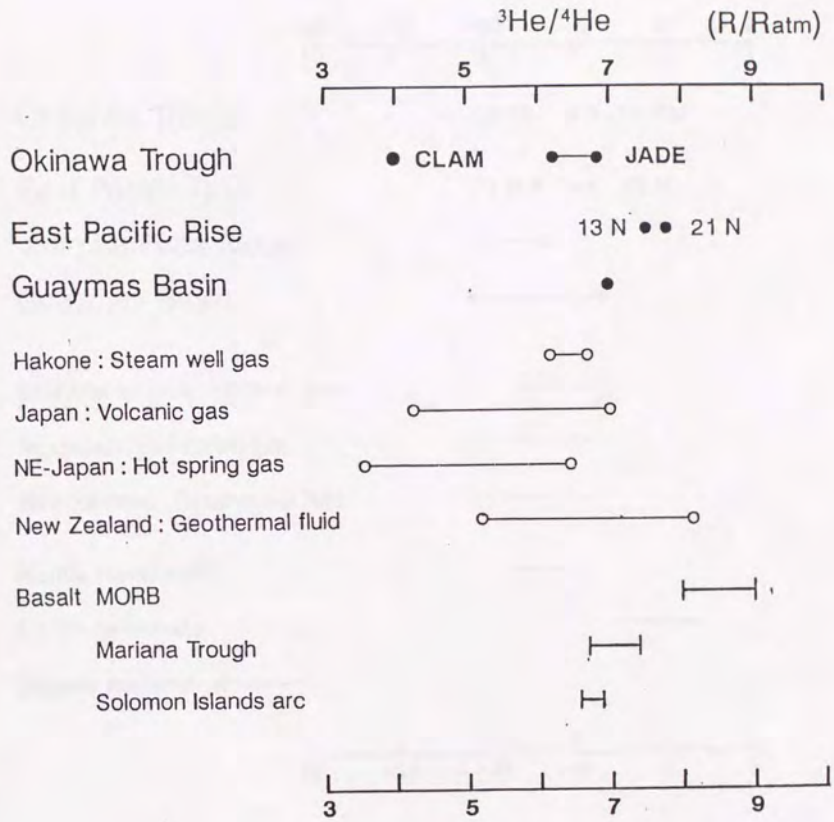

Fig. 5-2 Compilation of He isotopic compositions of hydrothermal fluids and other magmatic gases

Hakone: Steam well gas (Poreda and Craig, 1989)
Japan: Volcanic gas (Marty et al., 1989)
NE-Japan: Hot spring gas (Sano and Wakita, 1985)
N.Z.: Geothermal fluid (Torgersen et al., 1982)
MORB: Basalt (Kurz and Jenkins, 1981)
Mariana: Basalt (Sano et al., 1986)
Solomon: Basalt (Trull et al., 1990)

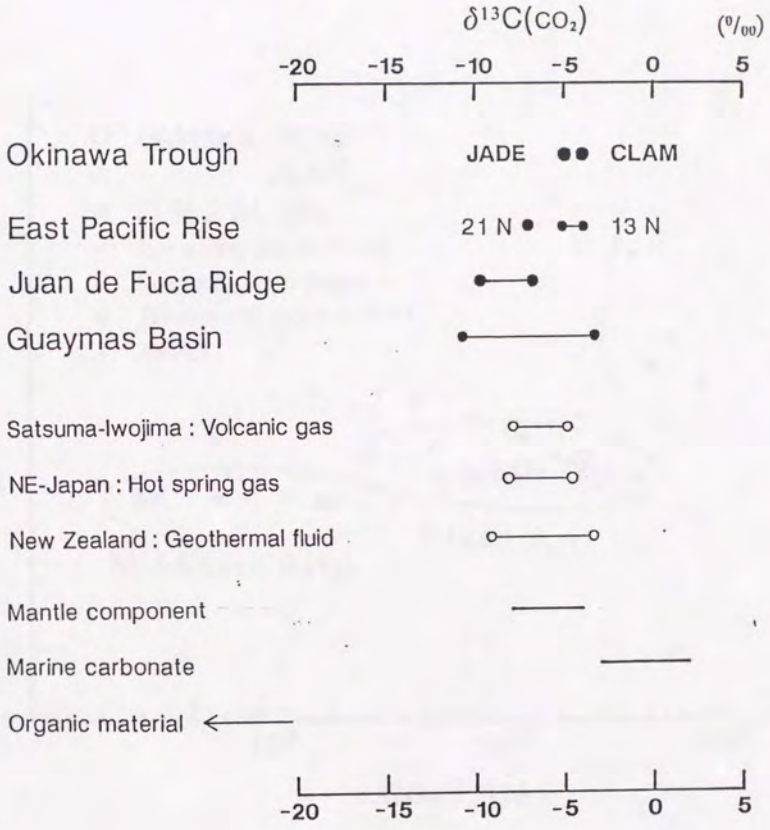

Fig. 5-3 Compilation of $\delta^{13}C(CO_2)$ of hydrothermal fluids and other magmatic gases

S.Iwojima: Volcanic gas (Matsubaya et al., 1975)
NE-Japan: Hot spring gas (Urabe 1985)
N.Z.: Geothermal fluid (Lyon and Hulston, 1984)

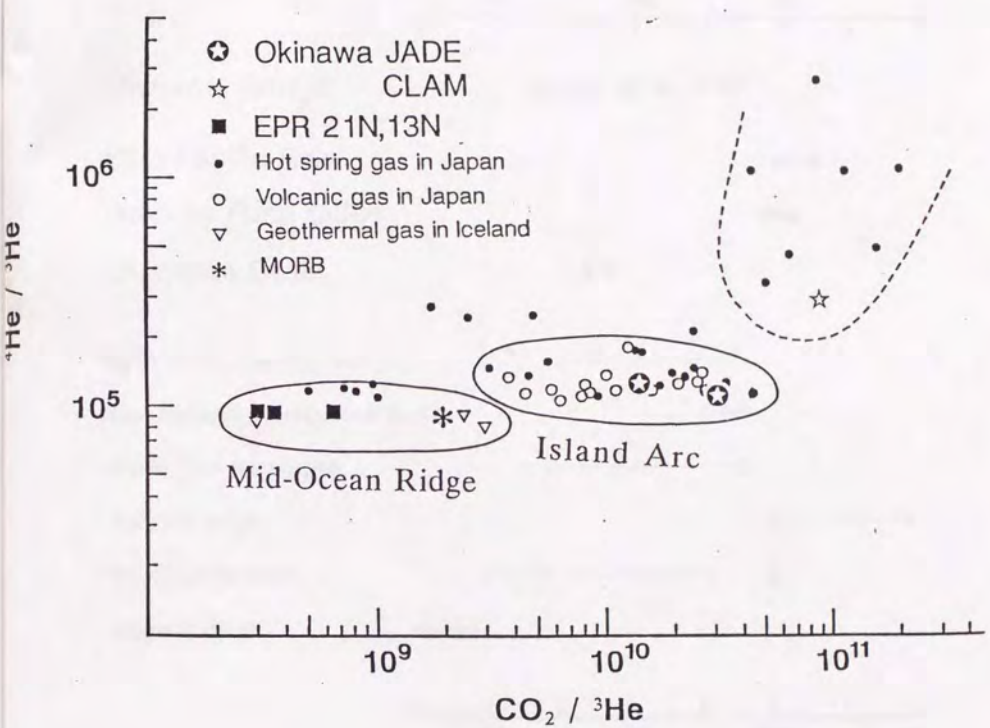

Fig. 5-4 $CO_2/^3He$-$^4He/^3He$ diagram for hydrothermal fluids and other magmatic gases

Japan: Hot spring gas (Urabe 1985)
Japan: Volcanic gas (Marty et al., 1989)
Iceland: Geothermal gas (Sano et al., 1985a)
MORB: (Marty and Jambon, 1987)

CO_2 Concentration in the submarine hydrothermal fluids is corrected value for deep seawater bicarbonate.

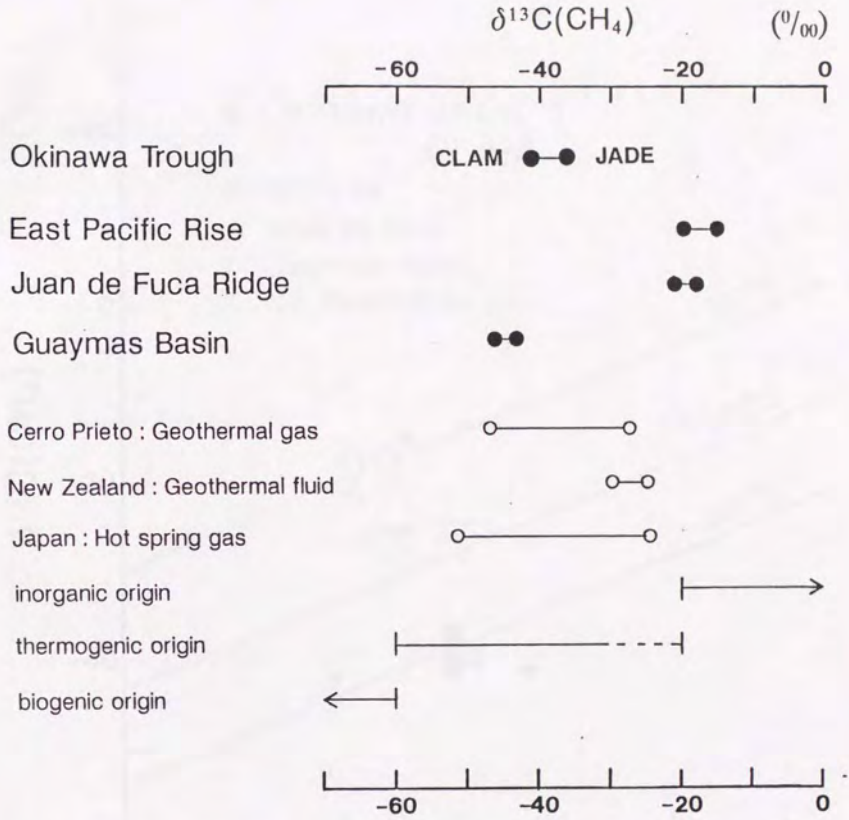

Fig. 5-5 Compilation of $\delta^{13}C(CH_4)$ of hydrothermal fluids and other magmatic gases

Cerro Prieto: Geothermal field gas (Des Marais et al., 1988)
N.Z.: Geothermal fluid (Lyon and Hulston, 1984)
Japan: Hot spring gas (Mizutani et al., 1989)

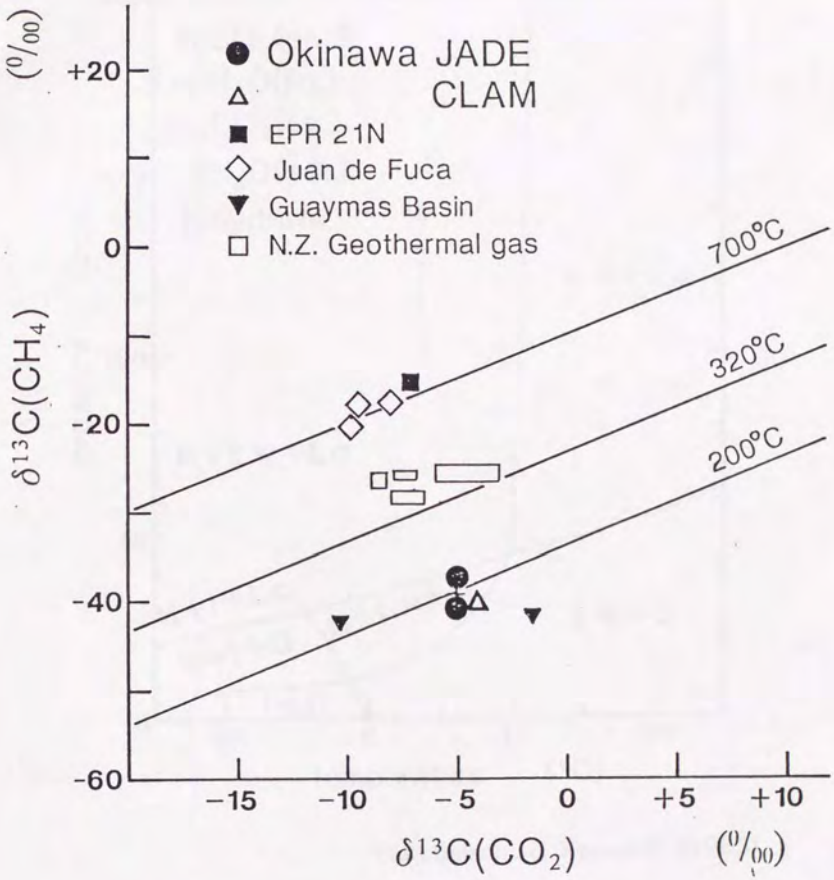

Fig. 5-6 Relationship between $\delta^{13}C(CO_2)$ and $\delta^{13}C(CH_4)$ of hydrothermal fluid and geothermal fluid.

Equilibrium isotopic fractionation values are based on Bottinga (1969)

N.Z.: Geothermal fluid (Lyon and Hulston, 1984)

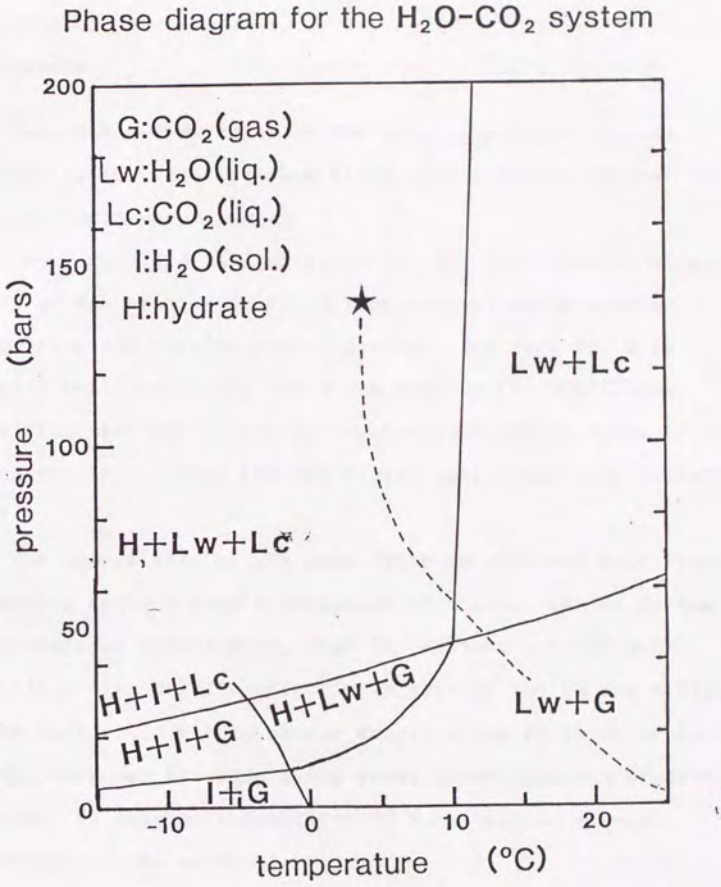

Fig. 5-7 The phase diagram for CO_2-H_2O system after (Takenouchi, 1971; Takenouchi et al., 1965).

A star mark indicates P-T condition on the seafloor at the discharge site. A dotted line represents vertical temperature profile in the water column above the Jade site.

Chapter 6.

Conclusions

Chemical compositions of the high temperature fluids obtained at the Jade and Clam sites in the middle Okinawa Trough back arc basin were studied.

The Jade fluid is similar to the MOR (Mid Oceanic Ridge) fluids so far studied in fluid temperature, major element composition and $^{3}He/^{4}He$ ratio. However, the Jade fluid is strongly enriched in CO_2 and K compared to the MOR fluids, indicating that the it has interacted with acidic rocks of the Island Arc type, while the MOR fluids interacted with tholeitic basalt.

The composition of the Jade fluid is affected significantly by species derived from degradation of organic matter during fluid-sediment interaction. High NH_3 content coupled with saturation with calcite effectively control the pH and alkalinity of the Jade fluid within narrow ranges close to those of the MOR fluids. Although the Jade fluid shows lower contents of metal elements, it retains the ability to form sulfide mineral deposition on the seafloor.

In the Clam site, fluids of 100°C are being discharged. Major element composition of the Clam fluid is explained by simple mixing of the high temperature fluid compositionally similar to the Jade fluid and entrained seawater at a shallow depths below the seafloor.

Fluid-sediment interaction affects the Clam fluid composition more significantly than it does the Jade fluid. The

oxidation of organic matter by reduction of sulfate derived from entrained seawater is responsible for the observed high alkalinity in the Clam fluid, which are the most characteristic features. Lowered temperature may cause extensive metal deposition at depth and thus depletion in heavy metal elements in the venting fluid. This mechanism explains the observation that only calcite deposition occurs at the Clam site by mixing of the hydrothermal fluid with ambient seawater.

As summarized here, the distinct geochemical signatures of the hydrothermal fluids in the middle Okinawa Trough back arc basin are created by combined effects of hydrothermal interaction within the continental crust and within thick sedimentary layer. Difference in flow rate between the Jade and Clam sites, which are probably caused by different thickness in sedimentary piles and other hydrological conditions, may be responsible for the differences in fluid temperature and composition between the two fluids. The Jade and Clam fluid are considered to represent two typical examples of hydrothermal fluids at the continental margins.

References

Akaku, K. (1988)
Geochemistry of mineral deposition from geothermal waters: deposition process of common minerals found in various geothermal fields and case study in the Fushime geothermal field.
Chinetsu, 25, 154-171.

Allard, P. (1983)
The origin of hydrogen, carbon, sulphur, nitrogen and rare gases in volcanic exhalations: evidence from isotope geochemistry.
in "Forecasting volcanic events"
(eds. Tazieff, H. and Sabroux, J.C., Elsevier, Amsterdam)
pp.337-386

Aoki, M. and Nakamura, K. (1989)
The occurrence of chimneys in Izena Hole No.2 ore body and texture and mineral composition of the sulfide chimneys.
JAMSTEC Tech. Rep. Deepsea Res., 197-210.

Arnorsson, S., Sigurdsson, S. and Svavarsson, H. (1982)
The chemistry of geothermal waters in Iceland. 1. Calculation of aqueous speciation from 0 to 370°C.
Geochim. Cosmochim. Acta, 46, 1513-1532.

Auzende, J.M., Honza, E., Boespflug, X., Deo, S., Eissen, J.P., Hashimoto, J., Huchon, P., Ishibashi, J., Iwabuchi, Y., Jarvis, P., Joshima, M., Kisimoto, K., Kuwahara, Y., Lafoy, Y., Matsumoto, T., Maze, J.P., Mitsuzawa, K., Monma, H., Naganuma, T., Nojiri, Y., Ohta, S., Otsuka, K., Okuda, Y., Ondreas, H., Otsuki, A., Ruellan, E., Sibuet, M., Tanahashi, M., Tanaka, T. and Urabe, T. (1990)
Active spreading and hydrothermalism in North Fiji Basin (SW Pacific): Results of Japanese French Cruise Kaiyo 87.
Marine Geophysical Researches, 12, 269-283.

Baker, E.T. and Lupton, J.E. (1990)
Changes in submarine hydrothermal ^{3}He/heat ratios as an indicator of magmatic/tectonic activity.
Nature, 346, 556-558.

Berndt, M.E., Seyfried, W.E.Jr and Janecky, D.R. (1989)
Plagioclase and epidote buffering of cation ratios in mid-ocean

ridge hydrothermal fluids: Experimental results in and near the supercritical region.
Geochim. Cosmochim. Acta, 53, 2283-2300.

Bischoff, J.L. and Rosenbauer, R.J. (1985)
An empirical equation of state for hydrothermal seawater (3.2 percent NaCl).
Am. J. Sci. 285, 725-763.

Bluth, G.J. and Ohmoto, H. (1988)
Sulfide-sulfate chimneys on the East Pacific Rise, 11° and 13°N latitudes. Part 2: sulfur isotopes.
Can. Mineral., 26, 505-515

Bottinga (1969)
Calculated fractionation factors for carbon and hydrogen isotope exchange in the system calcite-carbon dioxide-graphite-methane-hydrogen-water vapor.
Geochim. Cosmochim. Acta, 33, 49-64

Bowers, T.S., Jackson, K.J., Helgeson, H.C. (1984)
Equilibrium activity diagrams
Springer-Verlag, Berlin, 397pp.

Bowers, T.S. and Taylor, H.P.Jr. (1985)
An integrated chemical and stable-isotope model of the origin of midocean ridge hot spring systems.
J. Geophys. Res., 90, 12583-12606.

Bowers, T.S. and Von Damm, K.L. and Edmond, J.M. (1985)
Chemical evolution of mid-ocean ridge hot springs.
Geochim. Cosmochim. Acta, 49, 2239-2252.

Bowers, T.S., Campbell, A.C., Measure, C.I., Spivack, A.J., Khadem, M. and Edmond, J.M. (1988)
Chemical controls on the composition of vent fluids at 13-11°N and 21°N, East Pacific Rise.
J. Geophys. Res. 93, 4522-4536.

Bowers, T.S. (1989)
Stable isotope signatures of water-rock interaction in mid-ocean ridge hydrothermal systems: sulfur, oxygen, and hydrogen.
J. Geophys. Res., 94, 5775-5786.

Butterfield, D.A., Massoth, G.J., McDuff, R.E., Lupton, J.E. and Lilley, D. (1990)
Geochemistry of hydrothermal fluids from Axial Seamount Hydrothermal Emissons Study vent field, Juan de Fuca Ridge: Subseafloor boiling and subsequent fluid-rock interaction.
J. Geophys. Res. 95, 12895-12921.

Campbell, A.C., Bowers, T.S., Measures, C.I., Falkner, K.K., Khadem, M. and Edmond, J.M. (1988a)
A time series of vent fluid composiitons from 21 N, East Pacific Rise (1979, 1981, 1985), and the Guaymas Basin, Gulf of California (1982, 1985).
J. Geophys. Res., 93, 4537-4549.

Campbell, A.C., Palmer, M.R., Klinkhammer, G.P., Bowers, T.S., Edmond, J.M., Lawrence, J.R., Casey, J.F., Thompson, G., Humphris, S., Rona, P. and Karson, J.A. (1988b)
Chemistry of hot springs on the Mid-Atlantic Ridge.
Nature, 335, 514-519.

Corliss, J.B., Dymond, J., Gordon, L.I., Edmond, J.M., Von Herzen, R.P. Ballard, R.D., Green, K., Williams, D., Bainbridge, A., Crane, K. and Van Andel, T.H. (1979)
Submarine thermal springs on the Galapagos Rift.
Science, 203, 1073-1083.

Craig, H., Welhan, J.A., Kim, K., Poreda, R. and Lupton, J.E. (1980)
Geochemical studies of the 21°N EPR hydrothermal fluids
EOS, 61, 992.(abstaract)

Craig, H., Horibe, Y., Farley, K.A., Welhan, J.A., Kim, K.-R. and Hey, R.N. (1987)
Hydrothermal vents in the Mariana Trough: Results of the first Alvin dives.
EOS, 68, 1531.(abstract)

Deines, P. (1980)
The isotopic composition of reduced organic carbon.
in "Handbook of environmental isotope geochemistry"
(eds. Fritz, P. and Fontes, J.Ch., Elseivier, Amsterdam)
pp.329-406.

Des Marais, D.J., Stallard, M.L., Nehring, N.L. and Truesdell,

A.H. (1988)
Carbon isotope geochemistry of hydrocarbons in the Cerro Prieto geothermal field, Baja California Norte, Mexico.
Chem. Geol. 71, 159-167.

Edmond, J.M., Measures, C., McDuff, R.E., Chan, L.H., Collier, R. Grant, B., Gordon, L.I. and Corliss, J.B. (1979)
Ridge crest hydrothermal activity and the balance of the major and minor elements in the ocean; the Galapagos data.
Earth Planet. Sci. Lett., 46, 1-18

Ellis, A.J. and Golding, R.M. (1963)
The solubility of carbon dioxide above 100°C in water and in sodium chlorige solutions.
Am. J. Sci., 261, 47-60.

Evans, W.C., White, L.D. and Rapp, J.B. (1988)
Geochemistry of some gases in hydrothermal fluids from the Southern Juan de Fuca Ridge
J. Geophys. Res., 93, 15305-15313

Fournier, R.O. (1983)
A method of calculating quartz solubilities in aqueous sodium chloride solutions.
Geochim. Cosmochim. Acta, 47, 579-586

Gamo, T. and Horibe, Y. (1980)
Precise determination of dissolved gases in sea water by shipboard gas chromatography.
Bull. Chem. Soc. Jpn. 53, 2839-2842.

Gamo, T., Ishibashi, J., Sakai, H. and Tilbrook, B. (1987a)
Methane anomalies in seawater above the Loihi submarine summit area, Hawaii.
Geochim. Cosmochim. Acta, 51, 2857-2864.

Gamo, T., Ishibashi, J., Sakai, H., Kodera, M., Igarashi, G., Ozima, M., Akagi, T. and Masuda, A. (1987b)
Geochemistry of hydrothermal solutions in the Okinawa Trough.
JAMSTEC Tech. Rep., Deepsea Res., 213-224.

Gamo, T., Sakai, H., Kim, E.-S., Shitashima, K. and Ishibashi, J. (1991)
High alkalinity due to sulfate reduction in the CLAM hydrothermal

field, Okinawa Trough.
Submitted to Earth Planet. Sci. Lett.

Gerling, E.K., Mamyrin, B.A., Tolstikhin, I.N. and Yakovleva, S.S. (1971)
Isotope composition of helium in rocks.
Geokhimiya, 1971, 608-617.

Grienko, V.A., Grieneko, L.N. and Zagryazhskaya, G.D. (1969)
Kinetic isotope effect in high temperature reduction of sulfate.
Geokhimiya, 4, 484-491.

Halbach, P., Nakamura, K.-I., Wahsner, M., Lange, J., Sakai, H., Kaeselitz, L., Hansen, R.-D., Yamano, M., Post, J., Prause, B., Seifert, R., Michaelis, W., Teichmann, F., Kinoshita, M., Maerten, A., Ishibashi, J., Czervinski, S. and Bulm, N. (1989)
Probable modern analogue of kuroko-type massive sulphide deposits in the Okinawa Trough back-arc basin.
Nature, 338, 496-499.

Hajash, A. and Chandler, G.W. (1981)
An experimental investigation of high-temperature interactions between seawater and rhyolite, andesite, basalt and peridotite.
Contrib. Mineral. Petrol., 78, 240-254.

Henley, R.W., Truesdell, A.H., Barton, P.B.Jr. and Whitney, J.A. (1984)
Fluid-mineral equilibria in hydrothermal system.
Society of Economic geologists., 267pp.

Hoefs, J. (1987)
Stable isotope geochemistry. 3rd ed.
241pp., Springer-Verlag, Berlin.

Honma, H., Kusakabe, M., Kagami, H., Iizumi, S., Sakai, H., Kodama, Y. and Kimura, M. (1987)
Major and trace element abundances and D/H, $^{18}O/^{16}O$, $^{87}Sr/^{86}Sr$ and $^{143}Nd/^{144}Nd$ ratios in rocks of the Okinawa Trough.
JAMSTEC Tech. Rep., Deepsea Res., 197-211.

Ishibashi, J., Gamo, T., Sakai, H., Nojiri, Y., Igarashi, G., Shitashitam, K. and Tsubota, H. (1988)

Geochemical evidence for hydrothermal activity in the Okinawa Trough.
Geochem. J., 22, 107-114.

Ishizuka, H., Kawanobe, Y. and Sakai, H. (1990)
Petrology and geochemistry of volcanic rocks dredged from the Okinawa Trough, an active back-arc basin.
Geochem. J., 24, 75-92.

Japanese DELP Research group (1986)
Report on DELP 1984 cruise in the middle Okinawa Trough 1: general outline.
Bull. Earthq. Res. Inst. Univ. Tokyo, 61, 159-165.

Kadko, D.C., Rosenberg, N.D., Lupton, J.E., Collier, R.W. and Lilley, M.D. (1990)
Chemical reaction rates and entrainment within the Endeavour Ridge hydrothermal plume.
Earth Planet. Sci. Lett., 99, 315-335.

Kato, Y., Nakamura K., Iwabuchi, Y., Hashimoto, J. and Kaneko, Y. (1989)
Geology and topography in the Izena Hole of the middle Okinawa Trough - the results of diving surveys in 1987 and 1988 -.
JAMSTEC Tech. Rep., Deepsea Res., 163-182.

Kerridge, J.F., Haymon, R.M. and Kastner, M. (1983)
Sulfur isotope systematic at the 21°N site, East Pacific Rise.
Earth Planet. Sci. Lett., 66, 91-100.

Kimura, M. (1985)
Back-arc rifting in the Okinawa Trough.
Mar. Petrol. Geol., 2, 222-240.

Kimura, M., Kaneoka, I., Kato, Y., Yamamoto, S., Kushiro, I., Tokuyama, H., Kinoshita, H., Isezaki, N., Masaki, H., Ohsida, A., Uyeda, S. and Hilde, T.W.C. (1986)
Report on DELP 1984 cruise in the middle Okinawa Trough 5: topography and geology of the central grabens and their vicinity.
Bull. Earthq. Res. Inst. Univ. Tokyo, 61, 269-310.

Kimura, M. (1988)
Topography, geology and hydrothermal activity in and around the Okinawa Tourgh.

Chikyukagaku (Geochemistry), 22, 65-74.

Kimura, M., Uyeda, S., Kato, Y., Yamano, M., Gamo, T., Sakai, H., Kato, S., Izawa, E. and Oomori, T. (1988)
Active hydrothermal mounds in the Okinawa Trough backarc basin, Japan.
Tectonophysics, 145, 319-324.

Kitahara, Y., Isezaki, N. and Katao, H. (1986)
Report on DELP 1984 cruise in the middle Okinawa Trough 3: measurement of the three components of the geomagnetic field.
Bull. Earthq. Res. Inst. Univ. Tokyo, 61, 203-249.

Koski, R.A., Lonsdale, P.F., Shanks, W.C., Berndt, M.E. and Howe, S. (1985)
Mineralogy and geochemistry of a sediment-hosted hydrothermal sulfide deposit from the Southern Trough of Guaymas Basin, Gulf of California
J. Geophys. Res., 90, 6695-6707.

Koski, R.A., Shanks, W.C., Bohrson, W.A. and Oscarson, R.L. (1988)
The composition of massive sulfide deposits from the sediment-covered floor of Escanaba Trough, Gorda ridge: Implications for depositional processes.
Can. Mineral. 26, 655-673.

Kurz, M.D. and Jenkins, W.J. (1981)
The distribution of helium in oceanic basalt glasses.
Earth Plane. Sci. Lett., 53, 41-54.

Lee, C.-S., Shor, G.G.Jr., Bibee, L.D., Su, R.S. and Hilde, T.W. (1980)
Okinawa Trough: Origin of a back-arc basin
Marine Geology, 35, 219-241.

Letouzey, J. and Kimura, M. (1985)
Okinawa Trough genesis: structure and evolution of a backarc basin developed in a continent.
Mar. Petrol. Geol., 2, 111-130.

Lilley, M.D., Baross, J.A. and Gordon, L.I. (1983)
Reduced gases and bacteria in hydrothermal fluids: The Galapagos Spreading Center and 21°N East Pacific Rise

in "Hydrothermal processes at seafloor spreading centers"
(eds. P.A.Rona, K.Bostrom, L.Laubier, K.L.Smith, Plenum Press,
New York, 798pp.)
pp.441-449.

Lilley, M.D., Baross, J.A., Butterfield, D.A., Olson, E.J> and
McDuff, R.E. (1989)
Volatiles in Endeavour Vent Fluids.
EOS, 70, 1163 (abstract)

Lupton, J.E., Klinkhammer, G.P., Normark, W.R., Haymon, R.,
Macdonald, K.C., Weiss, R.F. and Craig, H. (1980)
Helium-3 and manganese at the 21°N East Pacific Rise hydrothermal
site.
Earth Planet. Sci. Lett., 50, 115-127.

Lupton, J.E. (1983a)
Terrestrial inert gases: Isotope tracer studies and clues to
primordial components in the mantle.
Ann. Rev. Earth Planet. Sci., 11, 371-414.

Lupton, J.E. (1983b)
Fluxes of Helium-3 and heat from submarine hydrothermal systems:
Guaymas Basin versus 21°N EPR.
EOS, 64, 723(abstract).

Lupton, J.E., Baker, E.T. and Massoth, G.J. (1989)
Variable ^{3}He/heat ratios in submarine hydrothermal systems:
evidence from two plumes over the Juan de Fuca ridge.
Nature, 337, 161-164.

Lyon, G.L. and Hulston, J.R. (1984)
Carbon and hydrogen isotopic compositions of new Zealand
geothermal gases.
Geochim. Cosmochim. Acta, 48, 1121-1171.

Malahoff, A., McMurtry, G.M., Wilthire, J.C. and Yeh, H.W. (1982)
Geology and chemistry of hydrothermal deposits from active
submarine volcano Loihi, Hawaii.
Nature, 298, 234-237.

Marty, B. and Jambon, A. (1987)
C/^{3}He in volatile fluxes from the solid Earth: implications for
carbon geodynamics.

Earth Planet. Sci. Lett., 83, 16-26.

Marty, B., Jambon, A. and Sano, Y. (1989)
Helium isotopes and CO_2 in volcanic gases of Japan
Chem. Geol., 76, 25-40.

Masuda, H., Ishibashi, J., Kato, Y., Gamo, T. and Sakai, H. (1987)
Oxygen isotope ratio and trace element composition of hydrothermal sediments from Okinawa trough, collected with SHINKAI2000, dive 231.
JAMSTEC Tech. Rep., Deepsea Res., 225-231.

Matsubaya, O, Ueda, A., Kusakabe, M., Matsuhisa, Y., Sakai, H. and Sasaki, A. (1975)
An isotopic study of the volcanoes and the hot springs in Satsuma Iwo-jima and some areas in Kyushu.
Rep. Geol. Surv. Jpn., 26, 375-392.

Merlivat, L., Pineau, F and Javoy, M. (1987)
Hydrothermal vent waters at 13°N on the East Pacific Rise: isotopic composition and gas concentration.
Earth Planet. Sci. Lett., 84, 100-108.

Michard, G., Albarede, F., Michard, A., Minster, J.F., Charlou, J.L. and N. Tan (1984)
Chemistry of solutions from the 13°N East Pacific rise hydrothermal site.
Earth and Planet. Sci. Lett., 67, 297-307.

Mizutani, Y., Tokiwa, M. and Satake, H. (1989)
Hydrogen and carbon isotopic compositions of methane in N_2- O_2-rich gases from Central Japan.
Geochem. J., 23, 65-73.

Momma, H., Hashimoto, J., Tanaka, T. and Deepsea Research Group (1989)
Preliminary report of deep tow surveys in the Okinawa Trough (DK88-2-OKN-Leg1,2).
JAMSTEC Tech. Rep., 21, 203-221.

Mottl, M.J. (1983a)
Hydrothermal processes at seafloor spreading centers: application of basalt-seawater experimental results.

in "Hydrothermal processes at seafloor spreading centers"
pp.391-409.
ed. P.A.Rona, K.Bostrom, L.Laubier, K.L.Smith
New York, Plenum Press, 798pp.

Mottl, M.J. (1983b)
Metabasalts, axial hot springs and the sturcture of hydrothermal systems at mid-ocean ridges.
Geol. Soc. Am. Bull. 94, 161-180.

Nagumo, S., Kinoshita, H., Kasahara, J., Ouchi, T., Tokuyama, H., Asanuma, T., Koresawa, S. and Akiyoshi, H. (1986)
Report on DELP 1984 cruise in the middle Okinawa Trough 2: seismic structural studies.
Bull. Earthq. Res. Inst. Univ. Tokyo, 61, 167-202.

Naka, J. and Deep Sea Research Group. (1989)
Volcanic products of the Iheya Ridge, Central Okinawa Trough.
JAMSTEC Tech. Rep., Deepsea Res., 245-257.

Nakamura, K., Kato, Y., Kimura, M., Ando, M. and Kyo, M. (1989)
Occurrence and distribution of the hydrothermal ore deposits at the Izena Hole in the Okinawa Trough - summary of the knowledge in 1988.
JAMSTEC Tech. Rep., Deepsea Res., 183-189.

Nakamura, K., Marumo, K. and Aoki, M. (1990)
Discovery of a black smoker vent and a pockmark emitting CO_2-rich fluid on the seafloor hydrothermal mineralization field at the Izena Cauldron in the Okinawa Trough.
JAMSTEC Tech. Rep., Deepsea res., 33-50.

Ohmoto, H. and Rye, R.O. (1979)
Isotopes of sulfur and carbon
in "Geochemistry of Hydrothermal Ore Deposits, 2nd. edition"
(ed. Barnes, H.L., John Willey & Sons, Canada, 798pp.)
pp.509-567

Ohmoto, H. and Lasaga, A.C. (1982)
Kinetics of reactions between aqueous sulfates and sulfides in hydrothermal systems.
Geochim. Cosmochim. Acta, 46, 1727-1745.

Oshima, S., Takanashi, M., Kato, S., Uchida, M., Okazaki, I.,

Sakai, H., Gamo, T., Kim, E.-S., Tsutsumi, M., Tanaka, T., Ishibashi, J., Wakita, H., Yamano, M. and Oomori, T. (1990b)
Venting of carbon dioxide-rich fluid and hydrate formation in the Mid-Okinawa Trough Backarc Basin.
Science, 248, 1093-1096.

Sakai, H., Yamano, M., Tanaka, T., Gamo, T., Kim, E.-S., Ishibashi, J., Shitashima, K., Matsumoto, T., Oomori, i, T., Yanagisawa, F. and Tsutsumi, M. (1990c)
Geochemical studies of the hydrothermal system at the Izena Cauldron using "Shinkai 2000" --reports on dive numbers 413 and 415, and on the liquid CO_2 bubbles and hydrate collected these during dive number 424.
JAMSTEC Tech. Rep., Deepsea Res., 69-85.

Sano, Y. and Wakita, H. (1985)
Geographical distribution of $^3He/^4He$ ratios in Japan: implications for arc tectonics and incipient magmatism.
J. Geophys. Res., 90, 8279-8741.

Sano, Y., Urabe, A., Wakita, H., Chiba, H. and Sakai, H. (1985)
Chemical and isotopic compositions of gases in geothermal fluids in Iceland.
Geochem. J., 19, 135-148.

Sano, Y., Nakamura, Y., Wakita, H. and Ishii, T. (1986)
Light noble gases in basalt glasses from Mariana Trough.
Geochim. Cosmochim. Acta, 50, 2429-2432.

Sano, Y., Wakita, H. and Giggenbach W.F. (1987)
Isalnd arc tectonics of New Zealand manifested in helium isotope ratios.
Geochim. Cosmochim. Acta, 51, 1855-1860.

Sano, Y. and Wakita, H. (1988)
Precise measurement of helium isotopes in terrestrial gases
Bull. Chem. Soc. Jpn., 61, 1153-1157.

Schoell, M. (1988)
Multiple origins of methane in the Earth
Chem. Geol. 71, 1-10.

Seyfried, W.E.Jr. and Bischoff, J.L. (1979)

Low temperature basalt alteration by seawater: an experimental study at 70°C and 150°C.
Geochim. Cosmochim. Acta, 43, 1937-1947.

Seyfried, W.E.Jr. and Bischoff, J.L. (1981)
Experimental seawater-basalt interaction at 300 °C, 500 bars, chemical exchange, secondary mineral formation and implications for the transport of heavy metals.
Geochim. Cosmochim. Acta, 45, 135-147.

Seyfried, W.E.Jr. and Mottl, M.J. (1982)
Hydrothermal alteration of basalt by seawater under seawater-dominated conditions.
Geochim. Cosmochim. Acta, 46, 985-1002.

Seyfried, W.E.Jr., Janecky, D.R. and Mottl, M.J. (1984)
Alteration of the oceanic crust: implications for geochemical cycles of lithium and boron.
Geochim. Cosmochim. Acta, 48, 557-569.

Seyfried, W.E.Jr., Berndt, M.E. and Seewald, J.S. (1988)
Hydrothermal alteration processes at Mid-Ocean Ridges: Constraints from diabase alteration experiments, hot-spring fluids and composition of the oceanic crust.
Can. Mineral., 26, 787-804.

Shanks, W.C.3 and Bischoff, J.L. and Rosenbauer, R.J. (1981)
Seawater sulfate reduction and sulfur isotope fractionation in basaltic systems: Interaction of seawater with fayalite and magnetite at 200-350°C.
Geochim. Cosmochim. Acta, 45, 1977-1995.

Shanks, W.C.3 and Seyfried, W.E.Jr. (1987)
Stable isotope studies of vent fluids and chimney minerals, Southern Juan de Fuca Ridge: sodium metasomatism and seawater fulfate reduction.
J. Geohphys. Res., 92, 11387-11399.

Shiraki, R., Sakai, H., Endoh, M. and Kishima, N. (1987)
Experimental studies on rhyolite- and andesite-seawater interactions at 300°C and 1000 bars.
Geochim. J., 21, 139-148.

Sibuet, J.-C., Letouzey, J., Barbier, F., Charvet, J., Foucher,

J.-P., Hilde, T.W.C., Kimura, M., Chao, L.-Y., Marset, B., Muller, C. and Stephan, J.-F. (1987)
Back arc extension in the Okinawa Trough
J. Geophys. Res., 92, 14041-14063.

Simoneit, B.R. (1985)
Hydrothermal petroleum: genesis, migration, and deposition in Guaymas Basin, Gulf of California.
Can. J. Earth Sci., 22, 1919-1929.

Spivack, A.J. and Edmond, J.M. (1987)
Boron isotope exchange between seawater and the oceanic crust.
Geochim. Cosmochim. Acta, 51, 1033-1043.

Takenouchi, S. and Kennedy, G.C. (1965)
The solubility of carbon dioxide in NaCl solutions at high temperatures and pressures.
Am. Jour. Sci., 263, 445-454.

Takenouchi, S. (1971)
Study of CO_2-bearing fluid inclusions by means of the freezing stage microscope.
Mining Geology, 21, 286-300.

Tanaka, T., Mitsuzawa, K. and Hotta, H. (1989)
"SHINKAI2000" diving surveys in the east of Iheya Small Ridge in the central Okinawa Trough.
JAMSTEC Tech. Rep., Deepsea Res., 267-281.

Tanaka, T., Hotta, H., Sakai, H., Ishibashi, J., Oomori, T.and Iizawa, E. and Oda, N. (1990)
Occurrence and distribution of hydrothermal deposits in the Izena Hole. Central Okinawa Trough.
JAMSTEC Tech. Rep., Deepsea Res., 11-26.

Thornton, E.C. and Seyfried, W.E.Jr. (1987)
Reactivity of organic-rich sediment in seawater at 350°C, 500 bars: Experimental and theoretical constraints and implications for the Guaymas Basin hydrothermal system.
Geochim. Cosmochim. Acta 51, 1997-2010.

Torgersen, T., Lupton, J.E., Sheppard, D.S. and Giggenbach, W.F. (1982)
Helium isotope variations in the thermal areas of New Zealand

J. Volcanol. Geotherm. Res., 12, 283-298

Truesdell, A.H. and Hulston, J.R. (1980)
Isotopic evidence on environments of geothermal systems
in "Handbook of environmental isotope geochemistry"
(eds. Fritz, P. and Fontes, J.Ch., Elseivier, Amsterdam)
pp.179-226.

Trull, T.W., Perfit, M.R. and Kurz, M.D. (1990)
He and Sr isotopic constraints on subduction contributions to
Woodlark Basin volcanism, Solomon Islands.
Geoochim. Cosmochim. Acta, 54, 441-453.

Ueda, A. and Sakai, H. (1984)
Sulfur isotope study of Quaternary volcanic rocks from the
Japanese Islands Arc.
Geochim. Cosmochim. Acta, 48, 1837-1848.

Urabe, A. (1985)
Chemical and isotopic compositions of natural gases in Japan.
Thesis for Ph.D. Univ.Tokyo pp.178

Urabe, T. (1989)
Mineralogical characteristics of the hydrothermal ore body at
Izena Hole No.1 in comparison with kuroko deposits.
JAMSTEC Tech. Rep., Deepsea Res., 191-196.

Uyeda, S., Kimura, M., Tanaka, T., Kaneoka, I., Kato, Y. and
Kushiro, I. (1985)
Spreading center of the Okinawa Trough
JAMSTEC Tech. Rep., Deepsea Res., 123-142.

Von Damm, K.L., Edmond, J.M., Grant, B., Measures, C.I., Walden,
B., Weiss, R.F. (1985a)
Chemistry of submarine hydrothermal solutions at 21°N, East
Pacific Rise.
Geochim. Cosmochim. Acta, 49, 2197-2220.

Von Damm, K.L., Edmond, J.M., Measures, C.I. and Grant, B.
(1985b)
Chemistry of submarine hydrothermal solutions at Guaymas Basin,
Gulf of California.
Geochim. Cosmochim. Acta, 49, 2221-2237.

Von Damm, K.L. and Bischoff, J.L. (1987)
Chemistry of hydrothermal solutions from the Southern Juan de Fuca Ridge.
J. Geophys. Res. 92, 11334-11346.

Von Damm, K.L. (1990)
Seafloor hydrothermal activity: black smoker chemistry and chimneys.
Ann. Rev. Earth Planet. Sci., 18, 173-204.

Weiss, R.F. (1971)
Solubility of helium and neon in water and seawater.
J. Chem. Eng. Data, 16, 235-41

Welhan, J.A. and Craig, H. (1983)
mehtane, hydrogen and helium in hydrothermal fluids at 21°N on the East Pacific Rise
in "Hydrothermal processes at seafloor spreading centers"
(eds. P.A.Rona, K.Bostrom, L.Laubier, K.L.Smith, Plenum Press, New York, 798pp)
pp.391-409.

Welhan, J.A. and Lupton, J.E. (1987)
light hydrocarbon gases in Guaymas basin hydrothermal fluids: Thermogenic versus abiogenic origin.
Am. Assoc. Petrol. Geol. Bull., 71, 215-223.

Welhan, J.A. (1988)
Origins of methane in hydrothermal systems
Chem. Geol., 71, 183-198.

Welhan, J.A., Poreda, R.J., Rison, W. and Craig, H. (1988)
Helium isotopes in geothermal and volcanic gases of the Western United States, 1. Regional variability and magmatic origin.
J. Volcanol. Geotherm. Res., 34, 185-199.

Woodruff, L.G. and Shanks, W.C.3 (1988)
Sulfur isotope study of chimney minerals and vent fluids from 21°N, East Pacific Rise: Hydrothermal sulfur sources and disequilibrium sulfate reduction.
J. Geophys. Res., 93, 4562-4572.

Yamano, M., Uyeda, S., Kinoshita, H. and Hilde, T.W.C. (1986a)
Report on DELP 1984 cruise in the middle Okinawa Trough 4: heat

flow measurements.
Bull. Earthq. Res. Inst. Univ. Tokyo, 61, 251-267.

Yamano, M., Uyeda, S., Furukawa, Y. and Dehghani, G.A. (1986b)
Heat flow measurements in the northern and middle Ryukyu arc area on R/V Sonne in 1984.
Bull. Earthq. Res. Inst. Univ. Tokyo, 61, 311-327.

Yamano, M., Uyeda, S., Foucher, J.-P. and Sibuet, J.-C. (1989)
Heat flow anomaly in the middle Okinawa Trough
Tectonophysics, 159, 307-318.

Yoshimura, Y., Yanagimoto, Y. and Nakagome, O. (1985)
Assessment of the Geothermal potential of the Fushime Area Kyushsu, Japan
Chinetsu, 22, 167-194

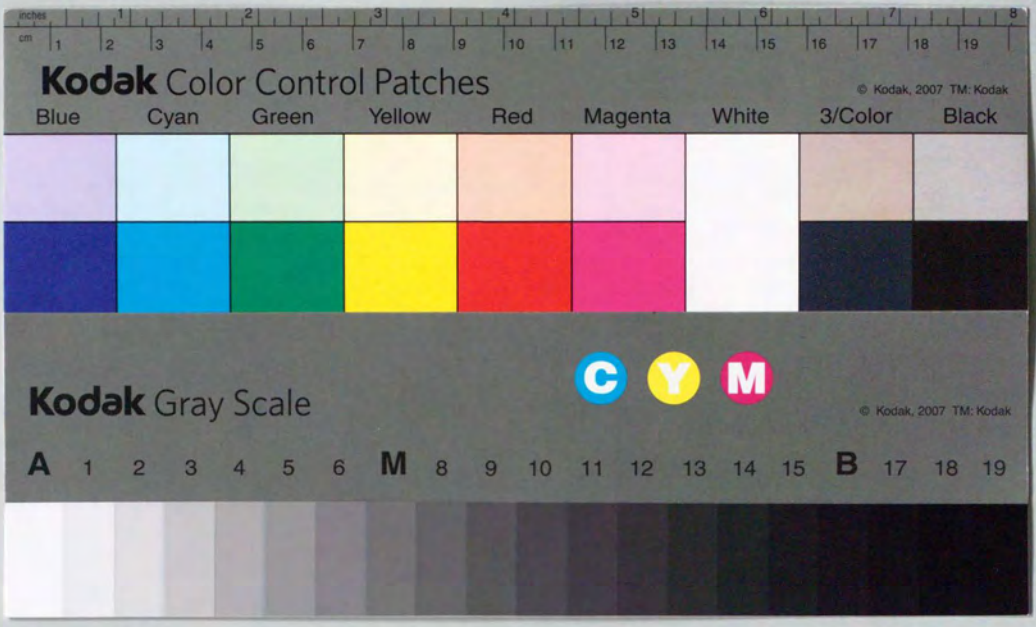
inches
cm
Kodak Color Control Patches
© Kodak, 2007 TM: Kodak
Blue
Cyan
Green
Yellow
Red
Magenta
White
3/Color
Black
Kodak Gray Scale
C
Y
M
© Kodak, 2007 TM: Kodak
A 1 2 3 4 5 6 M 8 9 10 11 12 13 14 15 B 17 18 19